A new approach to solving a spectral problem in a perturbed periodic waveguide

A thesis submitted by
Kieran J-B Robert
for the degree of Doctor of Philosophy

Department of Computer Science
University of Wales, Cardiff
December 2007

ProQuest LLC
789 East Eisenhower Parkway
P.O. Box 1346
Ann Arbor, MI 48106-1346

STATEMENT 1

This thesis is being submitted in partial fulfillment of the requirements for the degree of PhD.

Signed ..Kieran Rose..... (candidate) Date ..23/05/2008.....

STATEMENT 2

This thesis is the result of my own independent work/investigation, except where otherwise stated. Other sources are acknowledged by explicit references.

Signed ..Kieran Rose..... (candidate) Date ..23/05/2008.....

STATEMENT 3

I hereby give consent for my thesis, if accepted, to be available for photocopying and for inter-library loan, and for the title and summary to be made available to outside organisations.

Signed ....Kieran Rose..... (candidate) Date ...23/05/2008.....

Abstract

This thesis presents a numerical investigation of a problem on a semi infinite waveguide. The domain considered here is of a much more general form than those that have been considered using classical techniques. The motivation for this work originates from the work in [28], where unlike here, a perturbation technique was used to solve a simpler problem.

Acknowledgements

I would like to thank my two supervisors whose help allowed numerous unexpected challenges which arose in the computations to be overcome. Professor Marco Marletta's background in numerical analysis was especially useful for explaining certain computational problems which arose during the course of the PhD and also for the debugging advice which saved considerable amounts of time. Professor Malcolm Brown made many useful suggestions for debugging and his knowledge was useful in explaining some of the results and in allowing me to develop my understanding of the theory behind the results, thus allowing me to see that the numerical results in the PhD were in accordance with theory.

Contents

Chapter 1

Introduction

In this thesis we examine certain boundary value problems associated with periodic second order partial differential equations on waveguides. A waveguide is a domain in $\Re^n$ which is topologically cylindrical. This domain can either be finite, infinite or semi infinite. The problem that we shall treat is that of a semi infinite waveguide with a periodic potential which we perturb by attaching a domain to the other end of the waveguide, as illustrated in Fig 1.1. The region where these two domains meet is called the interface

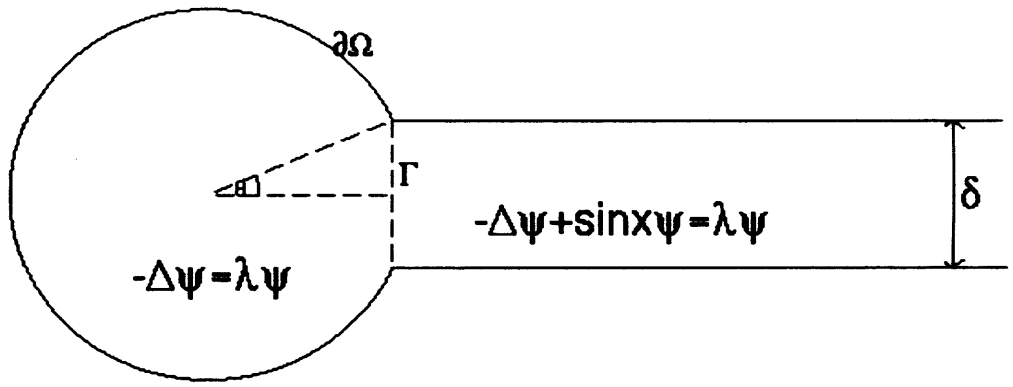

Figure 1.1: The domain consisting of a perturbed semi infinite waveguide

which we shall denote by Γ. The first step in solving this problem will be to find a Dirichlet to Neumann map at Γ in the waveguide. A Dirichlet to Neumann map when applied to Dirichlet data (usualy on the boundary of a domain, or partial domain) gives us Neumann data. In the case of Fig 1.1 it can be represented as the following map

$$\psi|_\Gamma \to \left.\frac{\partial \psi}{\partial n}\right|_\Gamma$$

on the interface Γ. In order to calculate this map we shall use the Floquet theory since we have a periodic potential on the waveguide to obtain both the solution with Dirichlet and Neumann boundary conditions on Γ. Knowing the Dirichlet to Neumann map on Γ and the boundary condition in the perturbing domain we may use finite differences and finite element methods to solve the problem in the perturbed region which in our case is a modified circular domain. Given this solution in the modified circular domain, we may find the solution ψ on Γ. With ψ defined on Γ and given the equation in the waveguide we can then find the solution over one period of the periodic potential, in the waveguide. For this we will use the method of continuous orthonormalisation.

Although a number of papers have considered trapped modes (eigenfunctions) in waveguides, there does not appear to be any work considering such a general periodic structure.

Many significant contributions have been made by Linton and his coworkers. For instance, in [3], Callan, Linton and Evans consider a waveguide obstructed by a circular obstacle, but with a constant potential. By using Hankel functions to solve the Helmholtz equation, the authors establish the existence of trapped modes. In [22] McIver shows the non-uniqueness of a water wave problem by constructing a potential that does not radiate to infinity. In [25] the authors P.McIver, Linton and M.McIver construct trapped modes belonging to eigenvalues that are embedded in the spectrum of the relevant operator. In [18] Linton and Evans seek the solution of the Helmholtz

equation for a parallel-plate waveguide with a symmetric obstacle about the centreline of the guide and solutions are sought using integral equations. In [24], McIver, Linton, McIver and Zhang use a boundary element technique to find embedded trapped modes of an infinitely long waveguide with an obstacle of the form $|\frac{x}{a}|^\nu + |\frac{y}{b}|^\nu = 1$ centred at the lower left corner of the tube and to study the effect on these modes when $\nu \to \infty$. In [23], McIver, Linton and Zhang use the matched eigenfunction technique to show that further modes exist in the vicinity of a rectangular block. In [11] Evans and Linton look for trapped modes in a cylinder with a rectangular indentation. In [2] Aslanyan, Parnovski and Vassiliev consider the situation as in [10] except that the obstacle is shifted from the axis of symmetry and the corresponding complex resonances are studied.

We stress that our use of the term 'periodic' differs from that of Linton, who often considers a finite sequence of identical equally spaced obstacles **across** the waveguide: our approach would be better adapted to dealing with infinitely many identical equally spaced obstacles placed along the axis of the waveguide strip.

Evans, Vassiliev and Levitin [10] devised a simple but elegant argument based on geometrical symmetries to prove the existence of embedded trapped modes for the Helmholtz equation in quite general geometries. We exploit this later on to find embedded trapped modes for our periodic Schrödinger operator.

In chapter 2, we introduce band gaps, the essential spectrum, look at a simple non perturbed waveguide and we then use the Levinson theorem to deal with non separable, rapidly decaying potentials. In chapter 3 we further expand the type of potential which we may study by introducing the Floquet theory and so allowing us to deal with periodic potentials. In chapter 4 we look at self adjoint boundary conditions and formulate a system of Schrödinger equations with a potential perturbed by a compactly supported perturbation such that we may find a Dirichlet to Neumann map. The original material is in chapter 5 where we are able to use the methods developed in chapter 4 to find a Dirichlet to Neumann map in order to find eigenvalues of the problem illustrated in Fig 1.1 which will involve the finite differences method. In chapter 6 we will use the finite element method to find the eigenvalues found in chapter 5 and finally in chapter 7 we make a comparison of the results.

Chapter 2

The Schrödinger equation with decaying potentials on waveguides

Introduction

In this first part of the thesis we shall be concerned with a numerical investigation of the spectra of both the Sturm-Liouville problem and the Schrödinger equation in a waveguide. We shall confine ourselves to examples of the latter in which separation of variables may be employed to reduce the problem to a system of Sturm-Liouville problems. We therefore commence this discussion by introducing the Sturm-Liouville equation.

2.1 Sturm-Liouville equation on the half-line

We shall consider the Sturm-Liouville equation

$$-y'' + qy = \lambda y \quad x \in [a, \infty), \quad \lambda \in \mathbf{C} \text{ and } a > -\infty \tag{2.1}$$

where we assume that $q \in L_{\text{loc}}[a, \infty)$ and satisfies the conditions

$$\exists X > a \text{ such that } \int_a^X |q| < \infty,$$

and

$$\exists X > a \text{ such that } \int_X^\infty |q|^2 < \infty.$$

A point a which satisfies the above conditions is a regular point, otherwise it is said to be an irregular or singular point. A point that is not singular is called a regular point. It is well known that under these assumptions on q,

(2.1) is in the so called *limit-point* case at infinity. For such problems, with a strictly complex λ, up to a constant multiple there is a unique solution that lies in $L^2[a,\infty)$. Thus no boundary conditions are required, or even allowed at infinity, see [6, chapter 9].

The spectrum of the self-adjoint operator (which must be real) generated by the left-hand side of (2.1) is known to contain an essential spectrum σ_{ess} which covers a half line $[0,\infty)$, possibly, with both (finitely or infinitely) many eigenvalues to the left of 0 and possibly some in the essential spectrum. (See [9, IX,Theorem 2.1] for details).

In order to generate a well posed spectral problem we impose the so called self-adjoint boundary condition at a, see [6, chapter 7,problem 15]. Thus we also assume that there are real constants A_1 and A_2 not both of which are zero such that

$$A_1 y(a) + A_2 y'(a) = 0$$

where a is a regular point.

2.2 Liouville-Green expansion

As we stated above our goal will be to use numerical procedures to investigate the spectrum of this Sturm-Liouville problem (and later the Schrödinger equation in two dimensions). However as the problem is posed over $[a,\infty)$ we must first approximate it by one on a finite interval $[a,X]$, $a < X < \infty$ and by imposing a boundary condition at X, which will now depend upon

the spectral parameter λ. In order to do this we calculate an approximation, using the Liouville Green expansion, to the (unique up to a constant multiple) decaying solution in $[X, \infty)$. We now explain how this is performed.

The following theorem is quoted from [7, 2.2.1] in the special case where $p = 1$.

Theorem

Let q be nowhere zero and have locally absolutely continuous derivatives in $[a, \infty)$. Let

$$\frac{(q-\lambda)'}{q-\lambda} = o\left(\frac{1}{\sqrt{q-\lambda}}\right) \quad \text{as} \quad x \to \infty$$

and let

$$\left(\frac{(q-\lambda)'}{\sqrt{(q-\lambda)^3}}\right)' \in L(X, \infty).$$

Let

$$\Re(\sqrt{q-\lambda+r^2}) \text{ have one sign in } [X, \infty),$$

where

$$r = \frac{(q-\lambda)'}{4(q-\lambda)}.$$

Then (2.1) has solutions y_1 and y_2 such that

$$y_1(X) \approx (q(X)-\lambda)^{-\frac{1}{4}} e^{\int_a^X \sqrt{q(t)-\lambda+r^2(t)}dt}, \tag{2.2}$$

$$y_1'(X) \approx (q(X)-\lambda)^{\frac{1}{4}} e^{\int_a^X \sqrt{q(t)-\lambda+r^2(t)}dt}, \tag{2.3}$$

and similarly for y_2 containing $-\int_a^X \sqrt{q(t)-\lambda+r^2(t)}dt$ in the exponential term.

Using the approximations (2.2) and (2.3) we may replace (2.1) by the following problem on the compact interval $[a, X]$ with $(a < X < \infty)$

$$-y''(x) + q(x)y(x) = \lambda y(x) \text{ with } A_1 y(a) + A_2 y'(a) = 0$$

and

$$\frac{y'(X)}{y(X)} = \sqrt{q(X)-\lambda}.$$

2.3 Schrödinger Equations on Waveguides with decaying potentials

As we said in the introduction, our motivation in discussing the Sturm-Liouville equation is as a tool in the investigation of the two dimensional Schrödinger spectral problem in a waveguide. We work with a model two dimensional problem over the domain $\Omega := [a, \infty) \times [0, \delta]$. It is

$$-\Delta\psi(x, y) + q(x, y)\psi(x, y) = \lambda\psi(x, y) \tag{2.4}$$

over this domain and boundary conditions $\psi(x, y)|_{\partial\Omega} = 0$.

For the simplified case where $q(x, y) = 0$ then by separation of variables,

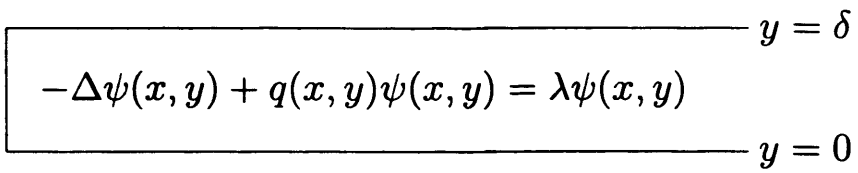

Figure 2.1: The domain and the PDE

and use of the geometry and boundary conditions we obtain the ansatz

$$\psi(x,y) = \sum_{k=1}^{\infty} \phi_k(x) \sin\left(\frac{k\pi}{\delta} y\right). \tag{2.5}$$

This leads to the sequence of ordinary differential equations

$$-\phi_k''(x) + \frac{k^2\pi^2}{\delta^2}\phi_k(x) = \lambda\phi_k(x) \tag{2.6}$$

for $k \in \{1, 2, ..., \infty\}$. These equations have solutions

$$\phi_k(x) = A_k \cos\left(\sqrt{\lambda - \frac{k^2\pi^2}{\delta^2}}\, x\right) + B_k \sin\left(\sqrt{\lambda - \frac{k^2\pi^2}{\delta^2}}\, x\right)$$

for $k \in \{1, 2, ..., \infty\}$ from which we can see that the essential spectrum of problem (2.4) starts at $\lambda = \frac{\pi^2}{\delta^2}$, ie

$$\sigma_{\text{ess}} = [w^2, \infty)$$

where $w = \frac{\pi}{\delta}$. This follows from considering the decomposed partial differ-

ential operator $L = \bigoplus_{k\in\mathbf{N}} L_k$ where

$$L_k = -\frac{d^2}{dx^2} + \frac{k^2\pi^2}{\delta^2}$$

equipped with boundary condition $\phi(0) = 0$. We therefore have

$$\sigma_{\text{ess}}(L_k) = \left[\frac{k^2\pi^2}{\delta^2}, \infty\right).$$

It is known that the essential spectrum of L is the union of the essential spectra of the L_k ie

$$\sigma_{\text{ess}}(L) = \bigcup_{k\in\mathbf{N}} \left[\frac{k^2\pi^2}{\delta^2}, \infty\right) = \left[\frac{\pi^2}{\delta^2}, \infty\right). \tag{2.7}$$

In relation to material that will be presented later in the thesis it will be of interest to see what happens to the spectrum if we cut the domain in half about the axis of symmetry. We will now proceed to investigate what happens in this case. It can be seen that if we cut the domain in half as Fig 2.2 illustrates.

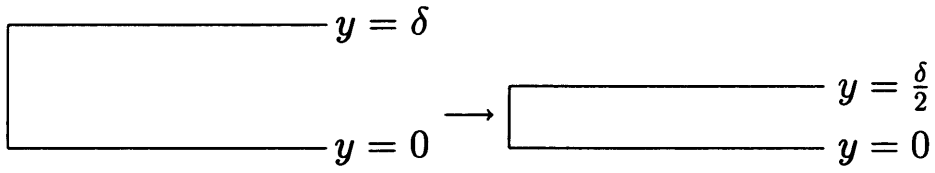

Figure 2.2: The domain on the left which we chop in half on the right

this has the effect of changing δ to $\frac{\delta}{2}$ and thus if we continue to impose Dirichlet boundary conditions on the boundary at $y = 0$ and $y = \frac{\delta}{2}$ then (2.5) becomes

$$\psi(x,y) = \sum_{k=1}^{\infty} \phi_k(x) \sin\left(\frac{2k\pi}{\delta} y\right)$$

and thus the essential spectrum is

$$\sigma_{\text{ess}} = [4w^2, \infty) \tag{2.8}$$

where $w = \frac{\pi}{\delta}$ is as above. We see that the essential spectrum has thus been shifted to the right on the real axis.

It will also be of interest to consider what happens if by contrast we impose Neumann boundary conditions at $y = \frac{\delta}{2}$ but keep Dirichlet boundary conditions at $y = 0$ after slicing the waveguide in half. In this case (2.5) becomes

$$\psi(x,y) = \sum_{k=1}^{\infty} \phi_k(x) \sin\left(\left(k - \frac{1}{2}\right) \frac{2\pi}{\delta} y\right) \tag{2.9}$$

and (2.6) becomes

$$-\phi_k''(x) + \left(k - \frac{1}{2}\right)^2 \frac{4\pi^2}{\delta^2} \phi_k(x) = \lambda \phi_k(x) \tag{2.10}$$

for $k \in \{1, ..., \infty\}$, from which it can be seen that the spectrum is the same as the case where we have Dirichlet boundary conditions at both $y = 0$ and $y = \delta$.

If we now add in a compactly supported perturbation $q(x,y)$, then it is

well known that it will not affect the position of the essential spectrum, see [9, IX2.1], however it may induce eigenvalues below the essential spectrum or embedded in it. If $q(x,y)$ in (2.4) is a potential which induces eigenvalues in the spectrum, then if we cut the tube in half as in Fig 2.2 and impose Dirichlet boundary conditions at $y = 0$ and $y = \frac{\delta}{2}$, some of the eigenvalues previously in the new spectrum may now be below the essential spectrum. This can be seen if one compares (2.7) with (2.8). This will be useful later since we will only be able to find eigenvalues that are not in the essential spectrum and thus cutting the waveguide in half is a way of revealing eigenvalues that would otherwise be hidden in the essential spectrum.

We now return to (2.4) and again (for a different ϕ) we use the ansatz (2.5) and we consider the case where $q \neq 0$. Substituting this into (2.4) and integrating over y we obtain

$$-\phi_k''(x)+\frac{k^2\pi^2}{\delta^2}\phi_k(x)+\frac{2}{\delta}\phi_k(x)\sum_{m=1}^{\infty}\int_0^{\delta} q(x,y)\sin\left(\frac{k\pi}{\delta}y\right)\sin\left(\frac{m\pi}{\delta}y\right)dy = \lambda\phi_k(x) \tag{2.11}$$

for $k = \{1, 2, ..., \infty\}$, where we assume that the sum is convergent (this will later be provided when q is sufficiently smooth). This system is rewritten in matrix form as

$$-\Phi''(x) + Q(x)\Phi(x) = \lambda\Phi(x) \tag{2.12}$$

where $\Phi(x) = [\phi_1(x), \phi_2(x), ..., \phi_\infty(x)]^T$ and

$$Q_{km}(x) = \frac{2}{\delta}\int_0^\delta q(x,y)\sin\left(\frac{k\pi}{\delta}y\right)\sin\left(\frac{m\pi}{\delta}y\right)dy + \frac{k^2\pi^2}{\delta^2} \text{ iff } k = m \quad (2.13)$$

and

$$Q_{km}(x) = \frac{2}{\delta}\int_0^\delta q(x,y)\sin\left(\frac{k\pi}{\delta}y\right)\sin\left(\frac{m\pi}{\delta}y\right)dy \text{ iff } k \neq m. \quad (2.14)$$

It will be our goal to solve the problem illustrated in Fig 2.1 using the expansion in (2.5) where ϕ this time is defined in (2.11). In the case where $q(x,y)$ is only dependent on x and not y, the system decouples and the asymptotes of section (2.2) may be used to define a boundary condition at some point X, $a < X < \infty$.

When the system does not decouple we use the Levinson theorem [7, 1.3.1] to obtain equivalent results as we now show.

2.4 The Levinson theorem

We now present a short account of the Levinson theorem taken from [7]. The differential equation (2.12) can be written as

$$\begin{pmatrix} \Phi(x) \\ \Phi'(x) \end{pmatrix}' = \left[\begin{pmatrix} 0 & I \\ Q(\infty) - \lambda I & 0 \end{pmatrix} + \begin{pmatrix} 0 & 0 \\ Q(x) - Q(\infty) & 0 \end{pmatrix}\right]\begin{pmatrix} \Phi(x) \\ \Phi'(x) \end{pmatrix}.$$

Let $SDS^{-1} = \begin{pmatrix} 0 & I \\ Q(\infty) - \lambda I & 0 \end{pmatrix}$ where D is a diagonal matrix, $\tilde{R}(x) = \begin{pmatrix} 0 & 0 \\ Q(x) - Q(\infty) & 0 \end{pmatrix}$ and $Z(x) = S^{-1} \begin{pmatrix} \Phi(x) \\ \Phi'(x) \end{pmatrix}$. This leads to the expression

$$Z'(x) = (D(x) + R(x))Z(x) \tag{2.15}$$

where $R = S^{-1}\tilde{R}S - S^{-1}S'$. If $q(x,y)$ in (2.13) and (2.14) decays sufficiently fast such that $q(x,y) \in L^2(a,\infty)$ then $Q(\infty) = \text{diag}\left(\frac{\pi^2}{\delta^2}, \frac{4\pi^2}{\delta^2}, ...\right)$ which means that S is independent of x and thus $R = S^{-1}\tilde{R}S$ and we thus have a necessary condition for the Levinson theorem namely

$$\int_a^\infty |R(x)|dx < \infty$$

since $q(x,y) \in L^2(a,\infty)$ and thus from (2.15), has solutions of the form

$$Z_k(x) = (e_k + o(1))e^{\int_a^x \sqrt{\frac{k^2\pi^2}{\delta^2} - \lambda}dt}$$

and

$$Z_k(x) = (e_k + o(1))e^{-\int_a^x \sqrt{\frac{k^2\pi^2}{\delta^2} - \lambda}dt}.$$

If we truncate the sum in (2.11) at N then the matrix D has the form

$$D = \text{diag}\left(\sqrt{\frac{\pi^2}{\delta^2} - \lambda}, ..., \sqrt{\frac{N^2\pi^2}{\delta^2} - \lambda}, -\sqrt{\frac{\pi^2}{\delta^2} - \lambda}, ..., -\sqrt{\frac{N^2\pi^2}{\delta^2} - \lambda}\right)$$

and thus for the left half of matrix S we have $S_{kk} = 1$ and $S_{(k+N)k} = \sqrt{\frac{k^2\pi^2}{\delta^2} - \lambda}$ and on the right half we have $S_{k(k+N)} = 1$ and $S_{(k+N)(k+N)} = -\sqrt{\frac{k^2\pi^2}{\delta^2} - \lambda}$ with all other entries being zero. Since $\begin{pmatrix} \Phi(x) \\ \Phi'(x) \end{pmatrix} = SZ(x)$ then (2.11) has L^2 solutions of the form

$$\phi_k(x) \approx e^{-\int_a^x \sqrt{\frac{k^2\pi^2}{\delta^2} - \lambda} dt}$$

and

$$\phi_k'(x) \approx -\sqrt{\frac{k^2\pi^2}{\delta^2} - \lambda} e^{-\int_a^x \sqrt{\frac{k^2\pi^2}{\delta^2} - \lambda} dt}.$$

A full discussion of the Levinson theorem is contained in [7].

2.5 Results for an exponentially decaying potential in the 2 dimensional Schrödinger equation

In this section we shall calculate the eigenvalues of the Schrödinger equation over the two dimensional domain as above consisting of a tube of infinite length and width δ, namely $([0, \infty) \times [0, \delta])$. We shall reduce the PDE to an infinite system of ODEs and we will then use the Liouville Green expansion on each ODE in order to approximate its solution at a certain point X along the tube, thus reducing the domain from $([0, \infty) \times [0, \delta])$ to $([0, X] \times [0, \delta])$

together with λ dependent boundary conditions at X. Before doing this we shall review some of the available software for solving these types of problems and a selection of the work done in this area.

There are two main pieces of software for solving Sturm-Liouville problems numerically, both of which use a shooting method, these are SLEIGN by Paul Bailey (1966) and SLEDGE written by Steven Pruess, Charles Fulton and Yuantao Xie. A more advanced version of SLEIGN, SLEIGN2 by P. Bailey, T. Zettl and N. Everitt, released in 1991, [27] can handle arbitrary self-adjoint, regular or singular, separated or coupled boundary conditions. These codes are designed to compute eigenvalues and eigenfunctions of regular and singular self-adjoint Sturm-Liouville problems. SLEDGE can also obtain information on endpoints by checking certain inequalities and can also calculate a spectral density function. In order to solve a Sturm-Liouville problem SLEDGE uses a piecewise approximation of coefficients of the differential equation while SLEIGN and SLEIGN2 make use of the Prüfer transform. The NAG library contains the routines D02KAF and D02KDF written in FORTRAN and is based on the scaled Prüfer transform of Pryce and a shooting method. They both find a specified eigenvalue of a SLP on a finite range and D02KDF has an advantage over D02KAF in that it can deal with discontinuities in the coefficient function of a SLP.

The code which we shall use here is that described in [19] called SL09F and SL10F and were available on NETLIB. Here a new spectral function is described for a vector Sturm-Liouville problem and a miss distance function

is used to find the eigenvalues. The codes SL11F and SL12F are based on matrix oscillation theory and shooting and SL12F additionally uses coefficient approximation. They are used in [20] where the code solves a differential equation whose solution is a unitary matrix.

It is well known that the problem of interval truncation and discretisation can introduce spurious eigenvalues as a form of spectral pollution and we can avoid this by using shooting. In [17], Levitin and Shargorodsky look at the phenomenon of spectral pollution resulting from trying to approximate the spectrum of a self-adjoint operator with a projection method. The paper has several detailed examples of the methods used to deal with the phenomenon. The authors introduce a second order relative spectrum to detect spectral pollution in the standard projection method. For different reasons there are spurious eigenvalues when working with the equations of fluid motion as in [30]. In this work Walker and Straughan are confronted with the problem of spurious eigenvalues when attempting to solve a porous convection problem and they make use of the compound matrix and the beta tau method to eliminate spurious eigenvalues. According to Gardner [12] who motivated the work in [30], these spurious eigenvalues are due to singularities in the matrix resulting from the discretisation of the differential equation.

In this chapter we shall use a shooting method to solve certain problems. Shooting methods don't suffer from the phenomenon of spectral pollution.

2.5.1 Application to a rapidly decaying negative potential

We note that when $q(x,y)$ is a function only of x the equation in (2.12) decouples and the Liouville-Green asymptotics [7, 2.2] apply to each equation separately. We now calculate a boundary condition at X for $X < \infty$ for the example problem (2.4) where $q(x,y) = -30e^{-x}\cos x$.

Let $q(x,y) = -30e^{-x}\cos x$ in (2.4) after substituting into (2.5) we obtain

$$-\phi_k''(x) + \left(\frac{k^2\pi^2}{\delta^2} - 30e^{-x}\cos x\right)\phi_k(x) = \lambda\phi_k(x)$$

for $k \in \{1, 2, ..., \infty\}$.

Applying (2.2) and (2.3) to the above equations gives for $X > a$

$$\phi_n(X) \approx \frac{e^{-\int_a^X \sqrt{\frac{n^2\pi^2}{\delta^2} - 30e^{-t}\cos t + \frac{900e^{-2t}(\sin t + \cos t)^2}{4\left(\frac{n^2\pi^2}{\delta^2} + 30e^{-t}\cos t - \lambda\right)^2} - \lambda}\,dt}}{\left(\frac{n^2\pi^2}{\delta^2} - 30e^{-X}\cos X - \lambda\right)^{\frac{1}{4}}} \tag{2.16}$$

and

$$\phi_n'(X) \approx -\frac{e^{-\int_a^X \sqrt{\frac{n^2\pi^2}{\delta^2} - 30e^{-t}\cos t + \frac{900e^{-2t}(\sin t + \cos t)^2}{4\left(\frac{n^2\pi^2}{\delta^2} + 30e^{-t}\cos t - \lambda\right)^2} - \lambda}\,dt}}{\left(\frac{n^2\pi^2}{\delta^2} - 30e^{-X}\cos X - \lambda\right)^{-\frac{1}{4}}} \tag{2.17}$$

respectively. The code in [21] which we use to compute a numerical approximation of the solutions requires the boundary condition to be of the form

$y'(X) = Ay(X)$ for $X > 0$ and thus (2.16) and (2.17) become

$$\phi'(X) = -\phi(X)\sqrt{\frac{n^2\pi^2}{\delta^2} - 30e^{-X}\cos X - \lambda}. \tag{2.18}$$

If δ is sufficiently small then the term $\frac{\pi^2}{\delta^2}$ dominates $-30e^{-x}\cos x$ so that

$$q \approx \frac{n^2\pi^2}{\delta^2} - \lambda$$

for $x > X$ and large X and thus (2.18) becomes

$$\phi'(X) \approx -\phi(X)\sqrt{\frac{n^2\pi^2}{\delta^2} - \lambda}.$$

This approximation is equivalent to setting $q(X) = 0$ and thus $-30e^{-x}\cos x$ acts as a compactly supported perturbation in $[a, X)$ and thus does not change the essential spectrum.

In our case we choose $\delta = 0.73$ and thus $\frac{\pi^2}{\delta^2} \approx 18.52$ with $a = -1$. The chosen value of δ is mainly an intuitive guess as this δ allows a certain number of eigenvalues to be below the essential spectrum while not producing too many. We impose the following boundary conditions

$$y(-1) = 0 \text{ and } y'(X) = -y(X)\sqrt{\frac{n^2\pi^2}{\delta^2} - \lambda}$$

and we choose several values for X in order to compare accuracy. Table (2.1) gives the eigenvalues to our problem where we truncate (2.11) at $N = 5$. We

note that since the system decouples then the eigenvalues do not depend on N.

$X = 5$	$X = 8$	$X = 11$	$X = 14$
-16.502020	-16.502019	-16.502019	-16.502013
-0.77175819	-0.77175678	-0.77175776	-0.77175930
11.396364	11.397026	11.397032	11.396997
19.352632	18.832586	18.641448	18.586329

Table 2.1: Eigenvalues for $\delta = 0.73$, $N = 5$ at various X

The negative potential $-30e^{-x}\cos x$ induces eigenvalues below the essential spectrum which start at $\frac{\pi^2}{\delta^2} = 18.52$. From table 2.1 it can be seen that the eigenvalues below the essential spectrum are quite stable with respect to X. We note that the last eigenvalue in the table is in the essential spectrum. We now discuss the case of a non separable potential.

2.5.2 Application to a non separable potential

For the following non separable potential

$$q(x,y) = -30e^{-\sqrt{x^2+(y-\frac{\delta}{2})^2}}$$

for $y \in [0,\delta]$ and $x \in [a,X]$ we use the FORTRAN code in [21] to integrate out the y dependence to obtain the following potential

$$Q_{mn}(x) = -30\int_0^\delta e^{-\sqrt{x^2+(y-\frac{\delta}{2})^2}}\sin\left(\frac{m\pi}{\delta}y\right)\sin\left(\frac{n\pi}{\delta}y\right)dy + \frac{n^2\pi^2}{\delta^2}\delta_{mn}.$$

We use the Levinson theorem [7, 1.3.1] to derive the boundary condition at X; namely $y'(X) = -y(X)\sqrt{\frac{k^2\pi^2}{\delta^2} - \lambda}$. In table (2.2), again we truncate (2.11) at $N = 5$.

$X = 5$	$X = 8$	$X = 11$	$X = 14$
-1.616036	-1.616047	-1.616037	-1.616061
7.977970	7.977978	7.977982	7.977962
13.829375	13.829459	13.829113	13.829361
17.299980	17.287788	17.286995	17.28774
19.194344	18.617109	18.542617	18.524077

Table 2.2: Eigenvalues for $\delta = 0.73$, $N = 5$ at various X

In table (2.3) we truncate (2.11) at $N = 10$.

$X = 5$	$X = 8$	$X = 11$	$X = 14$
-1.616043	-1.616055	-1.616045	-1.616064
7.977970	7.977976	7.977982	7.977963
13.829375	13.829450	13.829111	13.829360
17.299980	17.287788	17.286997	17.287735
19.194343	18.617108	18.542616	18.524077

Table 2.3: Eigenvalues for $\delta = 0.73$, $N = 10$ at various X

Of interest is the error made from truncating the domain. Looking at tables 2.2 and 2.3, it can be seen that interval truncation produces a more significant error than truncating the sum at N which we now analyse.

2.5.3 Analysis of the error caused by truncating at X

This leads us to the following observation. Our approximation at $x = X$ is equivalent to the assumption that $q(X, y) = 0$. We may therefore write two

differential equations, one for the non truncated problem

$$-\phi_k''(x) + Q(x)\phi_k(x) = \lambda\phi_k(x) \text{ and } -\phi_k''(x) + \tilde{Q}(x)\phi_k(x) = \tilde{\lambda}\phi_k(x)$$

where $\tilde{Q}(x) = Q(x)$ for $x \in [-1, X]$ and $\tilde{Q}(x) = 0$ for $x > X$. Subtracting these two equations from one another and integrating we obtain

$$(\lambda - \tilde{\lambda}) \int_{-1}^{\infty} \phi_k(x)^2 dx = \int_X^{\infty} Q(x)\phi_k^2(x)dx.$$

Let A be a normalisation constant so that $A^2 \int_0^{\infty} \phi_k^2(x)dx = 1$. Thus we obtain

$$\lambda - \tilde{\lambda} = A^2 \int_X^{\infty} Q(x)\phi_k^2(x)dx$$

or

$$\lambda - \tilde{\lambda} < A^2 \max_{x\in[X,\infty)} Q(x) \int_X^{\infty} e^{-2\sqrt{\frac{k^2\pi^2}{\delta^2} - \lambda}x dx}$$

which lead to

$$\lambda - \tilde{\lambda} < \frac{A^2 Q(X)}{2\sqrt{\frac{k^2\pi^2}{\delta^2} - \lambda}} e^{-2\sqrt{\frac{k^2\pi^2}{\delta^2} - \lambda}X}.$$

As can be seen, there is an exponential decay in the truncation error as we move the point of truncation X to the right of zero.

In this chapter we examined Schrödinger problems with decaying potentials while in the next chapter we will introduce Floquet's theory which allows us to deal with periodic potentials. We also look at certain conditions necessary for self adjointness.

Chapter 3

Sequences of ODEs on $\Re^+$ with band-gap spectral structure

In this chapter we shall consider the general class of problems of the form

$$-\Psi''(x) + Q(x)\Psi(x) = \lambda\Psi(x) \;\; x \in \Re^+ \tag{3.1}$$

where Q is an $n \times n$ matrix with the property that $Q(x + 2\pi) = Q(x)$ and $\Psi(x) = [\psi_1(x), \psi_2(x), ..., \psi_n(x)]^T$ and

$$A_1\Psi(0) + A_2\Psi'(0) = 0. \tag{3.2}$$

where A_1 and A_2 are $n \times n$ matrices.

We shall consider (a) the conditions on the matrices A_1 and A_2 which ensure that the operator underlying this ODE problem is self-adjoint; (b) the Floquet theory associated with the ODE problem; (c) the band-gap spectral structure of the underlying operator, as characterised through Floquet multipliers.

The role of this chapter is to provide a complete and rigorous description of the theory behind a system of ODEs which will arise in later chapters as an approximation to a single PDE on a waveguide. We should emphasise that this chapter is largely a review of known results, provided for the convenience of the reader. The construction of the self-adjoint operator associated with our system of ODEs may be found in a number of sources, including [14] and [26]. The Floquet theory is also quite classical, although in textbooks it is usually developed for a single ODE (see, e.g., [8]); for systems of ODEs there is a good review in the recent article of Clark, Gestezy, Holden and Levitan

[5].

We define an operator by $Ly = -y'' + Qy$ on the domain

$$\mathcal{D}(L) = \{y \in (L^2(\Re^+))^n | -y'' + Qy \in (L^2(\Re^+)), A_1 y(0) + A_2 y'(0) = 0\}.$$

We wish to describe the conditions on A_1 and A_2 which ensure that L is self-adjoint. For self-adjointness the following are required

$$\langle Lf, g\rangle - \langle f, Lg\rangle = 0 \ \forall f, g \in D(L)$$

where $< g, f >= \int_0^\infty gf dx$. The matrix $Q(x)$ is a real symmetric matrix and thus cancels, viz for $f, g \in D(L)$

$$\langle Lf, g\rangle - \langle f, Lg\rangle = \int_0^\infty (-f'' + Qf)^* g dx - \int_0^\infty f^*(-g'' + Qg) dx$$

$$= \lim_{t\to\infty}[-(f'(x))^* g(x) + f^*(x)g'(x)]_0^t = f'^*(0)g(0) - f^*(0)g'(0),$$

by choosing f and g to have compact support. The boundary condition (3.2) can be rewritten as

$$(A_1+iA_2)f(0)+A_2(f'(0)-if(0)) = 0 \ \Rightarrow \ f(0) = -(A_1+iA_2)^{-1}A_2(f'(0)-if(0))$$

and

$$(A_1-iA_2)g(0)+A_2(g'(0)+ig(0)) = 0 \ \Rightarrow \ g(0) = -(A_1-iA_2)^{-1}A_2(g'(0)+ig(0)),$$

provided that we can ensure that $A_1 + iA_2$ and $A_1 - iA_2$ are invertible. We shall justify this later. Therefore after rewriting the result for $\langle Lf, g\rangle - \langle f, Lg\rangle$ we obtain

$$\langle Lf, g\rangle - \langle f, Lg\rangle = (f'(0) - if(0))^* g(0) - f^*(0)(g'(0) + ig(0)) \qquad (3.3)$$

$$= (f'(0) - if(0))^* [A_2^*(A_1 + iA_2)^{-*} - (A_1 - iA_2)^{-1}A_2](g'(0) + ig(0)).$$

Expression (3.4) is zero for all compactly supported $f, g \in \mathcal{D}(L)$ iff

$$A_2^*(A_1 + iA_2)^{-*} = (A_1 - iA_2)^{-1}A_2$$

$$\Leftrightarrow \quad (A_1 - iA_2)A_2^* = A_2(A_1^* - iA_2^*)$$

$$\Leftrightarrow \quad A_1A_2^* = A_2A_1^*.$$

We see that one condition for the operator L to be self-adjoint is that $A_1A_2^* = A_2A_1^*$.

We introduce the minimal operator L_0 and the maximal operator L_0^* where L_0 has deficiency indices $(2n, 2n)$ and L_0^* has deficiency indices (n, n). Note that for $\lambda \notin \Re$ the deficiency indices n_+ and n_- are the number of $L^2[0, \infty)$ solutions of $Lg = \pm iy$, see Naimark [26]. The self-adjointness of the operator L given the boundary condition (3.2) will now be proved based on [14, theorem 10.5.2]. Let $\{f_j\}_{j=0}^n$ be a set of n functions in $\mathcal{D}(L_0^*)$ linearly independent with respect to $\mathcal{D}(L_0)$.

For our operator L to be self-adjoint it is necessary and sufficient that the boundary conditions (3.2) be of the form (3.4) for some suitable choice of $f_1, ..., f_n$. For self-adjointness

$$\langle Lf_j, \Psi \rangle - \langle f_j, L\Psi \rangle = [f_j, \Psi]_0^\infty = -f_j'^*(0)\Psi(0) + f_j^*(0)\Psi'(0) \tag{3.4}$$

should be zero. Comparing this with (3.2) we see that

$$f_j'(0) = -A_1^* e_j \quad \text{and} \quad f_j(0) = A_2^* e_j \tag{3.5}$$

and thus it can easily be deduced that $A_1 f_j(0) + A_2 f_j'(0) = 0$ and so $\begin{pmatrix} f_j(0) \\ f_j'(0) \end{pmatrix}$ is a spanning set of $\ker(A_1|A_2)$ and

$$A_1 = \begin{pmatrix} -f_1'(0)^* \\ -f_2'(0)^* \\ \cdot \\ \cdot \\ \cdot \\ -f_n'(0)^* \end{pmatrix} \quad \text{and} \quad A_2 = \begin{pmatrix} f_1(0)^* \\ f_2(0)^* \\ \cdot \\ \cdot \\ \cdot \\ f_n(0)^* \end{pmatrix}.$$

The functions $f_1, ..., f_n$ are smoothly extended from these initial conditions as compactly supported elements of $\mathcal{D}(L_o^*)$.

It remains to show that $\{f_j\}_{j=1}^n$ are linearly independent with respect to $\mathcal{D}(L_0)$. Let us choose n compactly supported functions $\{g_j\}_{j=1}^n$ in $\mathcal{D}(L_0^*)$ such

that $\det([f_i, g_j]_0^\infty) \neq 0$. This leads to

$$[f_i, g_j]_0^\infty = -f_i'^*(0)g_j(0) + f_i(0)^* g_j(0) = e_i^*(A_1 g_j(0) + A_2 g_j'(0)).$$

It can be seen that $\begin{pmatrix} g_j(0) \\ g_j'(0) \end{pmatrix} \in \ker(A_1|A_2)$ and thus

$$[f_i, g_j]_0^\infty = e_i^*(A_1|A_2) \begin{pmatrix} g_j(0) \\ g_j'(0) \end{pmatrix}.$$

Choosing $\begin{pmatrix} g_j(0) \\ g_j'(0) \end{pmatrix} = \begin{pmatrix} A_1^* \\ A_2^* \end{pmatrix} e_j$, we get

$$[f_i, g_j]_0^\infty = A_1 A_1^* + A_2 A_2^* \neq 0.$$

From [14, theorem 10.5.2] we have shown that no self-adjoint extension exists for the operator (3.1) and (3.2) and thus the problem is self-adjoint.

3.1 Floquet's Theory for a Hamiltonian system of ODEs

Consider the following Hamiltonian system of ODEs

$$u'(x) = A(x)u(x) \quad x \in [0, \infty) \tag{3.6}$$

where A has the property that $A(x+2\pi) = A(x)$, $u(x)$ is a vector of the form $u(x) = [y_1(x), ..., y_{2N}(x)]^T$ with unspecified boundary conditions at 0. Equation (3.1) can be written in the form $Y'(x) = A(x)Y(x)$ where $Y(x) \in \Re^{2N\times 2N}$ and

$$A_{pq} = \begin{cases} 1 & q = p+N \\ Q_{(p-N)q}(x) - \lambda & p = q+N \\ Q_{(p-N)q}(x) & p \neq q+N \text{ and } p > N, q \leq N \\ 0 & \text{otherwise} \end{cases} \tag{3.7}$$

on $[0, \infty)$ with the property that $A(x+2\pi) = A(x)$ since $Q(x+2\pi) = Q(x)$. Then there exists solutions $u_1, ..., u_N$ with $2N$ components, and complex numbers $\rho_1, ..., \rho_N$ such that

$$u_j(x+2\pi) = \rho_j u_j(x) \quad \text{for} \quad 1 \leq \text{j} \leq \text{2N}. \tag{3.8}$$

The u_j are called Floquet eigenvectors and the ρ_j Floquet multipliers. We let $u_j(x) = Y(x)c_j, j = 1, 2, ..., 2N$, where c_j is a column vector of length $2N$ and Y a $2N \times 2N$ matrix.

Setting $Y(0) = I_{2N}$ we have $u_j(0) = c_j$ where I_{2N} is the $2N \times 2N$ identity matrix and thus solve the following

$$Y'(x)c_j = A(x)Y(x)c_j \text{ with } Y(0) = I_{2N}$$

over the interval $x \in [0, 2\pi]$. Using (3.8) we obtain the following eigenvalue problem

$$(Y(2\pi) - \rho_j I_{2N})c_j = 0.$$

We are interested in values of λ which are in the spectral gaps of the operator L. In the spectral gaps we have solutions with the following property;

$$u_+(x + 2\pi) = \rho_+ u(x) \text{ and } u_-(x + 2\pi) = \rho_- u(x) \tag{3.9}$$

where $|\rho_-| < 1$ and $|\rho_+| > 1$. In fact we can expect N Floquet multipliers to have the property that $|\rho_-| < 1$ and N others with property that $|\rho_+| > 1$. The case when $|\rho_j| < 1$ corresponds to the Floquet eigensolutions in $L^2(\Re_+)$. Any solution of equation (3.1) which lies in L^2 consists of a linear combination of the $L^2(\Re_+)$ eigenvectors of (3.6). In the essential spectrum $|\rho_j| = 1$ for some j and thus there exists solutions which are oscillatory.

Using $u_j(x) = Y(x)c_j$ we can rewrite (3.8) as

$$Y'(x)c_j = A(x)Y(x)c_j.$$

We can then impose the following boundary condition $Y(0) = I_{2N}$ and thus (3.9) becomes $Y(2\pi)c_j = \rho_j Y(0)c_j$. From this equation we can find, for a given value of λ in a gap, the N values ρ for the N solutions in $L^2(\Re^+)$. For a more technical introduction to the Floquet Theory of Hamiltonian systems see [5].

3.2 The spectral bands and gaps

In [1] Aceto, Ghelardoni and Marletta find the spectral gaps of the differential equation $-\phi_0''(x) + \sin(x)\phi_0(x) = \lambda\phi_0(x)$ which we quote here as $\sigma_0 = (-\infty, -0.3785) \cup (-0.3477, 0.5948) \cup (0.9181, 1.293) \cup (2.285, 2.343)$ where the gaps beyond the fourth have been ignored. Consider (2.11) with $q(x, y) = \sin(x)$ which leads us to

$$-\phi_n''(x) + \sin(x)\phi_n(x) + \frac{n^2\pi^2}{\delta^2}\phi_n(x) = \lambda\phi_n(x). \tag{3.10}$$

The spectrum of (3.10) which we shall denote by σ_n is that of σ_0 shifted to the right by $\frac{n^2\pi^2}{\delta^2}$. This can be easily seen when one replaces λ in (3.10) with $\lambda' = \lambda - \frac{n^2\pi^2}{\delta^2}$. Let σ be the union of the spectra of the sequence of equations in (3.10) for $n = \{1, 2, ...2N\}$ then it is well known that σ should be the union of the spectrum of each individual equation in (3.10) ie

$$\sigma = \cup_{k=1}^{\infty}\sigma_k.$$

Since the gaps die out so rapidly (theorem 5.2 [8]) it follows that, in our case, to a very good approximation we have $\sigma = \sigma_1$.

Below is a diagram showing the bands and gaps in the spectrum for different n. The black lines denote the spectrum and the gaps are the clear spaces. It can be seen how the spectrum is shifted to the right for every equation in (3.10) with different n by $\frac{n^2\pi^2}{\delta^2}$. In this example as illustrated in

Fig. 3.1 we have chosen $\delta = 2\sin(\frac{\pi}{10})$.

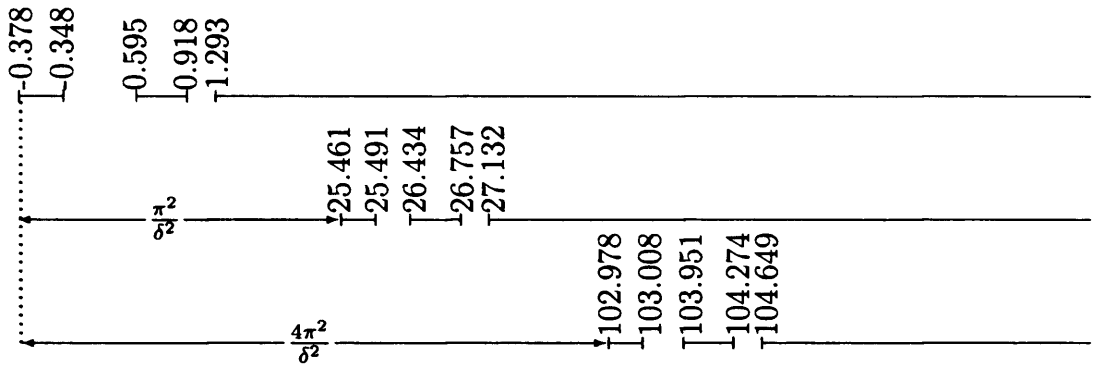

Figure 3.1: Spectrum and gaps of (3.10) for $n = 0, 1$ and 2.

In the following chapter we shall apply Floquet's theory to find eigenvalues of systems of ODE's containing a periodic potential with a compactly supported perturbation. The formulation will lay the foundations for finding the Dirichlet to Neumann map which will first appear in (5.17).

Chapter 4

A numerical algorithm for solving a perturbed periodic Hamiltonian system

In the previous chapter we considered a periodic potential Q. For such Q there are often no eigenvalues in the gaps, although this depends on the boundary conditions. By introducing a compactly supported perturbation, eigenvalues can be induced in the gaps. Thus we have a potential of the form $Q = Q_{periodic} + Q_{perturbed}$. We next illustrate this with a simple SLP example.

4.1 Solution of a simple ODE with a perturbation of a periodic potential

We consider two Sturm-Liouville problems over $[0, \infty)$ with self-adjoint boundary conditions at the end points and with potentials $\sin x$ and $\cos x$ respectively. Both problems have the same essential spectrum and it is well known that a compactly supported perturbation will leave the essential spectrum of the system invariant [9, IX 2.1]. In this example the compactly supported perturbation is $\frac{\epsilon}{1+x^2}$ where ϵ is a constant which when its absolute value is above a certain value results in eigenvalue accumulation [29].

Consider the two systems

$$z_1'' = (\sin x + q - \lambda)\, z_1 \quad \text{and} \quad z_2'' = (\cos x + q - \lambda)\, z_2 \tag{4.1}$$

with given boundary conditions $z_i(0)\cos\alpha_i + z_i'(0)\sin\alpha_i = 0$ for $i = \{1, 2\}$ and $q(x) = \begin{cases} \frac{\epsilon}{1+x^2} & x \in [0, 16\pi] \\ 0 & x > 16\pi \end{cases}$. We write the solution in the form $\begin{pmatrix} z_i \\ z_i' \end{pmatrix}$

where z_i is the solution to $-z_i'' + q(x)z_i = \lambda z_i$ for $i = \{1, 2\}$ and $q(x)$ is either $\sin x$ or $\cos x$. At 16π it is assumed the the solution is a linear combination of the vectors $e_1 = \begin{pmatrix} 1 \\ 0 \end{pmatrix}$ and $e_2 = \begin{pmatrix} 0 \\ 1 \end{pmatrix}$. Therefore given two fundamental solutions $\phi_1(x)$ and $\phi_2(x)$ of the differential equation with boundary conditions e_1 and e_2 at $x = 16\pi$ we can write the solutions Z and Z' as a linear combination of $\phi_1(16\pi)$ and $\phi_2(16\pi)$, ie

$$z(16\pi) = c_1\phi_1(16\pi) + c_2\phi_2(16\pi) \quad \text{and} \quad z'(16\pi) = c_1\phi_1'(16\pi) + c_2\phi_2'(16\pi).$$

Applying the Floquet theory to our case we have $Z(18\pi) = \rho Z(16\pi)$ where ρ is the Floquet multiplier and $Z'(18\pi) = \rho Z'(16\pi)$ *ie* $c_1\phi_1(18\pi)+c_2\phi_2(18\pi) = \rho(c_1\phi_1(16\pi)+c_2\phi_2(16\pi))$ and $c_1\phi_1'(18\pi)+c_2\phi_2'(18\pi) = \rho(c_1\phi_1'(16\pi)+c_2\phi_2'(16\pi))$. The last two equations can be rewritten in the form

$$\begin{pmatrix} \phi_1(18\pi) & \phi_2(18\pi) \\ \phi_1'(18\pi) & \phi_2'(18\pi) \end{pmatrix} \begin{pmatrix} c_1 \\ c_2 \end{pmatrix} = \rho \begin{pmatrix} \phi_1(16\pi) & \phi_2(16\pi) \\ \phi_1'(16\pi) & \phi_2'(16\pi) \end{pmatrix} \begin{pmatrix} c_1 \\ c_2 \end{pmatrix} \quad (4.2)$$

and in view of the boundary conditions at 16π we have

$$\begin{pmatrix} \phi_1(18\pi) & \phi_2(18\pi) \\ \phi_1'(18\pi) & \phi_2'(18\pi) \end{pmatrix} \begin{pmatrix} c_1 \\ c_2 \end{pmatrix} = \rho \begin{pmatrix} c_1 \\ c_2 \end{pmatrix}.$$

If λ is in one of the spectral gaps of the perturbed problem then $\rho \in \Re$ and from [1] the following values of λ correspond to gaps in the essential spectrum

$\lambda \in (-\infty, -0.378] \cup [-0.348, 0.595] \cup [0.918, 1.293]$ for the equations in (4.1). It is obvious that $\begin{pmatrix} c_1 \\ c_2 \end{pmatrix}$ is an eigenvector of (4.2) and it is known as a Floquet eigenvector. Thus the eigenvector $\begin{pmatrix} c_1 \\ c_2 \end{pmatrix}$ gives us the value of $\begin{pmatrix} c_1 \\ c_2 \end{pmatrix} = \begin{pmatrix} z(16\pi) \\ z'(16\pi) \end{pmatrix}$. These values define the boundary conditions on the right end of the interval $x \epsilon [0,\ 16\pi]$. We next turn our attention to the problem in $[0, 16\pi]$ with this initial condition at 16π and $\epsilon \neq 0$. We calculate $z(x)$ and $z'(x)$ in this interval as a function of λ, varying λ until the boundary condition is satisfied.

Results

The following are the eigenvalues found by satisfying $z\cos\alpha + z'\sin\alpha = 0$. ($\epsilon = -40$ and $\alpha = \frac{\pi}{8}$)

$-z_1'' + (\sin x + \frac{\epsilon}{1+x^2})z_1 = \lambda z_1$	$-z_2'' + (\cos x + \frac{\epsilon}{1+x^2})z_2 = \lambda z_2$
0.33532	0.01912
0.53651	0.38025
0.58302	0.52787
	0.57924

Table 4.1: The eigenvalues of the equations for z_1 and z_2

a comparison can be made with [1].

4.2 The Hamiltonian system

Our main result in this section will be formulated via a Hamiltonian System. For illustrative purposes we now recast problem (4.1) as a Hamiltonian System.

The equations in table 4.1 may be rewritten as the following system;

$$-\begin{pmatrix} z_1'' \\ z_2'' \end{pmatrix} + \begin{pmatrix} \sin x + \frac{\epsilon}{1+x^2} & 0 \\ 0 & \cos x + \frac{\epsilon}{1+x^2} \end{pmatrix} \begin{pmatrix} z_1 \\ z_2 \end{pmatrix} = \lambda \begin{pmatrix} z_1 \\ z_2 \end{pmatrix}. \quad (4.3)$$

The following transformation rotates the non-perturbed system ($\epsilon = 0$) by $\frac{\pi}{4}$

$$\begin{pmatrix} z_1 \\ z_2 \end{pmatrix} = \begin{pmatrix} \frac{1}{\sqrt{2}} & \frac{1}{\sqrt{2}} \\ \frac{1}{\sqrt{2}} & -\frac{1}{\sqrt{2}} \end{pmatrix} \begin{pmatrix} y_1 \\ y_2 \end{pmatrix}. \quad (4.4)$$

With this rotation we obtain

$$-\begin{pmatrix} y_1'' \\ y_2'' \end{pmatrix} + \begin{pmatrix} \frac{1}{\sqrt{2}} & \frac{1}{\sqrt{2}} \\ \frac{1}{\sqrt{2}} & -\frac{1}{\sqrt{2}} \end{pmatrix} \begin{pmatrix} \sin x + \frac{\epsilon}{1+x^2} & 0 \\ 0 & \cos x + \frac{\epsilon}{1+x^2} \end{pmatrix}$$

$$\begin{pmatrix} \frac{1}{\sqrt{2}} & \frac{1}{\sqrt{2}} \\ \frac{1}{\sqrt{2}} & -\frac{1}{\sqrt{2}} \end{pmatrix} \begin{pmatrix} y_1 \\ y_2 \end{pmatrix} = \lambda \begin{pmatrix} y_1 \\ y_2 \end{pmatrix}$$

which is better rewritten as

$$-\begin{pmatrix} y_1'' \\ y_2'' \end{pmatrix}+\frac{1}{2}\begin{pmatrix} \sin x+\cos x+\frac{\epsilon}{1+x^2} & \sin x-\cos x \\ \sin x-\cos x & \sin x+\cos x+\frac{\epsilon}{1+x^2} \end{pmatrix}\begin{pmatrix} y_1 \\ y_2 \end{pmatrix}=\lambda\begin{pmatrix} y_1 \\ y_2 \end{pmatrix}. \tag{4.5}$$

We find that (4.5) has the same essential spectrum as the two Sturm-Louiville systems in (4.3). The system in (4.5) may be rewritten in Hamiltonian form

$$JY'=(A+\lambda B)Y \tag{4.6}$$

where J is a symplectic matrix with property that $JJ^T=I$ and has the form

$$J=\begin{pmatrix} 0 & 0 & 1 & 0 \\ 0 & 0 & 0 & 1 \\ -1 & 0 & 0 & 0 \\ 0 & -1 & 0 & 0 \end{pmatrix}$$

A and B are the following real square matrices

$$A=\begin{pmatrix} \frac{1}{2}\left(\sin x+\cos x+\frac{\epsilon}{1+x^2}\right) & \frac{1}{2}\left(\sin x-\cos x\right) & 0 & 0 \\ \frac{1}{2}\left(\sin x-\cos x\right) & \frac{1}{2}\left(\sin x+\cos x+\frac{\epsilon}{1+x^2}\right) & 0 & 0 \\ 0 & 0 & -1 & 0 \\ 0 & 0 & 0 & -1 \end{pmatrix}$$

and

$$B = \begin{pmatrix} -1 & 0 & 0 & 0 \\ 0 & -1 & 0 & 0 \\ 0 & 0 & 0 & 0 \\ 0 & 0 & 0 & 0 \end{pmatrix}.$$

In order to solve this system we proceed in the same way as for solving (4.1), except in this case the initial conditions at $x = 16\pi$ are e_1, e_2, e_3 and e_4 (the usual 4×1 unit vectors). We thus set $\begin{pmatrix} y_1(16\pi) \\ y_2(16\pi) \\ y_3(16\pi) \\ y_4(16\pi) \end{pmatrix} = \begin{pmatrix} c_1 \\ c_2 \\ c_3 \\ c_4 \end{pmatrix}$. From the Hamiltonian system we have $y_1' = y_3$ and $y_2' = y_4$ and we let

$$\begin{pmatrix} y_1(x) \\ y_2(x) \\ y_3(x) \\ y_4(x) \end{pmatrix} = \begin{pmatrix} s_1(x) & t_1(x) & p_1(x) & q_1(x) \\ s_2(x) & t_2(x) & p_2(x) & q_2(x) \\ s_3(x) & t_3(x) & p_3(x) & q_3(x) \\ s_4(x) & t_4(x) & p_4(x) & q_4(x) \end{pmatrix} \begin{pmatrix} c_1 \\ c_2 \\ c_3 \\ c_4 \end{pmatrix}$$

where we set $s_1(16\pi) = 1$, $t_2(16\pi) = 1$, $p_3(16\pi) = 1$ and $q_4(16\pi) = 1$ with

the rest being equal to zero. From Floquet's theory this leads to

$$\begin{pmatrix} s_1(18\pi) & t_1(18\pi) & p_1(18\pi) & q_1(18\pi) \\ s_2(18\pi) & t_2(18\pi) & p_2(18\pi) & q_2(18\pi) \\ s_3(18\pi) & t_3(18\pi) & p_3(18\pi) & q_3(18\pi) \\ s_4(18\pi) & t_4(18\pi) & p_4(18\pi) & q_4(18\pi) \end{pmatrix} \begin{pmatrix} c_1 \\ c_2 \\ c_3 \\ c_4 \end{pmatrix} = \rho \begin{pmatrix} c_1 \\ c_2 \\ c_3 \\ c_4 \end{pmatrix} \tag{4.7}$$

where ρ is the Floquet multiplier and as in (4.1), it corresponds to λ being in a gap or in the essential spectrum depending on whether $\rho \in \Re$ or not. For a value of λ in a spectral gap we find both Floquet multipliers, whose absolute value are less than 1, and also the eigenvectors associated with these Floquet multipliers. These are associated with the decaying solution of our system and give boundary conditions at the point $x = 16\pi$ to the right of which the perturbation $\epsilon = 0$. These two eigenvectors generate the solution in $L^2[16\pi, \infty)$. Let these two L^2 eigenvectors be $\mathbf{u} = \begin{pmatrix} u_1 \\ u_2 \\ u_3 \\ u_4 \end{pmatrix}$ and

$\mathbf{v} = \begin{pmatrix} v_1 \\ v_2 \\ v_3 \\ v_4 \end{pmatrix}$. Thus we may write

$$\begin{pmatrix} y_1(x) \\ y_2(x) \\ y_3(x) \\ y_4(x) \end{pmatrix} = \begin{pmatrix} u_1(x) & v_1(x) \\ u_2(x) & v_2(x) \\ u_3(x) & v_3(x) \\ u_4(x) & v_4(x) \end{pmatrix} \begin{pmatrix} d_1 \\ d_2 \end{pmatrix} \tag{4.8}$$

here d_1 and d_2 are constants to be determined. We have the following boundary condition associated with our problem

$$z_i \cos \alpha_i + z_i^{'} \sin \alpha_i = 0$$

for $i \in \{1, 2\}$ and this suggests that we need to integrate (4.8) from $x = 16\pi$ to $x = 0$. Having found the L^2 Floquet eigenvectors of (4.7) we have the following boundary condition at $x = 16\pi$

$$\begin{pmatrix} y_1(16\pi) \\ y_2(16\pi) \\ y_3(16\pi) \\ y_4(16\pi) \end{pmatrix} = \begin{pmatrix} u_1(16\pi) & v_1(16\pi) \\ u_2(16\pi) & v_2(16\pi) \\ u_3(16\pi) & v_3(16\pi) \\ u_4(16\pi) & v_4(16\pi) \end{pmatrix} \begin{pmatrix} d_1 \\ d_2 \end{pmatrix}$$

together with (4.6) we may shoot back to $x = 0$ and obtain the solution vectors $\mathbf{u}(0)$ and $\mathbf{v}(0)$ with this solution at $x = 0$, from (4.4) and $z_i \cos\alpha_i + z_i' \sin\alpha_i = 0$ for $i = \{1, 2\}$. We obtain;

$$\frac{1}{2}\begin{pmatrix} \cos\alpha_1 & \cos\alpha_1 & \sin\alpha_1 & \sin\alpha_1 \\ \cos\alpha_2 & -\cos\alpha_2 & \sin\alpha_2 & -\sin\alpha_2 \end{pmatrix} \begin{pmatrix} u_1(0) & v_1(0) \\ u_2(0) & v_2(0) \\ u_3(0) & v_3(0) \\ u_4(0) & v_4(0) \end{pmatrix} \begin{pmatrix} d_1 \\ d_2 \end{pmatrix} = \begin{pmatrix} 0 \\ 0 \end{pmatrix}. \tag{4.9}$$

Since d_1 and d_2 are not zero the determinant of the matrix obtained by multiplying the two matrices on the left in (4.9) must be zero or

$$\det\left[\begin{pmatrix} \cos\alpha_1 & \cos\alpha_1 & \sin\alpha_1 & \sin\alpha_1 \\ \cos\alpha_1 & -\cos\alpha_1 & \sin\alpha_1 & -\sin\alpha_1 \end{pmatrix} \begin{pmatrix} u_1(x) & v_1(x) \\ u_2(x) & v_2(x) \\ u_3(x) & v_3(x) \\ u_4(x) & v_4(x) \end{pmatrix}\right] = 0. \tag{4.10}$$

All that is now required is to use some iterative scheme in order to find values of λ which satisfy (4.10). There is one more obstacle to overcome before we can solve this problem which is a consequence of the fact that the functions y_1, y_2, y_3 and y_4 are continuous however this does not mean that the eigenvectors $\mathbf{u}$ and $\mathbf{v}$ are continuous since the coefficients d_1 and d_2 can be discontinuous in such a way that the functions y_1, y_2, y_3 and y_4 remain continuous across the interval $x \in [0, 16\pi]$. This is what was found in

practise by our numerical experiment. It was found that d_1 and d_2 fluctuated suddenly between 1 or -1 with every increment of λ when we incremented λ over an interval which coincided with a spectral gap. Thus the determinant in (4.10) fluctuated between multiples of $+1$ and -1 of its absolute value. Thus the more values of λ along the interval that the determinant in (4.10) was calculated, the more often the determinant went from positive to negative giving an enormous number of incorrect eigenvalues amongst the correct ones.

In order to avoid this problem we make the transformation $R = V + iU$ where

$$U = \begin{pmatrix} u_1 & v_1 \\ u_2 & v_2 \end{pmatrix} \quad \text{and} \quad V = \begin{pmatrix} u_3 & v_3 \\ u_4 & v_4 \end{pmatrix}. \tag{4.11}$$

We may rewrite the equation for R as $I = VR^{-1} + iUR^{-1}$ and let $W = UR^{-1}$ where R is always invertible since either U or V or both U and V must be invertible. We then differentiate W to obtain the differential equation

$$W' = U'R^{-1} + U(R^{-1})'.$$

$(R^{-1})'$ can be replaced by $(R^{-1})' = -R^{-1}R'R^{-1}$ and thus we have

$$W' = U'R^{-1} - UR^{-1}R'R^{-1} \text{ or } W' = U'R^{-1} - WR'R^{-1}.$$

The initial matrix problem (4.6) with the solutions **U** and **V** can be

rewritten in the form

$$\begin{pmatrix} 0 & -I \\ I & 0 \end{pmatrix} \begin{pmatrix} U \\ V \end{pmatrix}' = \begin{pmatrix} \lambda I - Q & 0 \\ 0 & I \end{pmatrix} \begin{pmatrix} U \\ V \end{pmatrix}$$

where

$$Q = \begin{pmatrix} \frac{1}{2}(\sin x + \cos x) + \frac{\epsilon}{1+x^2} & \frac{1}{2}(\sin x - \cos x) \\ \frac{1}{2}(\sin x - \cos x) & \frac{1}{2}(\sin x + \cos x) + \frac{\epsilon}{1+x^2} \end{pmatrix}.$$

So with $V' = (Q - \lambda I)U$ and $U' = V$ we have $R' = (Q - \lambda I)U + iV$. Thus we obtain the following:

$$W' = VR^{-1} - W((Q - \lambda I)U + iV)R^{-1}.$$

Since $UR^{-1} = W$ and $VR^{-1} = I - iUR^{-1} = I - iW$ we finally obtain

$$W' - (\lambda - 1)W^2 + 2iW + WQW = I. \tag{4.12}$$

If we write $W = \begin{pmatrix} w_1 & w_3 \\ w_2 & w_4 \end{pmatrix}$ then we may write the matrix equation in (4.12) as the following four ordinary differential equations

$$w_1' - (\lambda - 1)(w_1^2 + w_2 w_3) + 2iw_1 + \frac{w_1^2}{2}(\sin x + \cos x) + \frac{w_1^2 \epsilon}{1 + x^2} + \frac{w_1 w_2}{2}(\sin x - \cos x)$$

$$+\frac{w_1w_3}{2}(\sin x-\cos x)+\frac{w_2w_3}{2}(\sin x+\cos x)+\frac{w_2w_3\epsilon}{1+x^2}=1;$$

$$w_2'-(\lambda-1)w_2(w_1+w_4)+2iw_2+\frac{w_1w_2}{2}(\sin x+\cos x)+\frac{w_1w_2\epsilon}{1+x^2}+\frac{w_2^2}{2}(\sin x-\cos x)$$
$$+\frac{w_1w_4}{2}(\sin x-\cos x)+\frac{w_2w_4}{2}(\sin x+\cos x)+\frac{w_2w_4\epsilon}{1+x^2}=0;$$

$$w_3'-(\lambda-1)w_3(w_1+w_4)+2iw_3+\frac{w_1w_3}{2}(\sin x+\cos x)+\frac{w_1w_3\epsilon}{1+x^2}+\frac{w_2^2}{2}(\sin x-\cos x)$$
$$+\frac{w_1w_4}{2}(\sin x-\cos x)+\frac{w_3^2}{2}(\sin x+\cos x)+\frac{w_3w_4\epsilon}{1+x^2}=0;$$

$$w_4'-(\lambda-1)(w_2w_3+w_4^2)+2iw_4+\frac{w_2w_3}{2}(\sin x+\cos x)+\frac{w_2w_3\epsilon}{1+x^2}+\frac{w_2w_4}{2}(\sin x-\cos x)$$
$$+\frac{w_3w_4}{2}(\sin x-\cos x)+\frac{w_4^2}{2}(\sin x+\cos x)+\frac{w_4^2\epsilon}{1+x^2}=1;$$

which are solved in MATLAB. We know the initial solution of all these equations at the right hand side of the interval (in our example at 16π) so we numerically solve the equation back to the origin for a chosen λ and look for a change in sign in the determinant, of this matrix in (4.9). That is, we seek the determinant of

$$D(W(\lambda))=\left|\begin{pmatrix}\frac{1}{\sqrt{2}}\cos\alpha_1 & \frac{1}{\sqrt{2}}\cos\alpha_1 & \frac{1}{\sqrt{2}}\sin\alpha_1 & \frac{1}{\sqrt{2}}\sin\alpha_1\\ \frac{1}{\sqrt{2}}\cos\alpha_2 & -\frac{1}{\sqrt{2}}\cos\alpha_2 & \frac{1}{\sqrt{2}}\sin\alpha_2 & -\frac{1}{\sqrt{2}}\sin\alpha_2\end{pmatrix}\begin{pmatrix}W\\ I-iW\end{pmatrix}\right|. \tag{4.13}$$

When a change occurs in the sign of both the real part and the imaginary part of the determinant in (4.13) then we have an eigenvalue of (4.3) with boundary condition $z_i\cos\alpha_i+z_i'\sin\alpha_i=0$ for $i=\{1,2\}$.

Results

Tables 4.3 and 4.2 contain some of the eigenvalues of (4.3) with $\epsilon = -40$ and the following boundary conditions; $z_1 \cos\alpha_1 + z_1' \sin\alpha_1 = 0$ and $z_2 \cos\alpha_2 + z_2' \sin\alpha_2 = 0$ where we have taken α_1 and α_2 to be $\frac{\pi}{8}$. In Table 4.2, the perturbation $\frac{\epsilon}{1+x^2}$ is non zero on the interval $x \in [0, 4\pi]$ and $\epsilon = 0$ for $x > 4\pi$.

$\Re(D(W(\lambda))) = 0$	$\Im(D(W(\lambda))) = 0$
-0.23217	-0.02362
0.02019	0.02019
0.09593	0.24645
0.37774	0.37774
0.39316	-
0.39831	0.39835
0.48884	0.41242

Table 4.2: Zeros of the real and imaginary parts of D(W(λ))

As can be seen the eigenvalues are 0.02019, 0.3777 and 0.3983 by reading off values of λ where $\Re(W(\lambda))$ and $\Im(W(\lambda))$ are simultaneously zero.

Below we have exactly the same example, except that the perturbation $\frac{\epsilon}{1+x^2}$ is non zero over the interval $x \in [0, 35\pi]$ and is zero for $x > 35\pi$.

In this case the eigenvalues are 0.0191, 0.3353, 0.3803, 0.5279, 0.5366, 0.5780, 0.5808, 0.5909, 0.5917 and 0.5918. As can be seen the perturbation induces eigenvalues in the gap $\lambda \in [-0.347, 0.594]$ and also increasing the range of the perturbation from $[0, 4\pi]$ to $[0, 35\pi]$ increases the number of these induced eigenvalues. Comparing these results with the work in [29] we see that there is a qualitative agreement in that the eigenvalues seem to

$\Re(D(W(\lambda))) = 0$	$\Im(D(W(\lambda))) = 0$	$\Re(D(W(\lambda))) = 0$	$\Im(D(W(\lambda))) = 0$
-0.23260	-0.02464	0.54517	0.57478
0.01912	0.01912	0.57796	0.57796
0.09367	0.23660	0.5803	-
0.33532	0.33532	0.58081	0.58080
0.34812	0.36905	0.58126	0.58175
0.38025	0.38025	0.59006	-
0.45102	0.51148	0.59085	0.59085
0.52787	0.52787	0.59147	-
0.53656	0.53650	0.59176	0.59170
0.53744	0.53917	0.59183	0.59196

Table 4.3: Zeros of the real and imaginary parts of D(W(λ))

accumulate towards the end of the gap. When ϵ is above some critical value we get an accumulation according to [29, theorem 3] which is what we see happening towards the right side of the gap. It can be seen that when we increase the range of the perturbation more eigenvalues are induced in the gap. Also most of the accumulation of eigenvalues is so close to the edge of the gap that we can only find a small number of eigenvalues numerically. These results agree quantitatively with [29, theorem 3] which in our case for accumulation at the right hand end of the gap, approximates the number of eigenvalues between any two points within the gap in terms of the distance between the second point to the right of the first and the edge of the gap.

We are now ready to apply these methods to obtain (5.17) which will allow us to obtain the eigenvalues of the problem in Fig 1.1, which have not been previously obtained.

Chapter 5

A PDE with band-gap spectral structure in a perturbed periodic waveguide

This chapter considers the numerical calculation of eigenfunctions for the Schrödinger operator in a domain with a regular cylindrical end, in which the potential appearing in the Schrödinger equation is periodic with respect to the axial variable measured along the cylinder. For definiteness we consider the configuration shown in Fig 5.1;

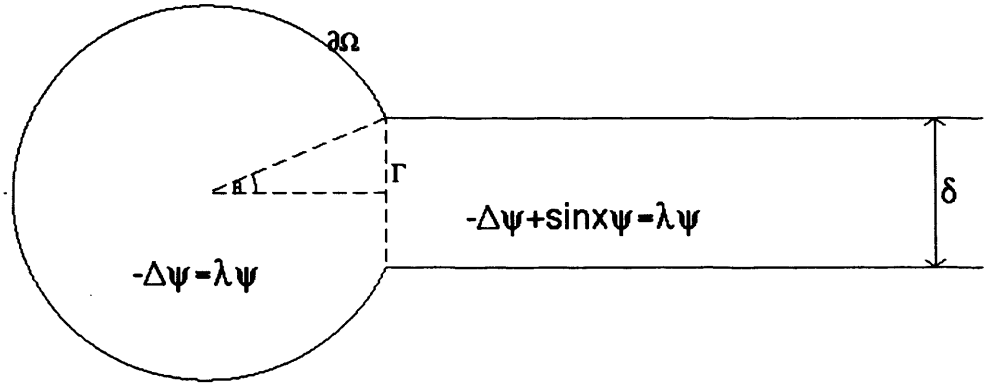

Figure 5.1: A domain with a regular cylindrical end in $\mathbb{R}^2$

in which a strip of width $\delta = 2\sin\theta$ is attached to the side of a disc of radius 1. In the composite domain[1], which we denote by Ω, we look for those λ for which the equation

$$-\Delta\psi + V(x,y)\psi = \lambda\psi \tag{5.1}$$

has a nontrivial solution satisfying the condition

$$\psi \in L^2(\Omega),$$

[1]This domain is also known as the frying pan model from its geometry

together with homogeneous boundary conditions on $\partial\Omega$

$$a(\cdot)\psi + b(\cdot)\frac{\partial\psi}{\partial n} = 0. \tag{5.2}$$

The functions a and b are assumed to be constant on the walls $|y| = \delta/2$ of the strip, at least for all sufficiently large x. The potential V is assumed to be 2π-periodic with respect to its first argument, at least for all sufficiently large x:

$$V(x + 2\pi, y) = V(x, y), \quad x \geq x_0, \ \ |y| < \delta/2 \tag{5.3}$$

where x_o is the x coordinate of Γ. In order to avoid technical complications we assume that V is continuous on $\overline{\Omega}$. The method used to solve the problem is a classical domain decomposition technique. The problem is reduced to a problem on a finite domain by cutting the attached strip at some point $x = x_1 > x_0$ (see Fig 5.1). We define the sub-domains

$$\Omega_0 = \Omega \bigcap \{(x, y) \,|\, x \leq x_1\},$$

$$\Omega_1 = \Omega \bigcap \{(x, y) \,|\, x > x_1\},$$

and the artificial boundary

$$\Gamma = \{(x_0, y) \,|\, |y| \leq \delta/2\}.$$

On Γ we introduce the Dirichlet to Neumann maps $\Lambda_0(\lambda)$ and $\Lambda_1(\lambda)$ as fol-

lows. Suppose that $f \in H^{3/2}(\Gamma)$. Let u be a solution of the boundary value problem consisting of the PDE (5.1) in Ω_0, the boundary condition (5.2) on $\partial\Omega_0 \setminus \Gamma$, and the boundary condition

$$u|_\Gamma = f \tag{5.4}$$

on Γ. Such a solution is guaranteed to exist uniquely for all but countably many values of λ, these being the eigenvalues of the problem in $L_2(\Omega_0)$ obtained by replacing (5.4) by the Dirichlet condition $u|_\Gamma = 0$. The map

$$u|_\Gamma \mapsto \left.\frac{\partial u}{\partial n}\right|_\Gamma$$

is the map which we denote by $\Lambda_0(\lambda)$. It is a linear map from $H^{3/2}(\Gamma)$ to $H^{1/2}(\Gamma)$. Correspondingly, if we can uniquely solve (5.1) in the infinite domain Ω_1 with the boundary condition (5.2) on $\partial\Omega_1 \setminus \Gamma$ and the condition (5.4) on Γ, then we can define a second map from $H^{3/2}(\Gamma)$ to $H^{1/2}(\Gamma)$, which is the map which we denote by $\Lambda_1(\lambda)$. Suppose (5.1), (5.2) has a nontrivial solution $\psi \in L_2(\Omega)$. Generically we may expect that

$$f := \psi|_\Gamma \neq 0.$$

(If not, we can always move Γ slightly to the right). This ψ then solves both

the inner and outer boundary value problems for this choice of f and hence

$$\Lambda_0(\lambda)f = -\Lambda_1(\lambda)f, \tag{5.5}$$

the minus sign being due to the change in the direction of the outward unit normal on Γ between Ω_0 and Ω_1. This means we can characterise eigenvalues as those λ for which

$$\ker(\Lambda_0(\lambda) + \Lambda_1(\lambda)) \neq \{0\}.$$

In this way the problem can be reduced to the interface Γ provided we can calculate Λ_0 and Λ_1. In fact, in this thesis, we take the slightly different but equivalent approach of solving the PDE (5.1) on the domain Ω_0 with the boundary condition (5.2) on $\partial\Omega_0 \setminus \Gamma$ and the λ-dependent boundary condition

$$\left.\frac{\partial\psi}{\partial n}\right|_\Gamma = -\Lambda_1(\lambda)\psi|_\Gamma \tag{5.6}$$

on the interface Γ. The main new contribution in this thesis is the algorithm for the calculation of the Dirichlet to Neumann map $\Lambda_1(\lambda)$ in the presence of the periodic potential V. In the remainder of this chapter, sections (5.2) to (5.5) are devoted to a description of our numerical algorithm and the necessary mathematical background for its development. Section (5.6) uses the algorithm to study some spectral properties of some periodic waveguide problems. For instance, we study the effect that the width of the tube has on the eigenvalue; we derive a theoretical expression for the rate of change

of the eigenvalue with respect to tube width and compare the results which this yields with those obtained from direct numerical calculation. Finally, we trace the evolution of an eigenvalue which lies in a spectral gap, but which becomes an embedded eigenvalue (embedded trapped mode) when the tube width becomes sufficiently small. We believe this may be the first time that it has been possible to observe, numerically, the evolution of a trapped mode from a spectral gap into a spectral band and out again.

Consider for definiteness the case with Dirichlet boundary conditions

$$\psi(x, \pm\delta/2) = 0, \quad x \geq x_0.$$

For each fixed x we represent the solution ψ using a Fourier series

$$\psi(x, y) = \sum_{n=1}^{\infty} \phi_n(x) \sin\left(\frac{n\pi}{\delta}\left(y + \frac{\delta}{2}\right)\right). \tag{5.7}$$

We have two main objectives:

1. To determine the infinite coupled system of differential equations which must be satisfied by the functions $\phi_n(\cdot)$ in order that the PDE be satisfied;

2. To determine an appropriate representation for the Dirichlet to Neumann map $\Lambda_1(\lambda)$ when the boundary datum f appearing in (5.4) has a corresponding Fourier expansion.

In fact, **2** is rather simple. If we suppose that

$$\psi(x_1, y) = f(y) = \sum_{n=1}^{\infty} \phi_{n,0} \sin\left(\frac{n\pi}{\delta}\left(y + \frac{\delta}{2}\right)\right),$$

then we shall evidently need to have the initial conditions

$$\phi_n(x_1) = \phi_{n,0}.$$

The Dirichlet to Neumann map $\Lambda_1(\lambda)$ will map f to the function g defined by

$$g(y) = -\psi_x(x_1, y) = -\sum_{n=1}^{\infty} \phi_n'(x_1) \sin\left(\frac{n\pi}{\delta}\left(y + \frac{\delta}{2}\right)\right).$$

We now proceed to derive the system of differential equations satisfied by $\phi_n(\cdot)$.

5.1 A circular domain with Dirichlet boundary conditions

Here we consider the simplest version of the non-perturbed problem, since we can solve it analytically and see what effect the perturbation will have on the eigenvalues of the original problem.

The problem is posed on a disc of radius 1 called Ω with boundary $\partial\Omega$ with the following equation

$$-\Delta\psi = \lambda\psi \tag{5.8}$$

on Ω and boundary condition $\psi|_{\partial\Omega} = 0$. We remind the reader that Δ takes the form

$$\Delta = \frac{1}{r}\frac{\partial}{\partial r}\left(r\frac{\partial}{\partial r}\right) + \frac{1}{r^2}\frac{\partial^2}{\partial\theta^2}$$

in polar coordinates. Then by separation of variables $\psi(r,\theta) = R(r)\Theta(\theta)$ we obtain

$$-\left[\frac{1}{rR}\frac{\partial}{\partial r}\left(r\frac{\partial R}{\partial r}\right) + \frac{1}{r^2\Theta}\frac{\partial^2\Theta}{\partial\theta^2}\right] = \lambda$$

and after choosing $\Theta(\theta) = \cos n\theta$ or $\Theta(\theta) = \sin n\theta$ we thus obtain the following well known equation

$$-\frac{1}{r}\frac{\partial}{\partial r}\left(r\frac{\partial R}{\partial r}\right) + \frac{n^2}{r^2}R = \lambda R.$$

This is Bessel's equation and the solutions are of the form $R(r) = J_n(\sqrt{\lambda}r)$ where n is the order of the Bessel function. The boundary condition $\psi(1,\theta)|_{\partial\Omega} = 0$ translates into

$$0 = J_n(\sqrt{\lambda}).$$

This means that the eigenvalues λ are the zeros squared of different order Bessel functions. The eigenfunctions are

$$J_n(\sqrt{\lambda}r)\{\sin n\theta, \cos n\theta\}$$

and it can be seen that eigenvalues not associated with zero order Bessel functions are doubly degenerate. Table 5.1gives eigenvalues associated with

(5.8) which we enumerate in increasing order.

n	λ	n	λ	n	λ
0	5.783186	0	30.47126	4	57.58294
1	14.68197	3	40.70647	2	70.85000
2	26.37462	1	49.21846	0	74.88701

Table 5.1: Eigenvalues in increasing order for the Laplacian of a circular domain of radius 1

5.2 The modified circular domain

The domain left of Γ in Fig 5.1, which we call the modified circular domain, is defined by

$$(x,y) = \{x \in [-1-\cos\theta, 0], y \in [-\sqrt{1-(x+\cos\theta)^2}, \sqrt{1-(x+\cos\theta)^2}]\}$$

or $(x,y) \in \Omega_0 \backslash ([0,2\pi] \times [-\frac{\delta}{2}, \frac{\delta}{2}])$. In this domain we apply the finite difference method to the discretised Laplacian. We will have to design a finite difference mesh in the modified part of the circular domain to fit the geometry and also to meet other requirements such as preserving accuracy. The corners in Fig 5.1 which are located where Γ and $\partial\Omega_0$ meet can lead to inaccuracies depending on how we apply the finite differences method in the domain. It is known that the use of geometric meshing minimises the error in this case.

There are numerous examples of such meshes, in [16] for instance Kuznetsov, Lipnikov and Shashkov claim to achieve the same accuracy with a geometric

mesh as with a uniformly refined grid with four times as many points. In [15] Kadalbajoo and Kumar use geometric mesh refinement to solve a singularly perturbed second order self-adjoint boundary value problem. In [13] Gilbert, Miller and Teng use the geometric partitioning algorithm to define mesh point positions and provide MATLAB code for doing this.

For our domain a geometric mesh involves placing more points near the corners as in Fig 5.6. In Fig 5.2 we have an example of a point with its four neighbouring points on the unevenly spaced mesh.

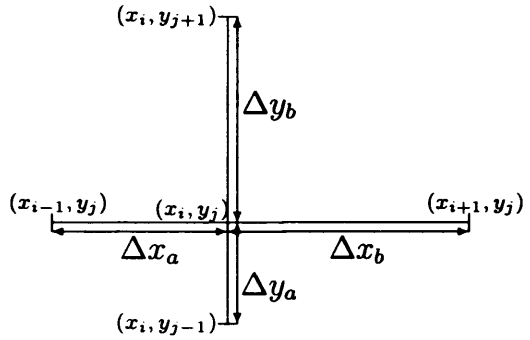

Figure 5.2: A section of mesh with the node in the middle unevenly separated from its four neighbouring nodes

If we discretise $\Delta\psi + \lambda\psi = 0$ based on the five nodes in Fig 5.2, then we obtain the corresponding five point discretised Laplacian

$$\frac{2}{\Delta x_b(\Delta x_a + \Delta x_b)}\psi(x_{i+1}, y_j) + \frac{2}{\Delta x_a(\Delta x_a + \Delta x_b)}\psi(x_{i-1}, y_j) +$$

$$\frac{2}{\Delta y_b(\Delta y_a + \Delta y_b))}\psi(x_i, y_{j+1}) + \frac{2}{\Delta y_a(\Delta y_a + \Delta y_b)}\psi(x_i, y_{j-1}) \tag{5.9}$$

$$-2\left(\frac{1}{\Delta x_a \Delta x_b} + \frac{1}{\Delta y_a \Delta y_b}\right)\psi(x_i, y_j) + \lambda\psi(x_i, y_j) = 0.$$

We now move on to discuss the construction of this mesh. In order to fully describe the domain we give the x and y coordinates for various mesh nodes in the domain in Fig 5.1. The interface Γ where the tube and the modified circular domain meet is located at $(0, y)$ where $y \in [-\frac{\delta}{2}, \frac{\delta}{2}]$ and $\delta =: 2\sin\theta$.

We now describe the algorithm for partitioning Γ. We begin by placing n evenly spaced nodes across Γ not including the corners and bisect the first and last interval. This means that the first two and last two intervals have width $\frac{\delta}{2(n+1)}$ while the remaining intervals each have a width of $\frac{\delta}{n+1}$. This is considered to be one iteration of the algorithm for dividing up Γ. Iterating again we cut every interval in two and again bisect the first and last intervals. This gives us a width of $\frac{\delta}{8(n+1)}$ for the first two and last two intervals, $\frac{\delta}{4(n+1)}$ for the third, fourth, fifth, third to last, fourth to last and fifth to last intervals. The remainder of the intervals each have a width of $\frac{\delta}{2(n+1)}$. Let p be the number of iterations of this algorithm and N the number of nodes on the interval, then

$$N = 2^{p-1}n + 2^{p+1} + 2^{p-1} - 3.$$

The points in Fig 5.3 have been labelled from 1 to 7 and 1 to 13 respectively and have been spaced using the algorithm just outlined above with two and three iterations respectively.

From these points we may draw lines extending to the left of Γ (parallel to the x axis) as in Fig 5.5 to the boundary of the domain on the left.

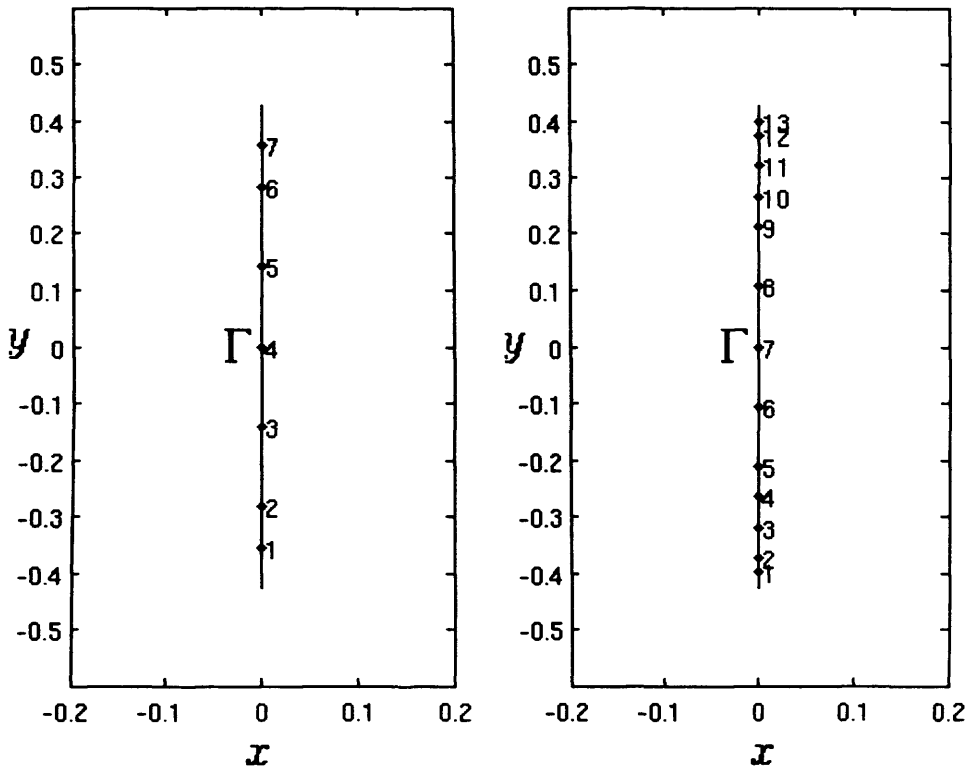

Figure 5.3: The interface Γ showing the location of points for $n = 5$ with $p = 1$ on the left and $n = 3$ with $p = 2$ on the right

These lines will determine the y coordinates of the nodes in the part of the domain where $(x, y) \in \Omega_0 \cap ([-1 - \cos\theta, 0] \times [-\frac{\delta}{2}, \frac{\delta}{2}])$. The x coordinates will be positioned in the same way as the nodes on Γ, that is, distributed geometrically in x for $x \in [-2\cos\theta, 0]$ as has been explained for Γ. We start by placing m evenly spaced nodes not including the edges over the interval $x \in [-2\cos\theta, 0]$ and dividing the first and last interval. We then perform a second iteration where we divide each interval into two and again we chop

the first and last interval in two. If we apply this algorithm p times and let M be the number of nodes across the interval then we obtain

$$M = 2^{p-1}m + 2^{p+1} + 2^{p-1} - 3.$$

The position of these points is illustrated by the vertical lines (parallel to the y axis) in Fig 5.5. The intercept of these vertical lines with the horizontal lines determines the coordinates of the nodes in the mesh as illustrated in Fig 5.6 for the points in $(x, y) \in ([-2\cos\theta, 0] \times [-\frac{\delta}{2}, \frac{\delta}{2}])$. As can be seen in Fig 5.5 we draw vertical and horizontal lines joining the intercepts of the lines passing through the geometrically spaced points with $\partial\Omega_0$ to locate mesh nodes for $(x, y) \in \Omega_0 \setminus ([-2\cos\theta, 2\pi] \times [-\frac{\delta}{2}, \frac{\delta}{2}])$.

Fig 5.6 shows the intercepts of these lines as mesh points and Fig 5.4 shows the part of the domain in Fig 5.6 for $(x, y) \in \{x \in [-1 - \cos\theta, -2\cos\theta], y \in [-\sqrt{1-(x+\cos\theta)^2}, \sqrt{1-(x+\cos\theta)^2}]\}$.

We introduce a numbering scheme for the node as in Fig 5.4. For any node (x_i, y_j) we number the x coordinate starting at the leftmost nodes. For any column (x_i, y_j) (where a column consists of the set of nodes with the same x coordinate and different y coordinates as in Fig 5.6) we number the y coordinate with the smallest y value; which in our case is from the base of the column. Using this convention and referring to Fig 5.4, we obtain $\psi(x_2, y_2) = \psi_3$, $\psi(x_1, y_1) = \psi_1$, $\psi(x_2, y_1) = \psi_2$, $\psi(x_2, y_3) = \psi_4$ and $\psi(x_3, y_3) = \psi_7$. Referring to Fig 5.4, let Δx_1, Δx_2 and Δx_3 be the x distances between certain

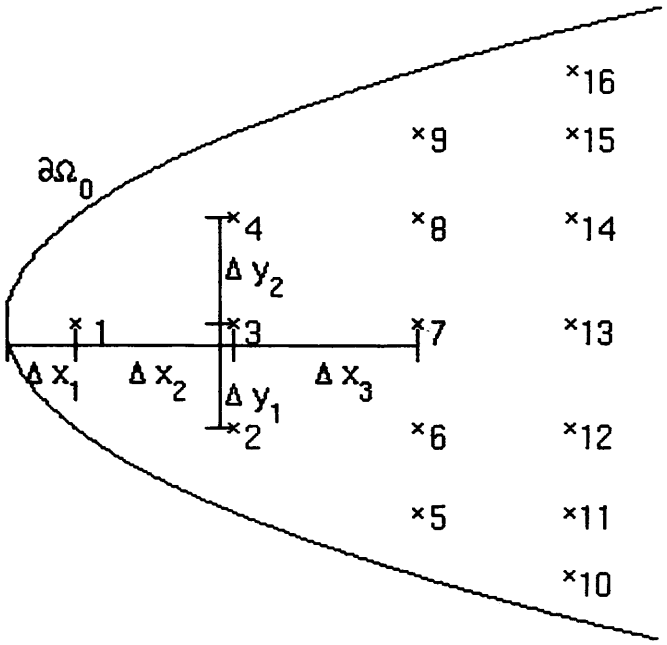

Figure 5.4: A section of the mesh left of $x = -2\cos\theta$

neighbouring nodes, and likewise Δy_1 and Δy_2 be the y distances between certain neighbouring nodes. Note that in this particular case $\Delta y_1 = \Delta y_2$ since the mesh is symmetric about the x axis. In order to illustrate the application of equation (5.9) to our mesh we treat the five nodes in equation (5.9) and in Fig (5.2) as corresponding to the set of nodes labelled 1, 2, 3, 4 and 7 in Fig 5.4. If we apply equation (5.9) to ψ_3 then from Fig 5.4 we obtain

$$\frac{2}{\Delta x_3(\Delta x_2 + \Delta x_3)}\psi_7 + \frac{2}{\Delta x_2(\Delta x_2 + \Delta x_3)}\psi_1 + \frac{2}{\Delta y_1(\Delta y_1 + \Delta y_2)}\psi_2 +$$

$$\frac{2}{\Delta y_2(\Delta y_1+\Delta y_2)}\psi_4-2\left(\frac{1}{\Delta x_2\Delta x_3}+\frac{1}{\Delta y_1\Delta y_2}\right)\psi_3+\lambda\psi_3=0. \qquad (5.10)$$

We will next demonstrate how the Dirichlet boundary conditions are accounted for. Keeping in mind that we have chosen $\psi(x_2,y_2)=\psi_3$ in Fig 5.4 then the Dirichlet boundary condition on $\partial\Omega_0$ is interpreted as $\psi(-1-\cos\theta,0)=0$, $\psi(-\cos\theta-\sqrt{1-\frac{\sin^2\theta}{2^{2(p-2)}(n+1)^2}},\frac{\sin\theta}{2^{p-2}(n+1)})=0$ and $\psi(-\cos\theta-\sqrt{1-\frac{\sin^2\theta}{2^{2(p-2)}(n+1)^2}},-\frac{\sin\theta}{2^{p-2}(n+1)})=0$, where the last two nodes are located above and below $\psi_4=\psi(x_2,y_3)$ and $\psi_2=\psi(x_2,y_1)$ respectively on $\partial\Omega$ and are thus unlabelled. If we treat ψ_1 in Fig 5.4 as "$\psi(x_i,y_j)$" in (5.9) then we obtain

$$\frac{2}{\Delta x_2(\Delta x_1+\Delta x_2)}\psi_3-2\left(\frac{1}{\Delta x_1\Delta x_2}+\frac{1}{\Delta y_1\Delta y_2}\right)\psi_1+\lambda\psi_1=0. \qquad (5.11)$$

More generally for a mesh with parameters M and N then the number of nodes is $\frac{1}{2}M^2+\frac{1}{4}N^2+\frac{1}{2}MN+M+N+\frac{3}{4}$. The mesh in Fig 5.6 has parameters $M=27$ and $N=11$ from $m=5$, $n=2$ and $p=2$ producing a total of 582 nodes. We label the nodes from $1,2,...,582$ and thus $\{\psi_k\}_{k=1}^{582}$. If we apply (5.9) at each node in the mesh of Fig 5.6 like we did for two nodes in (5.10) and (5.11), then we obtain 582 equations. Note that we have not yet dealt with the application of (5.9) at the boundary Γ. Suppose that we wish to apply (5.9) at a point of the boundary Γ, for example $\psi(x_{M+\frac{N}{2}+\frac{3}{2}},y_j)=\psi_{\frac{1}{2}M^2+\frac{1}{4}N^2+\frac{1}{2}MN+M+\frac{3}{4}+j}$ where $j\in\{2,...,N-1\}$. We know that there are no nodes to the right of Γ and thus $\psi(x_{M+\frac{N}{2}+\frac{5}{2}},y_j)$ is known as a fictitious node and will have to be eliminated from (5.9). For the time being we imagine

that we have zero Neumann boundary conditions on Γ which we approximate by $\psi(x_{M+\frac{N}{2}+\frac{5}{2}}, y_{j+1}) = \psi(x_{M+\frac{N}{2}+\frac{1}{2}}, y_j)$ which means that on Γ (5.9) becomes

$$\frac{2}{\Delta x_a^2}\psi(x_{M+\frac{N}{2}+\frac{1}{2}}, y_j) + \frac{2}{\Delta y_b(\Delta y_a + \Delta y_b))}\psi(y_{M+\frac{N}{2}+\frac{3}{2}}, y_{j+1})$$

$$+\frac{2}{\Delta y_a(\Delta y_a + \Delta y_b)}\psi(x_{M+\frac{N}{2}+\frac{3}{2}}, y_{j-1}) - 2\left(\frac{1}{\Delta x_a^1 2} + \frac{1}{\Delta y_a \Delta y_b}\right)\psi(x_{M+\frac{N}{2}+\frac{3}{2}}, y_j)$$

$$+\lambda\psi(x_{M+\frac{N}{2}+\frac{3}{2}}, y_j) = 0$$

where $\Delta x_b = \Delta x_a$ for $x_i \in \Gamma$. Note that if $j = 1$ or $j = N$ then we would have $\psi(x_{M+\frac{N}{2}+\frac{3}{2}}, y_{j-1}) = 0$ or $\psi(x_{M+\frac{N}{2}+\frac{3}{2}}, y_{j+1}) = 0$ respectively.

We let $\mathbf{\Psi} = [\psi_1, \psi_2, ..., \psi_{582}]^T$, then our 582 equations may be rewritten as

$$A\mathbf{\Psi} = \lambda\mathbf{\Psi}. \tag{5.12}$$

The eigenvalues of A are of course the approximate eigenvalues of our simplified problem with zero Neumann boundary conditions on Γ and zero Dirichlet boundary conditions on $\partial(\Omega_0 \setminus ([0, 2\pi] \times [-\frac{\delta}{2}, \frac{\delta}{2}])) \setminus \Gamma$.

In the following section we derive a Dirichlet to Neumann map which when modified allows us to deal with the application of (5.9) to nodes in Fig 5.6 on Γ.

Figure 5.5: Example of a mesh with $m = 5$, $n = 2$ and $p = 2$ with $\delta = 2\sin(0.14\pi)$ illustrating the location of mesh nodes

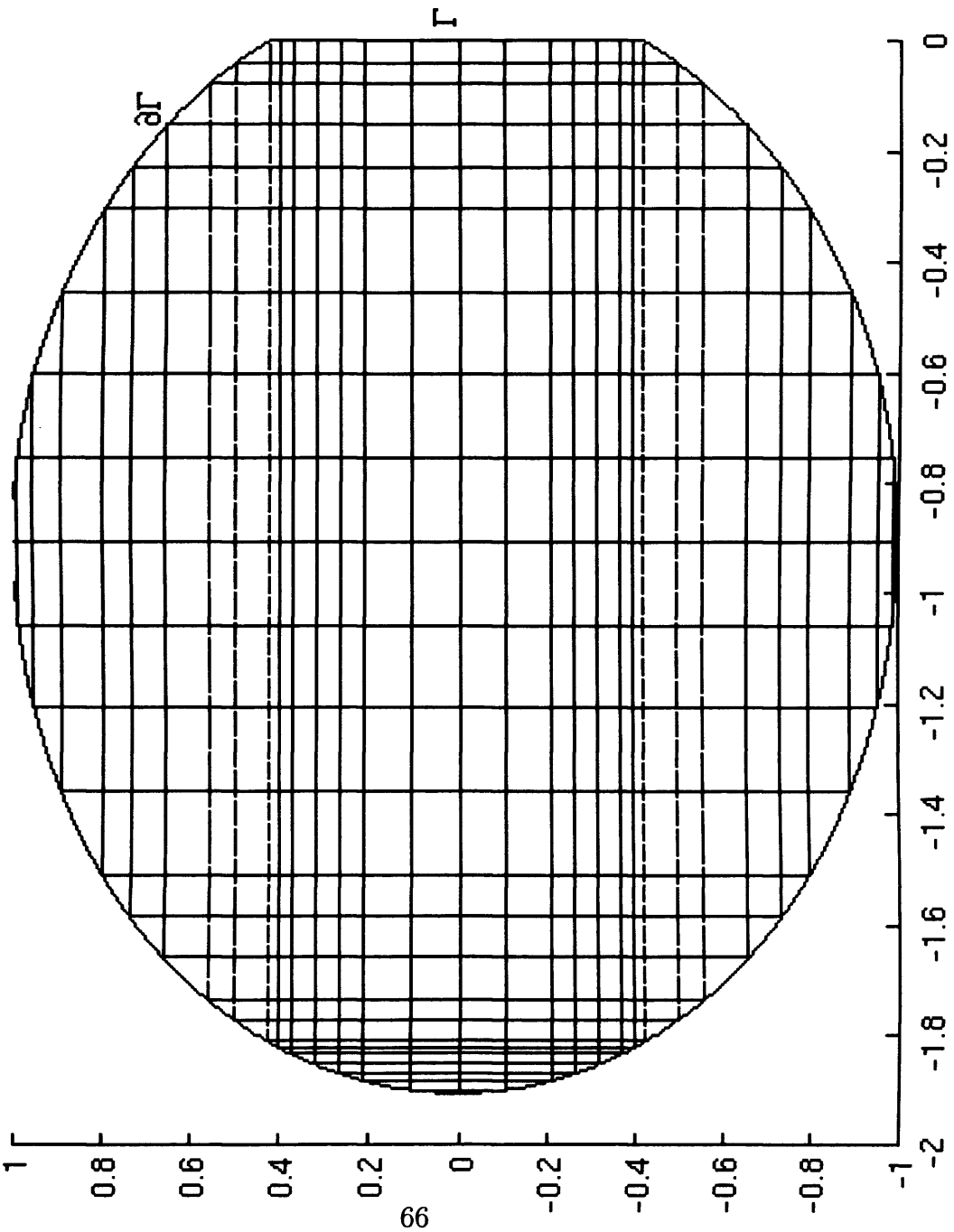

Figure 5.6: Example of a mesh with $m = 5$, $n = 2$ and $p = 2$ with $\delta = 2\sin(0.14\pi)$ illustrating the positioning of the mesh nodes

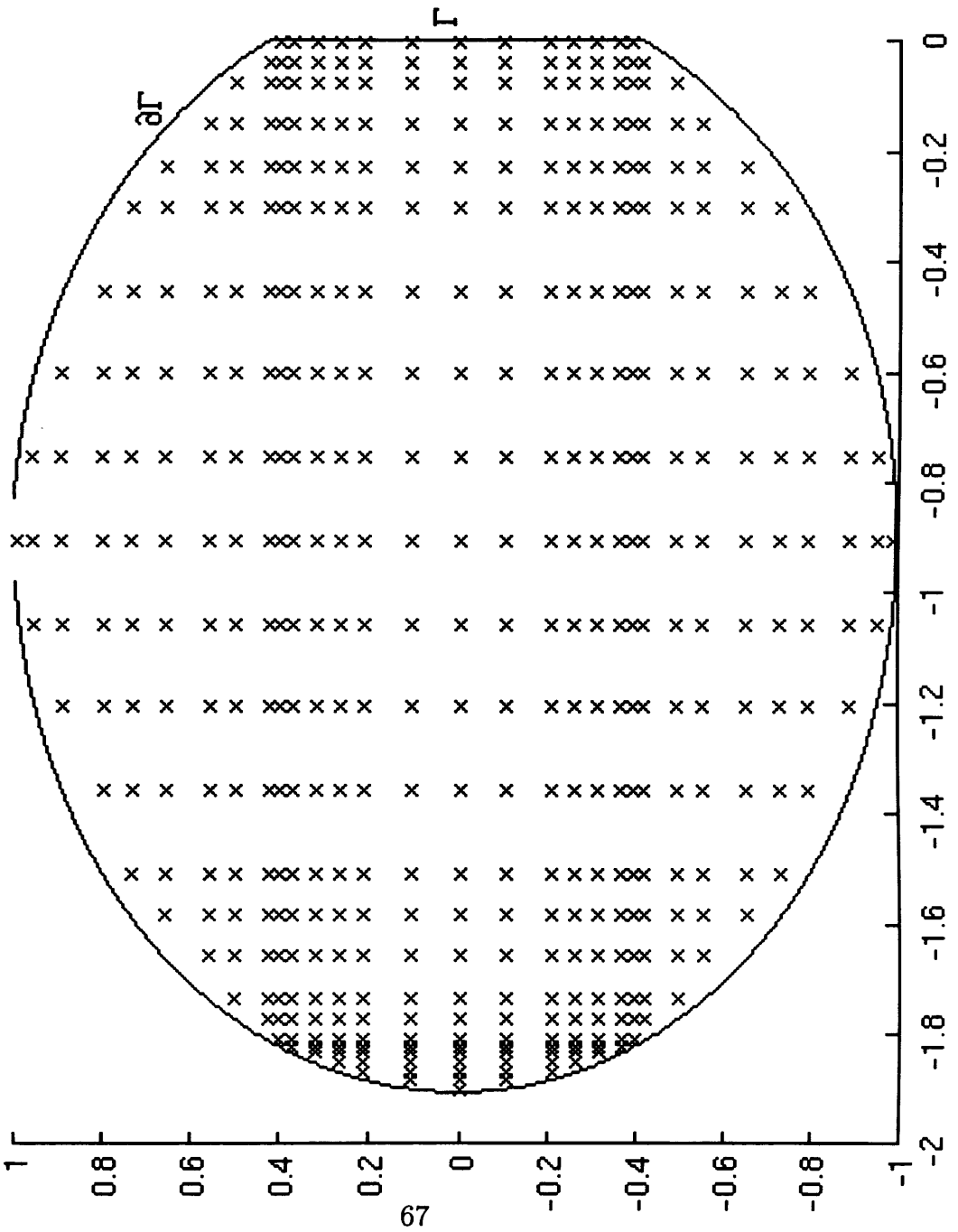

5.3 Calculation of the Dirichlet to Neumann map

In order to derive a Dirichlet to Neumann map at the interface Γ we must solve (3.6) making use of the matrices U and V in (4.11) which means we will be required to solve a problem of the form $Y'(x) = A(x)Y(x)$ when $A(x)$ is as in (3.7) and $Q(x)$ is as in (3.10),

$$Q(x) = \text{diag}\left(\frac{\pi^2}{\delta^2} + \sin x - \lambda, ..., \frac{Z^2\pi^2}{\delta^2} + \sin x - \lambda\right)$$

where (5.7) has been truncated at Z. This means that $Y(x)$ contains exponentially growing solutions with asymptotic behaviour for large n of the form $\phi_n(x) = A_n e^{x\sqrt{\frac{n^2\pi^2}{\delta^2}-\lambda}} + B_n e^{-x\sqrt{\frac{n^2\pi^2}{\delta^2}-\lambda}}$, which come from equations of the form $-\phi_n''(x) + \frac{n^2\pi^2}{\delta^2}\phi_n(x) = \lambda\phi_n(x)$.

To avoid this problem due to exponentially growing solutions dominating the decaying solutions in the matrix Y we shall change the representation of the variable Y to a form which restricts the growing solutions.

The Cayley transform has the desired properties since it will not converge to zero or ∞ as certain elements of $Y(x)$ tend to ∞ and we will make use of it to calculate the Floquet multipliers. The method is explained as follows. We choose

$$\Theta = (Y + iI)(Y - iI)^{-1} \tag{5.13}$$

as our Cayley transform where I is the $2Z \times 2Z$ identity matrix.

Differentiating (5.13) and using $Y' = AY$ we obtain

$$\Theta' = \frac{1}{2}(I - \Theta)A(I + \Theta) \tag{5.14}$$

and with $Y(0) = I_{2N}$ then $\Theta(0) = (I + iI)(I - iI)^{-1} = \frac{1+i}{1-i}I$. Let $u_j(x) = Y(x)c_j$ be the j^{th} Floquet eigensolution. From this we obtain

$$Y'(x)c_j = A(x)Y(x)c_j$$

hence $Y'(x) = A(x)Y(x)$ since c_j is constant and note that $Y(2\pi)c_j = \rho_j Y(0)c_j$ where ρ_j is the j^{rmth} Floquet multiplier. If we apply $\Theta(2\pi)$ as in (5.13) to $\mathbf{c}_j$ we obtain

$$\Theta(2\pi)\mathbf{c}_j = \frac{\rho_j + i}{\rho_j - i}\Theta(0)\mathbf{c}_j. \tag{5.15}$$

We see that finding an eigenvalue of $\Theta(2\pi)$ allows us to obtain the corresponding Floquet multipliers. We are interested in values of λ which are in the spectral gaps of equation (3.10). In these gaps values of ρ are real. In fact if λ is in a spectral gap, then of $2Z$ possible values of ρ, Z of these will have the property that $-1 < \rho < 1$ and $|\rho| > 1$ for the other Z. The case where $|\rho| < 1$ corresponds to the Floquet eigenvectors in L^2. The physically realistic solution down the tube consists of a linear combination of the $L^2[0, \infty)$ eigenvectors of (5.15).

Let $\Phi(0) = [\phi_1(0), ..., \phi_N(0)]^T$ and $\Phi'(0) = [\phi_1'(0), ..., \phi_N'(0)]^T$ be $Z \times 1$

column vectors containing the $\{\phi_k\}_{k=1}^{2N}$ in (5.7) and let X be a $2Z \times Z$ matrix of the $L^2[0,\infty)$ eigenvectors of $Y(2\pi)$ or $\Theta(2\pi)$ ie the c_j of (5.15). Let

$$X = \begin{pmatrix} U \\ V \end{pmatrix}.$$

Then $\exists \mathbf{d} \in c^N$ such that

$$\begin{pmatrix} \Phi(0) \\ \Phi'(0) \end{pmatrix} = \begin{pmatrix} U \\ V \end{pmatrix} \mathbf{d}$$

where $\mathbf{d}$ is a $Z \times 1$ vector. From these we obtain the following two equations

$$\Phi(0) = U\mathbf{d} \quad \text{and} \quad \Phi'(0) = V\mathbf{d} \tag{5.16}$$

from which we obtain

$$\Phi'(0) = VU^{-1}\Phi(0).$$

Thus we have the following expression for the Dirichlet to Neumann map

$$\Lambda(\lambda) = VU^{-1}|_{x=0}. \tag{5.17}$$

5.4 Calculation of the modified Dirichlet to Neumann map and its application

In section (5.3) we calculated the Dirichlet to Neumann map for a one dimensional domain in terms of the basis functions $\phi_i(x)$ for $i = \{1, ..., Z\}$ in (5.7). The interface Γ represents a two dimensional domain and thus $\Lambda(\lambda)$ in (5.17) will have to be modified as we now show.

Suppose we are given a set of Z evenly spaced nodes $y_1, y_2, ...y_Z$ on the interface Γ between the waveguide and the perturbation, and a function η with corresponding values $\eta(y_1), \eta(y_2), ...\eta(y_Z)$ where the function η has the property that $\eta(-\frac{\delta}{2}) = 0$ and $\eta(\frac{\delta}{2}) = 0$ with $\{y_1, y_Z\} \notin \{-\frac{\delta}{2}, \frac{\delta}{2}\}$. Then if we are given an arbitrary point $\xi \in (-\frac{\delta}{2}, \frac{\delta}{2})$ in this interval, we can estimate $\eta(\xi)$ by the following interpolate

$$\eta(\xi) = \frac{2}{Z+1} \sum_{k=1}^{Z} \sum_{m=1}^{Z} \eta(y_m) \sin\left(\frac{k\pi}{\delta}\left(y_m + \frac{\delta}{2}\right)\right) \sin\left(\frac{k\pi}{\delta}\left(\xi + \frac{\delta}{2}\right)\right). \tag{5.18}$$

We may substitute these Z nodes into (5.7) to obtain Z equations which can be written as the following matrix; $\Psi_R = F\Phi$. Here we have the vector $\Psi_R = (\psi(y_1), \psi(y_2), ..., \psi(y_Z))^T$ which denotes the values of ψ in the tube at $x = 0$ and at the evenly spaced nodes $y_1, y_2, ..., y_Z$ to the right of Γ together with $\Phi = (\phi_1(0), \phi_2(0), ..., \phi_Z(0))^T$ and F is the matrix

$$F_{kl} = \sin\left(\frac{k\pi l}{Z+1}\right)$$

for $\{k,l\} \in \{1,2,...,Z\}$. If on the interface Γ we have N geometrically spaced nodes corresponding to where the nodes on the geometric mesh coincide with Γ, we denote these by; $\xi_1, \xi_2, ..., \xi_N$, we may write

$$\Psi_L = G\Psi_R$$

where $\Psi_L = (\psi(y_1), ..., \psi(y_N))$ is the solution where the nodes on the geometric mesh intersect Γ, and $G = (G)_{mn}$ for $m \in \{1, ..., N\}$ and $n \in \{1, ..., Z\}$. Using the fact that in the tube $\{y_1, ..., y_Z\}$ are evenly spaced nodes we have $y_n = -\frac{\delta}{2} + \frac{n\delta}{Z+1}$ for $n \in \{1, ..., Z\}$ and substituting this into (5.18) we obtain

$$G_{mn} = \frac{2}{Z+1} \sum_{k=1}^{Z} \sin\left(\frac{k\pi n}{Z+1}\right) \sin\left(\frac{k\pi}{\delta}\left(\xi_m + \frac{\delta}{2}\right)\right). \tag{5.19}$$

From (5.16) $\Psi_R = FU\mathbf{d}$ and $\Psi_R' = FV\mathbf{d}$ since $\Phi(0) = U\mathbf{d}$ and $\Phi'(0) = V\mathbf{d}$ where $\mathbf{d}$ is an $Z \times 1$ column vector and with $\Psi_L = G\Psi_R$ and $\Psi_L' = G\Psi_R'$ so we are led to

$$\Psi_L = GFU\mathbf{d} \tag{5.20}$$

and

$$\Psi_L' = GFV\mathbf{d}.$$

The variable $\mathbf{d}$ in the expressions for Ψ_L and Ψ_R needs to be eliminated in order to obtain a relationship between Ψ_L and Ψ_L'. Since $GFU \in \Re_{N\times Z}$ and $GFV \in \Re_{N\times Z}$ we look for a least squares solution. Let $\hat{\mathbf{d}}$ be the

value of $\mathbf{d}$ that minimises the norm $||\Psi_L - GFU\mathbf{d}||$ then it is well known that if $\mathbf{d}$ is such a value then $(GFU)^T(\Psi_L - GFU\hat{\mathbf{d}}) = 0$. We thus obtain $\hat{\mathbf{d}} = (U^TF^TG^TGFU)^{-1}U^TF^TG^T\Psi_L$ and substituting this into $\Psi'_L = GFV\mathbf{d}$ where we write $\mathbf{d} = \hat{\mathbf{d}}$ which yields

$$\Psi'_L = GFV(U^TF^TG^TGFU)^{-1}U^TF^TG^T\Psi_L \tag{5.21}$$

from which we obtain

$$\Lambda(\lambda) = GFV(U^TF^TG^TGFU)^{-1}U^TF^TG^T \tag{5.22}$$

where $\Lambda(\lambda)$ is the Dirichlet to Neumann map to the left of Γ. We use this in equation (5.9) to eliminate $\psi(x_{i+1}, y_j)$ when applying equation (5.9) to $\psi(x_i, y_j)$ when $(x_i, y_j) \in \Gamma$.

We are now in a position to apply the Dirichlet to Neumann map where as stated previously, we wish to eliminate $\psi(x_{i+1}, y_j)$ when $(x_i, y_j) \in \Gamma$. Referring to the diagram (5.2) we consider $\psi(x_i, y_j)$ where $(x_i, y_j) \in \Gamma$ then we may interpret (5.21) as the following;

$$\frac{\psi(x_{i+1}, y_j) - \psi(x_{i-1}, y_j)}{2\Delta x_a} = \sum_{k=1}^{N} \Lambda_{jk}(\lambda)\psi(x_i, y_k). \tag{5.23}$$

Using (5.23) to eliminate $\psi(x_{i+1}, y_j)$ from (5.9) we obtain

$$\frac{2}{\Delta x_a^2}\psi(x_{i-1}, y_j) + \frac{2}{\Delta x_a}\sum_{k=1}^{N}\Lambda_{jk}(\lambda)\psi(x_i, y_k) + \frac{2}{\Delta y_a(\Delta y_a + \Delta y_b)}\psi(x_i, y_{j-1}) \tag{5.24}$$

$$+\frac{2}{\Delta y_b(\Delta y_a + \Delta y_b)}\psi(x_i, y_{j+1}) - 2\left(\frac{1}{\Delta x_a^2} + \frac{1}{\Delta y_a \Delta y_b}\right)\psi(x_i, y_j) + \lambda\psi(x_i, y_j) = 0.$$

The matrix corresponding to (5.9) can now be assembled with software packages such as MATLAB and so the eigenvalues of the complete domain and corresponding eigenfunctions of the modified circular part of the domain can be found. In assembling the matrix corresponding to (5.9) and (5.24) which we call A, it was necessary to form a sparse matrix where only the non-zero entries of the matrix corresponding to (5.9) are stored. The eigenfunction over the modified circular domain is calculated via an iterative technique using MATLAB. This involves guessing an initial value for λ in order to determine $\Lambda(\lambda)$ from which we form the matrix equation $A(\lambda)$ in (5.12) to obtain

$$A(\lambda)\Psi = \mu\Psi \tag{5.25}$$

where the eigenvalue μ of $A(\lambda)$ is obtained by using MATLAB's **eigs** function. The next step is to repeat the process by constructing $\Lambda(\mu)$ and thus finding the eigenvalues of $A(\mu)$. In obtaining the results in (5.7) for most eigenvalues it was found after two iterations that $\lambda - \mu$ was less than the error as a result of the discretisation and thus there was no point in performing more iterations. From MATLAB's **eigs** function we may also obtain

the eigenvector containing the values of Ψ at the nodes in figure (5.6), and based on the organisation of the matrix $A(\lambda)$ we can pick out from Ψ the value $\eta(y_1)$,...,$\eta(y_N)$ and thus we now ψ at Γ and so we obtain a boundary condition at the interface. This is essential for calculating the solution in the waveguide as shall be explained in the next section.

5.5 Continuous orthonormalisation and the solution in the waveguide

The version of this method which we shall employ here is based on the paper [31] and here this method will be explained in a self contained format specially adapted to solve our problem.

Let $W = \Phi(0)$ where $W \in \Re^{Z\times 1}$ is the initial condition of the problem $\Phi' = A\Phi$, $x \in [0, 2\pi]$ where A is as in (3.7). Let us form $\Psi_L \in \Re^{N\times 1}$ in (5.20) by taking the last N elements of Ψ in (5.25). From (5.20) we must have $\Psi_L = GFW$ and thus from least squares we obtain

$$W = (F^T G^T G F)^{-1} F^T G^T \Psi_L.$$

We also have $\Phi' = L\Phi$ at $x = 2\pi$ where L is the Dirichlet to Neumann map in (5.17) as we will be working to the right of the interface Γ. These two

equations may be written as

$$B\Phi(0) = W \quad \text{and} \quad C\Phi(2\pi) = 0.$$

Here $B = (I_Z\ 0)$ and $C = (L\ -I_Z)$ where I_Z is the $Z \times Z$ identity matrix.

Let $X' = AX$ where A is as before, and X is a solution. Now consider the equation

$$Y' = AY + YG \tag{5.26}$$

for Y as before and G is some matrix. The spaces spanned by the columns of X and Y will be the same if $X(0) = Y(0)$. Let

$$Y = XW \tag{5.27}$$

then $Y' = X'W + XW'$ so that $Y' - AY - YG = X'W + XW' - AXW - XWG$ which leads to $Y' - AY - YG = X(W' - WG)$. Hence if $W' = WG$ and $W(0) = I_N$ then $Y(0) = X(0)$ and Y defined by (5.27) will satisfy (5.26).

We can choose a G such that the solution of (5.26) has orthonormal columns. Let us denote these orthonormal columns by T_1. Then we have $T_1^T T_1 = I_N$ and after differentiating and substituting in (5.26) we obtain

$$G + G^T = -T_1^T(A^T + A)T_1.$$

This leads to an obvious solution $G = -T_1^T A T_1$ for G. For T_1 we now have

$T_1' = (I_{2N} - T_1 T_1^T) A T_1$. To find the initial value of T_1 we can perform a QR decomposition on B^T

$$B^T = Q \begin{pmatrix} R \\ 0 \end{pmatrix} \quad \text{or} \quad \mathrm{Q^T B^T} = \begin{pmatrix} R \\ 0 \end{pmatrix}.$$

The left side of the above equation can be multiplied by an anti-diagonal matrix U consisting of zeros except for ones on the anti diagonal. This leads to

$$T^T B^T = \begin{pmatrix} 0 \\ \hat{R} \end{pmatrix} \quad \text{or} \quad \mathrm{BT} = \begin{pmatrix} 0 & \hat{R}^T \end{pmatrix} \tag{5.28}$$

where $T^T = UQ^T$ and $\hat{R}$ is reverse lower triangular. In this case R is reverse lower triangular. The first N columns of T which we denote as T_1 are orthogonal to B and thus we may chose $T_1(0) = \begin{pmatrix} 0 \\ I_N \end{pmatrix}$. The remaining N columns will be called T_2. Let

$$z = (I_{2N} - T_1 T_1^T)\Phi \tag{5.29}$$

then we have $Bz = W$ since T_1 is orthogonal to B from (5.28). It can also be easily seen that $T_1^T z = 0$ by applying T_1^T to (5.29). This gives us boundary conditions for z for which we will seek a differential equation.

Next we need a transformation of the form $\Phi = Ty$ for $\Phi' = A\Phi$. This

leads to $y' = T^T ATy - T^T T' y$ which, if we partition T into $(T_1|T_2)$, we obtain

$$\begin{pmatrix} y_1 \\ y_2 \end{pmatrix}' = \begin{pmatrix} T_1^T AT_1 - T_1^T T_1' & T_1^T AT_2 - T_1^T T_2' \\ T_2^T AT_1 - T_2^T T_1' & T_2^T AT_2 - T_2^T T_2' \end{pmatrix} \begin{pmatrix} y_1 \\ y_2 \end{pmatrix}. \tag{5.30}$$

We wish to choose the transformation such that y_1 is the growing solution and y_2 the decaying solution and which also partially separates the equations. This can be done if we set $T_2^T AT_1 - T_2^T T_1' = 0$. This would lead to $T_1' = AT_1$ but would not give an orthogonal T_1. However $T_1' = AT_1 + T_1 G$ is orthogonal to T_2 and T_1 will remain orthogonal over the integration interval for some G in (5.26). We now wish to eliminate T_2' in (5.30) and thus we seek an expression for T_2'. Differentiating $T_1^T T_2 = 0$ and using the expression $T_1' = AT_1$ we get $T_1^T T_2' = -T_1^T A^T T_2$. Given that $T_1 T_1^T T_2' = -T_1 T_1^T A^T T_2$ and with $T_1 T_1^T + T_2 T_2^T = I_{2N}$ we are led to $T_2' = T_2 T_2^T T_2' - T_1 T_1^T AT_2$. Since from differentiation $T_2^T T_2 = I_N$ we obtain $(T_2^T T_2')^T + T_2^T T_2' = 0$ and so $T_2^T T_2'$ can be chosen to be 0 and likewise T_1. This finally leads to $T_2' = -T_1 T_1^T A^T T_2$ and so (5.30) becomes

$$\begin{pmatrix} y_1 \\ y_2 \end{pmatrix}' = \begin{pmatrix} T_1^T AT_1 & T_1^T (A + A^T) T_2 \\ 0 & T_2^T AT_2 \end{pmatrix} \begin{pmatrix} y_1 \\ y_2 \end{pmatrix}. \tag{5.31}$$

By the partitioning of T into $(T_1|T_2)$ and y into $(y_1\ y_2)^T$ and using the fact that $\Phi = Ty$ we may write $\Phi = T_1 y_1 + T_2 y_2$ which when substituted into $z = (I_{2N} - T_1 T_1^T)\Phi$ yields $z = (I_{2Z} - T_1 T_1^T)(T_1 y_1 + T_2 y_2)$ which upon using

the fact that $T_1^T T_1 = I_N$ and $T_1^T T_2 = 0$ gives us $z = T_2 y_2$. Differentiating and substituting in the expressions for T_1' and T_2' we obtain $z' = -T_1 T_1^T A^T T_2 y_2 + T_2 T_2^T A T_2 y_2$ and T_2 can be eliminated using $z = T_2 y_2$ and we may use $T_1 T_1^T + T_2 T_2^T = I_{2N}$ to eliminate $T_2 T_2^T$ to finally give

$$z' = (A - T_1 T_1^T (A + A^T))z.$$

This together with $Bz(0) = W$ and $T_1^T z = 0$ gives us

$$\begin{pmatrix} B \\ T_1^T \end{pmatrix} z(0) = \begin{pmatrix} W \\ 0 \end{pmatrix}$$

from which $z(0) = \begin{pmatrix} B \\ T_1^T \end{pmatrix}^{-1} \begin{pmatrix} W \\ 0 \end{pmatrix}$. We now have boundary conditions for T_1 and z at $x = 0$ as well as differential equations for T_1 and z thus T_1 and z can be found over the interval $x \in [0, 2\pi]$. We recall the boundary condition $C\Phi(2\pi) = 0$ which after substituting in $\Phi = T_1 y_1 + z$ yields $C\Phi(2\pi) = CT_1(2\pi)y_1(2\pi) + Cz(2\pi)$ or

$$y_1(2\pi) = -(CT_1(2\pi))^{-1} Cz(2\pi).$$

To summarise our equations and boundary conditions for T_1 and z, we have $z(0) = \begin{pmatrix} B \\ T_1^T \end{pmatrix}^{-1} \begin{pmatrix} W \\ 0 \end{pmatrix}$ with $z'(x) = (A - T_1 T_1^T (A + A^T))z(x)$

and $T_1(0) = \begin{pmatrix} 0 \\ I_N \end{pmatrix}$ with $T_1' = (I_{2N} - T_1 T_1^T) A T_1$. We now need to find $\Phi(x)$. From the equation $\Phi(x) = T_1(x) y_1(x) + z(x)$ all we need is $y_1(x)$ since from above $T_1(x)$ and $z(x)$ have been found. Let $Y_{11}'(x) = T_1^T A T_1 Y_{11}(x)$ with $Y_{11}(0) = I_N$ then from (5.31) we have $y_1'(x) = T_1^T A T_1 y_1(x) + T_1^T (A + A^T) z(x)$ then any solution y_1 can be written in the following form

$$y_1(x) = w_1(x) + Y_{11}(x) y_1(0) \tag{5.32}$$

where $w_1(0) = 0$ and $Y_{11}(0) = I_N$. The matrix $Y_{11}(x)$ is likely to become ill conditioned and thus an alternative is to consider $R_{11}(x) Y_{11}(x) = I_N$. Differentiating this equation and solving for R_{11}' leads to $R_{11}' = -R_{11} Y_{11}' Y_{11}^{-1} = -R_{11} T_1^T A T_1$. Letting $v_1(x) = R_{11}(x) w(x)$ then differentiating this gives us

$$v_1' = R_{11}' y_1 + R_{11} y_1' = -R_{11} T_1^T A T_1 y_1 + R_{11} (T_1^T A T_1 y_1 + T_1^T (A + A^T) z)$$

which after cancelling the first two terms yields

$$v_1'(x) = R_{11} T_1^T (A + A^T) z$$

with the boundary condition $v_1(0) = 0$ since $w(0) = 0$. Multiplying (5.32) by R_{11} we obtain at $x = 2\pi$ the following $R_{11}(2\pi) y_1(2\pi) = v_1(2\pi) + y_1(0)$. Thus starting at $x = 2\pi$ we can integrate backwards via a finite differences scheme whereby for each interval the solution on the right hand end of the

interval becomes the new boundary condition.

Figure 5.7: One interval of the finite differences scheme in the tube

Looking at Fig 5.7, it can be seen that over interval i from the left, we have the following iteration formula

$$y_1(x_i) = R_{11}^{(i)}(x_{j+1})y_1(x_{i+1}) - v^{(i)}(x_{i+1}).$$

Once we have the matrix $y_1(x_i)$ at every node x_i of the interval we use the transformation

$$\Phi(x_i) = T_1(x_i)y_1(x_i) + z(x_i).$$

The mesh on which we solve this problem is once again geometric. The smallest interval is between Γ and x_1 and the largest contains $x_{i+1} = 2\pi$.

5.6 Derivative of the eigenvalue λ with respect to the tube width δ

We set $\langle \psi, \psi \rangle = 1$ where $\dot{\psi} = \frac{\partial \psi}{\partial \delta}$ is over the domain Ω and differentiate $-\Delta\psi + V(x)\psi = \lambda\psi$ with respect to δ to obtain

$$-\Delta\dot{\psi} + V\dot{\psi} = \dot{\lambda}\psi + \lambda\dot{\psi} \tag{5.33}$$

where $\dot{\psi}$ denotes partial differentiation with respect to δ. Using Green's theorem for the inner product $\langle \Delta\dot{\psi}, \psi \rangle$ we have

$$\langle \Delta\dot{\psi}, \psi \rangle - \langle \dot{\psi}, \Delta\psi \rangle = \int_{\partial\Omega} \left(\psi \frac{\partial \dot{\psi}}{\partial \nu} - \dot{\psi} \frac{\partial \psi}{\partial \nu} \right) \cdot \mathbf{dl}$$

where $\partial\Omega$ denotes the boundary of the whole domain and ν the outwards normal. Substituting in (5.33) we obtain

$$\dot{\lambda} = -\langle \dot{\psi}, \Delta\psi \rangle - \int_{\partial\Omega} \left(\psi \frac{\partial \dot{\psi}}{\partial \nu} - \dot{\psi} \frac{\partial \psi}{\partial \nu} \right) \cdot \mathbf{dl} + \langle \dot{\psi}, \mathbf{V}\psi \rangle.$$

Since $\langle \dot{\psi}, (-\Delta + V)\psi \rangle = \langle \dot{\psi}, \lambda\psi \rangle$ we have

$$\dot{\lambda} = \langle \dot{\psi}, \lambda\psi \rangle - \int_{\partial\Omega} \left(\psi \frac{\partial \dot{\psi}}{\partial \nu} - \dot{\psi} \frac{\partial \psi}{\partial \nu} \right) \cdot \mathbf{dl}.$$

Since $\psi|_{\partial\Omega} = 0$ and $\langle \dot{\psi}, \psi \rangle = 0$ we are left with

$$\dot{\lambda} = \int_{\partial\Omega} \dot{\psi} \frac{\partial \psi}{\partial \nu} \cdot \mathbf{dl}. \tag{5.34}$$

Taking the total derivative of ψ with respect to δ we have

$$\frac{d\psi}{d\delta} = \frac{dx}{d\delta}\frac{\partial \psi}{\partial x} + \frac{dy}{d\delta}\frac{\partial \psi}{\partial y} + \dot{\psi} \tag{5.35}$$

where $\dot{\psi} = \frac{\partial \psi}{\partial \delta}$ and substituting (5.35) into (5.34) we obtain

$$\dot{\lambda} = \int_{\partial\Omega} \left(\frac{d\psi}{d\delta} - \frac{dx}{d\delta}\frac{\partial \psi}{\partial x} - \frac{dy}{d\delta}\frac{\partial \psi}{\partial y} \right) \frac{\partial \psi}{\partial \nu} \cdot \mathbf{dl}.$$

It can easily be seen that $\frac{dy}{d\delta} = \pm\frac{1}{2}$ for $y = \pm\frac{\delta}{2}$, $\frac{dx}{d\delta} = 0$ and $\frac{d\psi}{d\delta}|_{\partial\Omega} = 0$ (from the Dirichlet boundary condition) and so (5.35) reduces to

$$\dot{\psi}|_{y=\pm\frac{\delta}{2}} = \mp\frac{1}{2}\frac{\partial \psi}{\partial y}|_{y=\pm\frac{\delta}{2}} \quad \text{at} \quad y = \pm\frac{\delta}{2}.$$

Let i. j be the unit vectors where $i = \begin{pmatrix} 1 \\ 0 \end{pmatrix}$ and $j = \begin{pmatrix} 0 \\ 1 \end{pmatrix}$. In our case $\frac{\partial \psi}{\partial \nu} = \frac{\partial \psi}{\partial x}\mathbf{i} + \frac{\partial \psi}{\partial y}\mathbf{j}$ and since the boundaries of the waveguide are horizontal then $dy = 0$ and thus $\mathbf{dl} = -\mathbf{j}dx$ which upon substituting the expressions for $\dot{\psi}$ and $\mathbf{dl}$ into (5.34) we obtain

$$\dot{\lambda} = \int_0^\infty \frac{1}{2}\frac{\partial \psi(x, -\frac{\delta}{2})}{\partial y}\frac{\partial \psi(x, -\frac{\delta}{2})}{\partial y}(-\mathbf{j}\cdot\mathbf{j})dx + \int_\infty^0 -\frac{1}{2}\frac{\partial \psi(x, \frac{\delta}{2})}{\partial y}\frac{\partial \psi(x, \frac{\delta}{2})}{\partial y}(-\mathbf{j}\cdot\mathbf{j})dx$$

which simplifies to

$$\dot{\lambda} = -\frac{1}{2}\int_0^{\infty} \left|\frac{\psi(x,\frac{\delta}{2})}{\partial y}\right|^2 dx - \frac{1}{2}\int_0^{\infty} \left|\frac{\psi(x,-\frac{\delta}{2})}{\partial y}\right|^2 dx. \tag{5.36}$$

Substituting in (5.7) we obtain

$$\int_0^{\infty} \left|\frac{\partial\psi}{\partial y}(x,-\frac{\delta}{2})\right|^2 dx = \frac{\pi^2}{\delta^2}\sum_{m=1}^{N}\sum_{n=1}^{N} mn \int_0^{\infty} \phi_m(x)\phi_n(x)dx$$

and

$$\int_0^{\infty} \left|\frac{\partial\psi}{\partial y}(x,\frac{\delta}{2})\right|^2 dx = \frac{\pi^2}{\delta^2}\sum_{m=1}^{N}\sum_{n=1}^{N} mn\cos(m\pi)\cos(n\pi) \int_0^{\infty} \phi_m(x)\phi_n(x)dx.$$

Letting ρ_m be the Floquet multiplier of ϕ_m, we can rewrite the integral as

$$\int_0^{\infty} \phi_m(x)\phi_n(x)dx = \sum_{k=0}^{\infty} \rho_m^k \rho_n^k \int_o^{2\pi} \phi_m(x)\phi_n(x)dx.$$

Setting $\sum_{k=0}^{\infty} \rho_m^k \rho_n^k = \frac{1}{1-\rho_m\rho_n}$ we obtain for $\dot{\lambda}$ the following

$$\dot{\lambda} = -\frac{\pi^2}{2\delta^2}\sum_{m=1}^{N}\sum_{n=1}^{N} \frac{mn(1+\cos(m\pi)\cos(n\pi))}{1-\rho_m\rho_n} \int_0^{2\pi} \phi_m(x)\phi_n(x)dx. \tag{5.37}$$

5.7 Numerical results

Here we consider the domain in Fig 5.1 for different values of the mesh parameters m,n, p and θ. Table 5.2 gives eigenvalues as a function of the

mesh parameters m, n and p as well as a function of θ.

(m,n,p)	θ	λ_1	λ_2	λ_3	λ_4	λ_5	λ_6
(53,15,3)	0.09π	5.68499	14.0968	14.6771	24.8608	26.3358	29.6698
(53,15,4)	0.09π	5.68508	14.0972	14.6769	24.8622	26.3368	29.6731
(51,17,3)	0.1π	5.66031	13.9229	14.6742	24.0921	26.3153	-
(51,17,4)	0.1π	5.66038	13.9231	14.6741	24.0924	26.3166	-
(51,17,3)	0.11π	5.63231	13.7101	14.6702	-	-	-
(51,17,4)	0.11π	5.63235	13.7101	14.6703	-	-	-
(49,19,3)	0.12π	5.60071	13.4477	14.6651	-	-	-
(49,19,4)	0.12π	5.60074	13.4476	14.6653	-	-	-
(49,19,3)	0.13π	5.56536	13.1202	14.6584	-	-	-
(49,19,4)	0.13π	5.56535	13.1199	14.6588	-	-	-
(47,21,3)	0.14π	5.52592	12.7026	-	-	-	-
(47,21,4)	0.14π	5.52591	12.7023	-	-	-	-

Table 5.2: Eigenvalues for different mesh densities and various tube widths

In table 5.2, λ_5 goes from being below the essential spectrum to being in the first gap when θ changes from 0.09π eigenvalues as a function of θ.

θ	$\dot{\lambda}_1$	$\dot{\lambda}_2$	$\dot{\lambda}_3$	$\dot{\lambda}_4$	$\dot{\lambda}_5$	$\dot{\lambda}_6$
0.09π	-0.315	-2.24	-0.0268	-9.28	-0.203	-5.69
0.1π	-0.369	-2.85	-0.0382	-19.3	-0.295	-
0.11π	-0.429	-3.68	-0.0531	-	-	-
0.12π	-0.495	-4.85	-0.0721	-	-	-
0.13π	-0.570	-6.69	-0.0961	-	-	-
0.14π	-0.653	-10.01	-	-	-	-

Table 5.3: Rate of change of various eigenvalues with respect to tube width

Table 5.4 compares (5.37) with the numerical value for the rate of change of λ with respect to δ. Here we have used best fit polynomials to calculate $\dot{\lambda}$ at various values of θ in between the sampled points as in Tables 5.3 and

5.2. The results of this are illustrated in Table 5.4 where $\dot{\lambda}$ is obtained from the best fit polynomial to the data in Table 5.2 while $P_i'(\theta)$ is obtained by differentiating the best fit polynomial to the data in Table 5.3. The accuracy

θ	0.095π	0.105π	0.115π	0.125π	0.135π
$\dot{\lambda}_1$	-0.34	-0.40	-0.46	-0.53	-0.61
$P_1'(\theta)$	-0.41	-0.47	-0.54	-0.61	-0.69
$\dot{\lambda}_2$	-2.5	-3.2	-4.2	-5.6	-8.1
$P_2'(\theta)$	-2.9	-3.6	-4.5	-5.6	-7.3
$\dot{\lambda}_3$	-0.032	-0.045	-0.062	-0.083	-
$P_3'(\theta)$	-0.047	-0.064	-0.085	-0.11	-
$\dot{\lambda}_4$	-14.3	-	-	-	-
$P_4'(\theta)$	-12.8	-	-	-	-
$\dot{\lambda}_5$	-0.25	-	-	-	-
$P_5'(\theta)$	-0.35	-	-	-	-

Table 5.4: Comparison of theoretical and observed derivatives of λ with respect to δ

of the eigenvalues is of order $\pm 0.008\%$ for the eigenvalues that are most sensitive to changes in tube width and $\pm 0.003\%$ for those least sensitive. When we vary the width of the tube the variation in the eigenvalues between adjacent values of θ is $\pm 1.2\%$ for the most sensitive to $\pm 0.02\%$ for the least sensitive. Contour plots of the eigenfunctions are illustrated in Figs 5.8, 5.9, 5.10, 5.11, and 5.12.

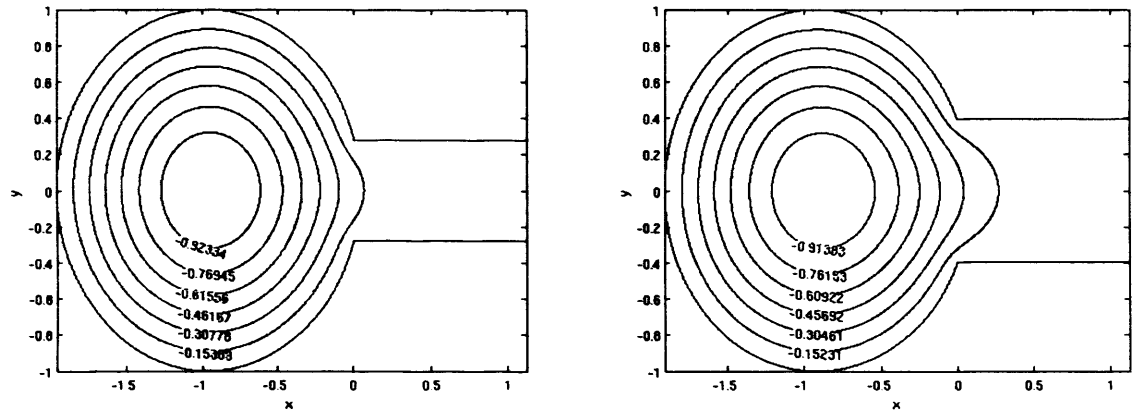

Figure 5.8: Contour plot of λ_1 for $\theta = 0.09\pi$ and $\theta = 0.13\pi$

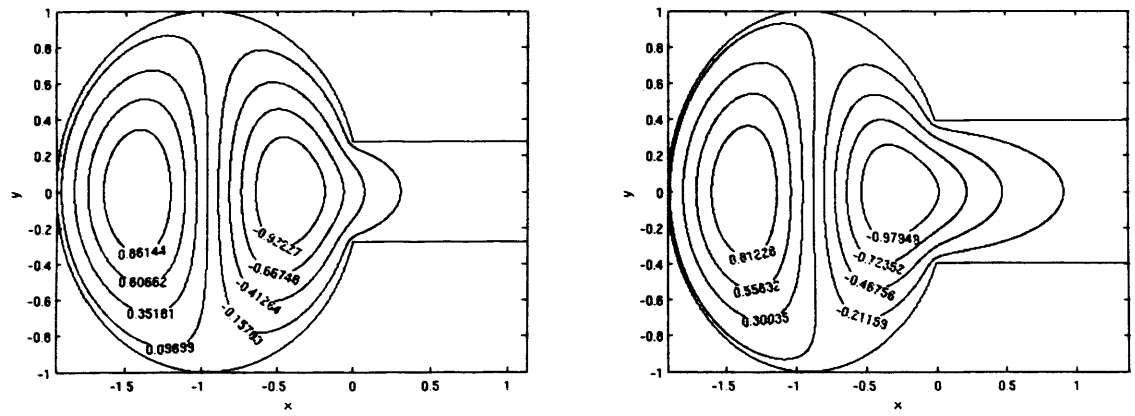

Figure 5.9: Contour plot of λ_2 for $\theta = 0.09\pi$ and $\theta = 0.13\pi$

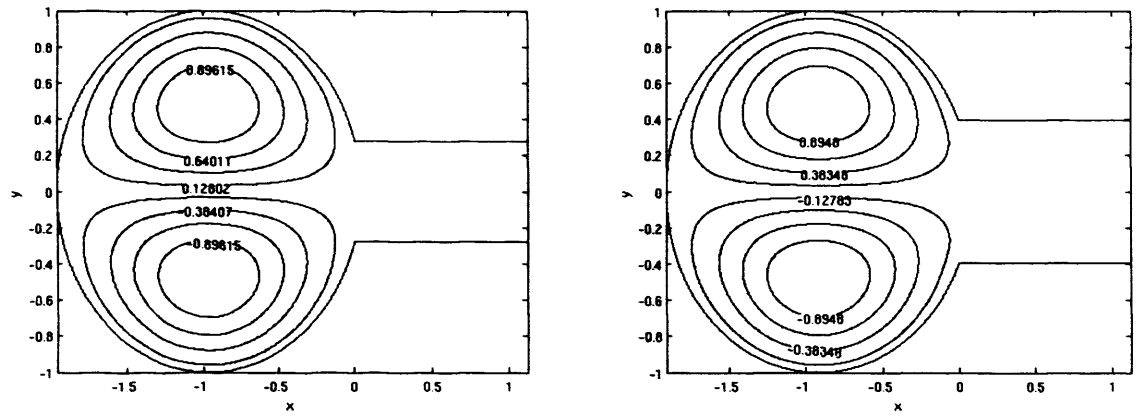

Figure 5.10: Contour plot of λ_3 for $\theta = 0.09\pi$ and $\theta = 0.13\pi$

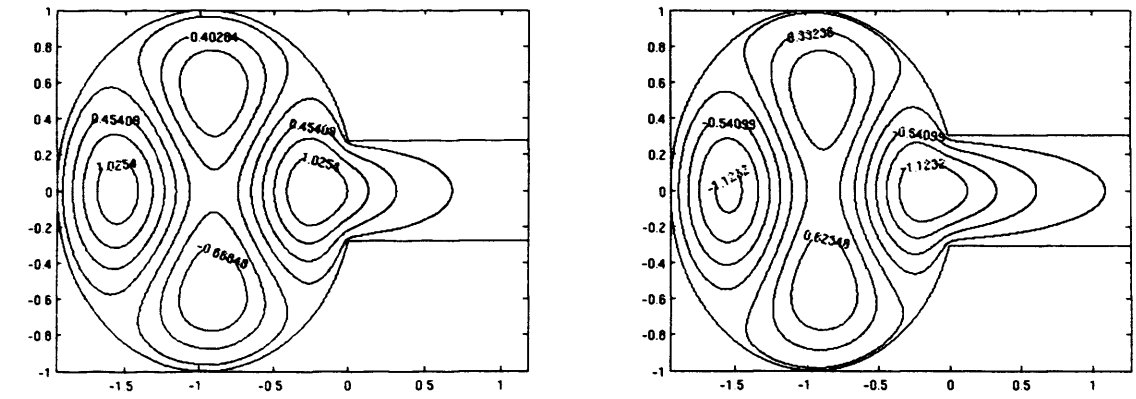

Figure 5.11: Contour plot of λ_4 for $\theta = 0.09\pi$ and $\theta = 0.1\pi$

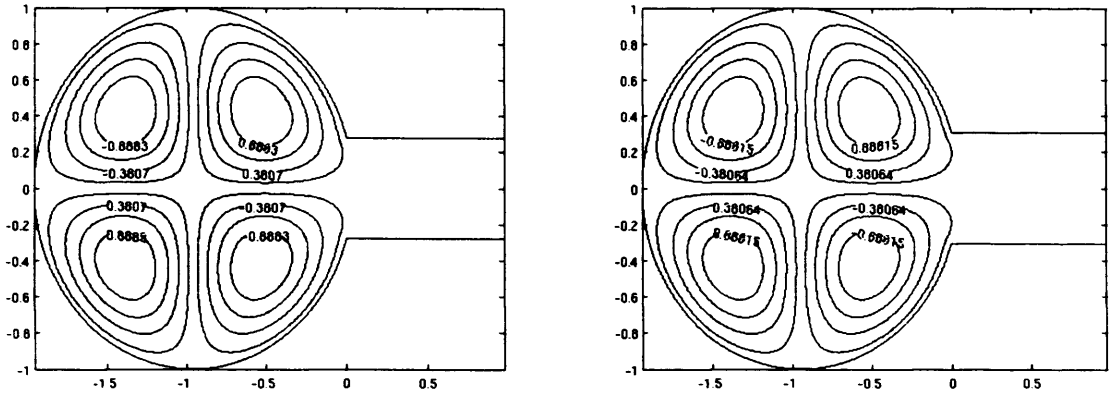

Figure 5.12: Contour plot of λ_5 for $\theta = 0.09\pi$ and $\theta = 0.1\pi$

5.8 The half domain with Dirichlet boundary conditions about the symmetry axis

We now proceed to cut the domain in half about the axis of symmetry, namely $y = 0$. First we impose zero Dirichlet boundary conditions on the whole domain resulting from this operation and secondly we shall impose Neumann boundary conditions on the original axis of symmetry. For the first case $\delta = \sin(\theta)$, and with Dirichlet boundary conditions on the whole boundary, equation (5.7) becomes

$$\psi = \sum_{n=1}^{Z} \phi_n(x) \sin\left(\frac{n\pi}{\delta} y\right)$$

and (5.18) becomes

$$\eta(\xi) = \frac{2}{Z+1} \sum_{k=1}^{Z} \sum_{l=1}^{Z} \eta(y_l) \sin\left(\frac{k\pi}{\delta} y_l\right) \sin\left(\frac{k\pi}{\delta} \xi\right).$$

(5.19) therefore becomes

$$G_{mn} = \frac{2}{Z+1} \sum_{k=1}^{Z} \sin\left(\frac{k\pi m}{Z+1}\right) \sin\left(\frac{k\pi}{\delta} \xi_n\right) \tag{5.38}$$

with ξ_n being the geometrically spaced points on the left. Table 5.5 contains the eigenvalues for five different mesh densities.

(m,n,p)	θ	λ_3	λ_5	λ_8	λ_{10}	λ_{12}
(53,7,3)	0.09π	14.6769	26.3343	40.5566	49.1709	57.1995
(53,7,4)	0.09π	14.6768	26.3360	40.5678	49.1905	57.2269
(51,9,3)	0.1π	14.6741	26.3131	40.4802	49.1586	56.9976
(51,9,4)	0.1π	14.6741	26.3152	40.4924	49.1772	57.0255
(51,9,3)	0.11π	14.6700	26.2837	40.3733	49.1403	56.7001
(51,9,4)	0.11π	14.6702	26.2866	40.3862	49.1570	56.7283
(49,11,3)	0.12π	14.6649	26.2446	40.2246	49.1101	56.2530
(49,11,4)	0.12π	14.6652	26.2481	40.2384	49.1252	56.2819
(49,11,3)	0.13π	14.6581	26.1928	40.0186	49.0598	55.5373
(49,11,4)	0.13π	14.6587	26.1970	40.0335	49.0729	55.5677
(47,13,3)	0.14π	14.6497	26.1254	39.7318	48.9635	-
(47,13,4)	0.14π	14.6504	26.1303	39.7476	48.9754	-

Table 5.5: The eigenvalues of the half domain with Dirichlet boundary conditions on the former axis of symmetry

The labelling of the eigenvalues is obtained by looking at Table 5.1. Since in the above problem we have Dirichlet boundary conditions at $y = 0$ then

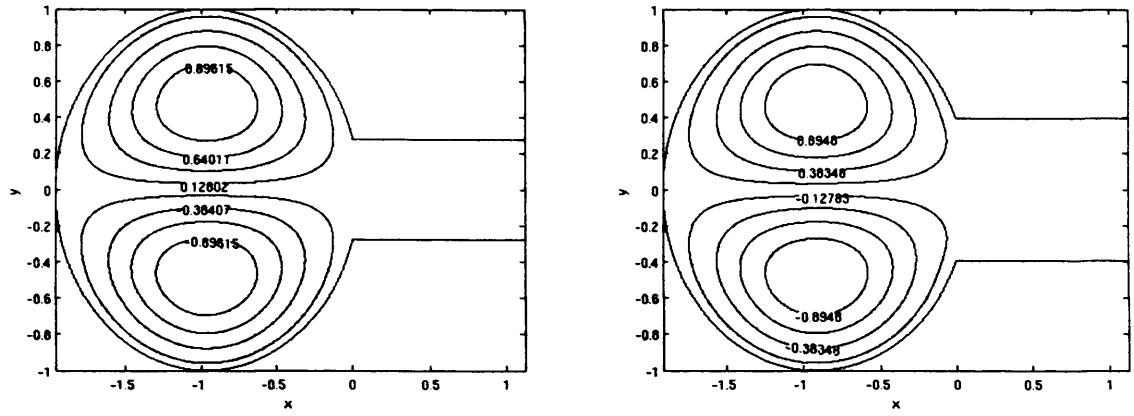

Figure 5.13: Contour plot of λ_3 for $\theta = 0.09\pi$ and $\theta = 0.13\pi$

these eigenvalues correspond to the eigenvalues associated with the solutions of the form $\Theta(\theta) = \sin\theta$ for our non-perturbed problem. These eigenfunctions are not able to penetrate so far into the tube and thus represent the larger eigenvalue of eigenvalue pairs after the degeneracy is lost due to the perturbation.

Figs 5.13, 5.14, 5.15, 5.16 and 5.17 are contour plots of various eigenvalues as we widen the tube with theoretical estimates of the derivative. Notice how more of the eigenfunction gets into the tube as we widen the tube. This leads to the hypothesis that the eigenvalue associated with the eigenfunction becomes more sensitive to fluctuations in tube width as one widens the tube. This is verified in the table of theoretical estimates for the derivative from (5.37).

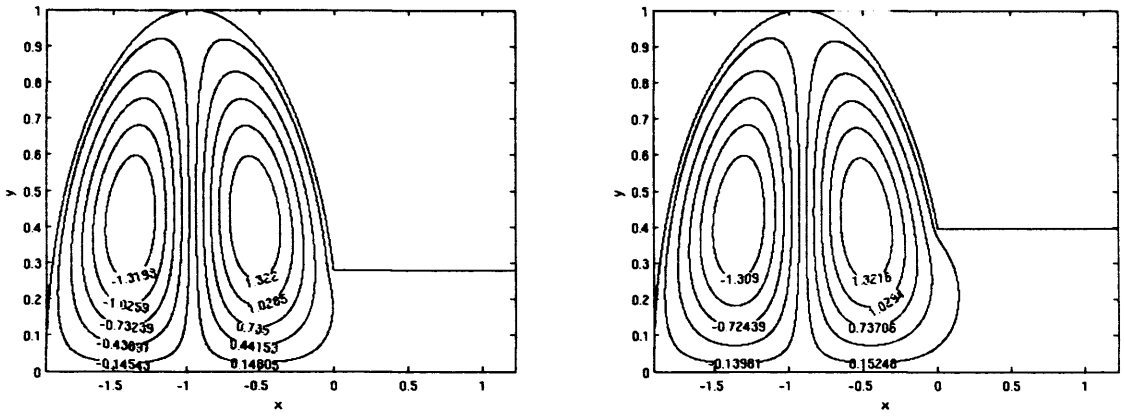

Figure 5.14: Contour plot of λ_5 for $\theta = 0.09\pi$ and $\theta = 0.13\pi$

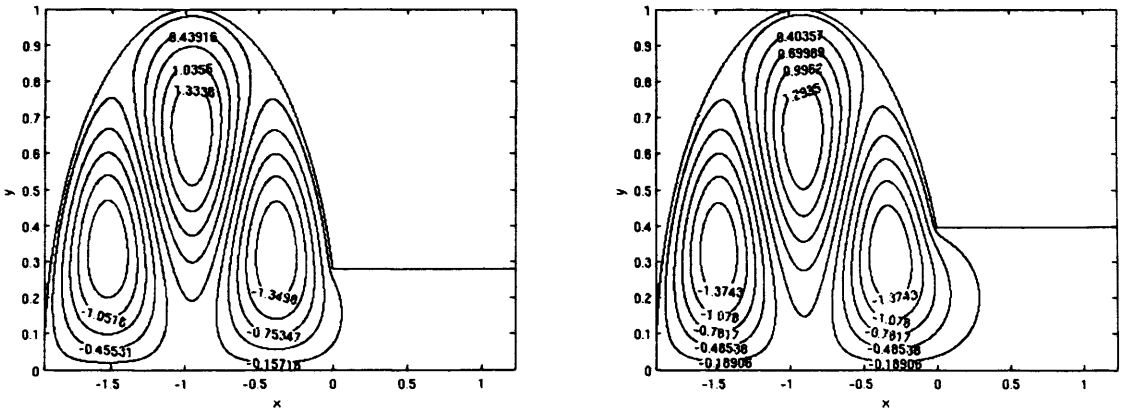

Figure 5.15: Contour plot of λ_8 for $\theta = 0.09\pi$ and $\theta = 0.13\pi$

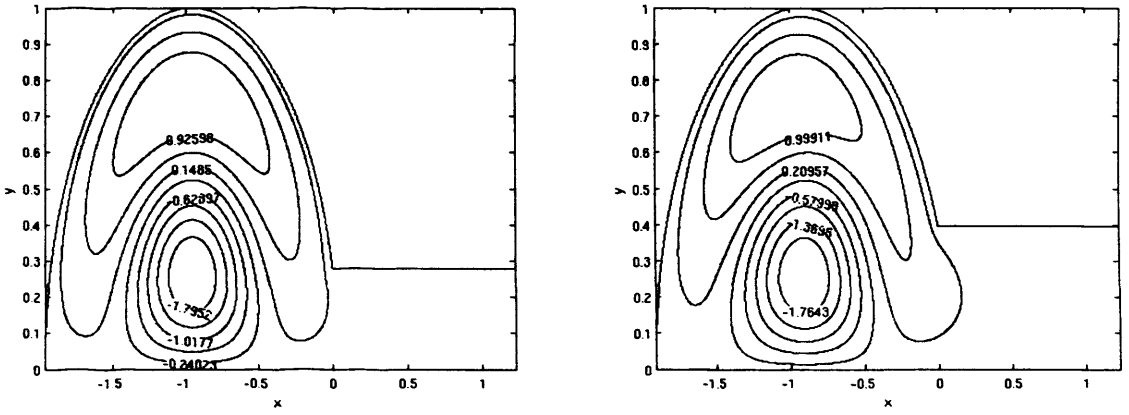

Figure 5.16: Contour plot of λ_{10} for $\theta = 0.09\pi$ and $\theta = 0.13\pi$

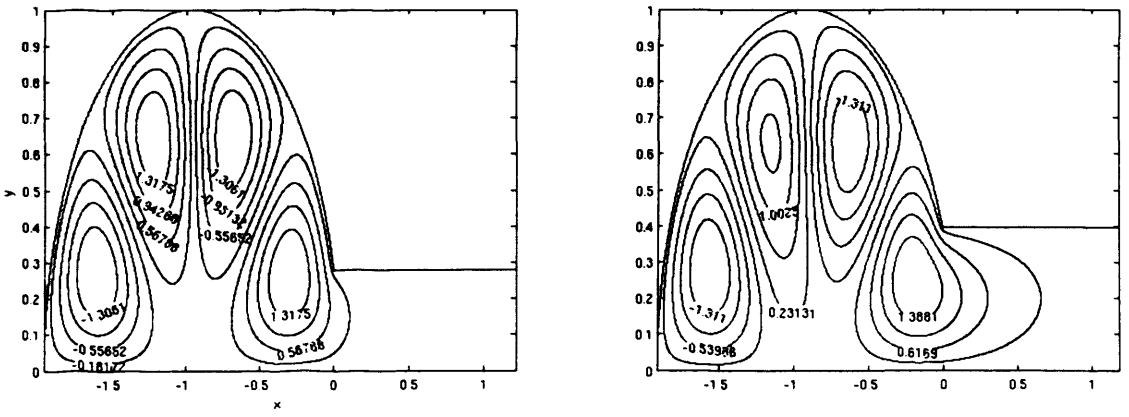

Figure 5.17: Contour plot of λ_{12} for $\theta = 0.09\pi$ and $\theta = 0.13\pi$

5.9 The half domain with Neumann boundary conditions on the symmetry axis

In the case where we impose Neumann boundary conditions on the original axis of symmetry (5.7) becomes

$$\psi(x,y) = \sum_{n=1}^{z+1} \phi_n(x) \cos\left(\left(n - \frac{1}{2}\right)\frac{\pi y}{\delta}\right)$$

where $\delta = \sin\theta$ and $z+1$ is the number of basis functions in the waveguide. Equation (5.18) is more complicated and it can't be obtained as in section 5.1 using simple intuition.

Firstly we need to consider the geometry to the right of the interface Γ. For the full domain there are Z evenly spaced points across the tube and by definition of Z, $Z = 2z+1$. Let y_l be the l^{th} evenly spaced point from the bottom of the interface for the complete domain. Since we have Neumann boundary conditions about the lines $y = 0$ then if we let η be the solution across the interface then for the points y_ν for $\nu \in \{1,...,z\}$ we have $y_\nu = -y_{2z+2-\nu}$ and from the Neumann boundary condition we have the symmetry relation $\eta(y_\nu) = \eta(y_{2z+2-\nu})$. Ignoring the term $\frac{1}{Z+1}$ in (5.18), then (5.18) becomes

$$\sum_{k=1}^{Z}\sum_{l=1}^{Z}\eta(y_l)\sin\left(\frac{k\pi}{\delta}\left(y_l+\frac{\delta}{2}\right)\right)\sin\left(\frac{k\pi}{\delta}\left(\xi+\frac{\delta}{2}\right)\right)$$

$$=\sum_{k=1}^{Z}\sum_{\nu=1}^{z}\eta(y_\nu)\sin\left(\frac{k\pi}{\delta}\left(y_\nu+\frac{\delta}{2}\right)\right)\sin\left(\frac{k\pi}{\delta}\left(\xi+\frac{\delta}{2}\right)\right)+$$

$$\sum_{k=1}^{Z}\eta(0)\sin\left(\frac{k\pi}{2}\right)\sin\left(\frac{k\pi}{\delta}\left(\xi+\frac{\delta}{2}\right)\right)+$$

$$\sum_{k=1}^{Z}\sum_{\nu=1}^{z}\eta(y_{2z+2-\nu})\sin\left(\frac{k\pi}{\delta}\left(y_{2z+2-\nu}+\frac{\delta}{2}\right)\right)\sin\left(\frac{k\pi}{\delta}\left(\xi+\frac{\delta}{2}\right)\right).$$

Writing $y_\nu = y_{2M+2-\nu}$ and $\eta(y_{2M+2-\nu}) = \eta(y_\nu)$ we obtain

$$\sum_{k=1}^{Z}\sum_{\nu=1}^{z}\eta(y_\nu)\left(\sin\left(\frac{k\pi}{\delta}\left(y_\nu+\frac{\delta}{2}\right)\right)+\sin\left(\frac{k\pi}{\delta}\left(-y_\nu+\frac{\delta}{2}\right)\right)\right)\sin\left(\frac{k\pi}{\delta}\left(\xi+\frac{\delta}{2}\right)\right)$$

$$+\sum_{k=1}^{Z}\eta(0)\sin\left(\frac{k\pi}{2}\right)\sin\left(\frac{k\pi}{\delta}\left(\xi+\frac{\delta}{2}\right)\right)$$

$$=\sum_{k=1}^{Z}\sum_{\nu=1}^{z}\eta(y_\nu)2\cos\left(\frac{k\pi}{\delta}y_\nu\right)\sin\left(\frac{k\pi}{2}\right)\sin\left(\frac{k\pi}{\delta}\left(\xi+\frac{\delta}{2}\right)\right)$$

$$+\sum_{k=1}^{Z}\eta(0)\sin\left(\frac{k\pi}{2}\right)\sin\left(\frac{k\pi}{\delta}\left(\xi+\frac{\delta}{2}\right)\right).$$

Further collecting like terms and using the fact that $Z = 2z + 1$ we see that

$\sin\left(\frac{k\pi}{2}\right)_{k=1,..N} = \sin\left(\frac{2\mu-1}{2}\pi\right)_{\mu=1,...M+1}$ leading to

$$\sum_{k=1}^{Z} \sin\left(\frac{k\pi}{2}\right)\left(2\sum_{\nu=1}^{Z}\eta(y_\nu)\cos\left(\frac{k\pi}{\delta}y_\nu\right)+\eta(0)\right)\sin\left(\frac{k\pi}{\delta}\left(\xi+\frac{\delta}{2}\right)\right)$$
$$=\sum_{\mu=1}^{z+1}\sin\left(\frac{2\mu-1}{2}\pi\right)\left(\sum_{\nu=1}^{z}\eta(y_\nu)2\cos\left(\frac{(2\mu-1)\pi}{\delta}y_\nu\right)+\eta(0)\right)\sin\left(\frac{(2\mu-1)\pi}{\delta}\left(\xi+\frac{\delta}{2}\right)\right).$$

Writing

$$\sin\left(\frac{(2\mu-1)\pi}{\delta}\left(\xi+\frac{\delta}{2}\right)\right)=\sin\left(\frac{2\mu-1}{\delta}\pi\xi\right)\cos\left(\frac{2\mu-1}{2}\pi\right)$$
$$+\cos\left(\frac{2\mu-1}{\delta}\pi\xi\right)\sin\left(\frac{2\mu-1}{2}\pi\right)$$

we finally obtain

$$\sum_{\mu=1}^{z+1}(-1)^{\mu+1}\left(2\sum_{\nu=1}^{z}\eta(y_\nu)\cos\left(\frac{2\mu-1}{\delta}\pi y_\nu\right)+\eta(0)\right)(-1)^{\mu+1}\cos\left(\frac{2\mu-1}{\delta}\pi\xi\right)$$
$$=\sum_{\mu=1}^{z+1}\left(2\sum_{\nu=1}^{z}\eta(y_\nu)\cos\left(\frac{(2\mu-1)\pi}{\delta}y_\nu\right)+\eta(0)\right)\cos\left(\frac{2\mu-1}{\delta}\pi\xi\right).$$

Since we cut the tube in half $\delta \longrightarrow 2\delta$ and with $z+1$ evenly spaced points in the half tube, then $y_\nu = \frac{\nu\delta}{z+1}$ for $\nu \in \{0,1,...,z\}$ and remembering that we must substitute $Z = 2z+1$ into (5.18) we obtain

$$\eta(\xi)=\frac{1}{z+1}\sum_{\mu=1}^{z+1}\left(2\sum_{\nu=1}^{z}\eta(y_\nu)\cos\left(\left(\mu-\frac{1}{2}\right)\frac{\pi\nu}{z+1}\right)+\eta(0)\right)\cos\left(\left(\mu-\frac{1}{2}\right)\frac{\pi\xi}{\delta}\right).$$

The matrix G in (5.19) becomes

$$G_{m1} = \frac{1}{z+1} \sum_{\mu=1}^{z+1} \cos\left(\left(k - \frac{1}{2}\right) \frac{\pi \xi_m}{\delta}\right) \tag{5.39}$$

$$G_{mn} = \frac{2}{z+1} \sum_{\mu=1}^{z+1} \cos\left(\left(\mu - \frac{1}{2}\right) \frac{\pi(n-1)}{z+1}\right) \cos\left(\left(\mu - \frac{1}{2}\right) \frac{\pi \xi_m}{\delta}\right) \quad n > 1.$$

Table 5.6 contains the eigenvalues obtained for various mesh densities and width of the tube.

(m,n,p)	θ	λ_1	λ_2	λ_4	λ_6
(53,7,3)	0.09π	5.68456	14.0923	24.8559	29.6679
(53,7,4)	0.09π	5.68466	14.0947	24.8569	29.6711
(51,9,3)	0.1π	5.66006	13.9214	24.0890	-
(51,9,4)	0.1π	5.66010	13.9215	24.0861	-
(51,9,3)	0.11π	5.63202	13.7084	-	-
(51,9,4)	0.11π	5.63202	13.7082	-	-
(49,11,3)	0.12π	5.60022	13.4448	-	-
(49,11,4)	0.12π	5.60041	13.4456	-	-
(49,11,3)	0.13π	5.56479	13.1170	-	-
(49,11,4)	0.13π	5.56496	13.1177	-	-
(47,13,3)	0.14π	5.52521	12.6989	-	-
(47,13,4)	0.14π	5.52560	12.7007	-	-

Table 5.6: Eigenvalues for various mesh densities with Dirichlet conditions on the former axis of symmetry

Equation (5.37) becomes

$$\dot{\lambda} = -\frac{\pi^2}{\delta^2} \sum_{m=1}^{z+1} \sum_{n=1}^{z+1} \frac{mn \cos n\pi \cos n\pi}{1 - \rho_m \rho_n} \int_0^{2\pi} \phi_m(x) \phi_n(x) dx.$$

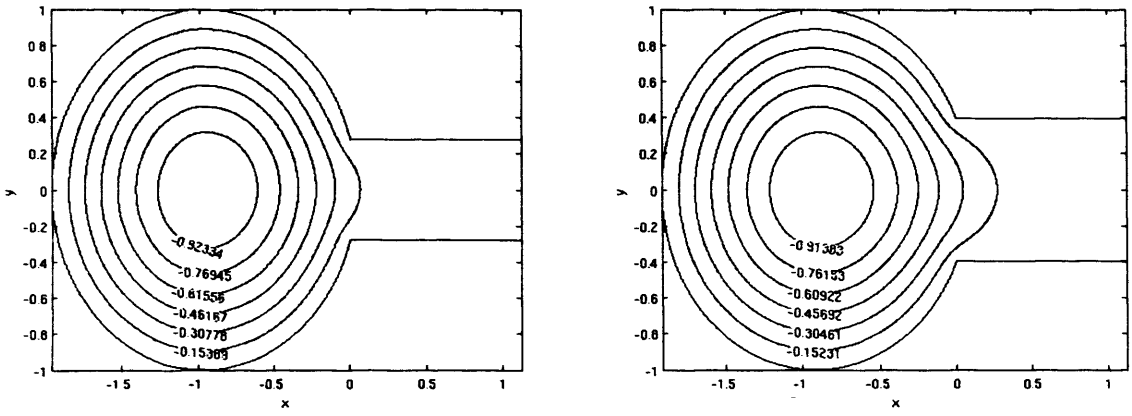

Figure 5.18: Contour plot of λ_1 for $\theta = 0.09\pi$ and $\theta = 0.13\pi$

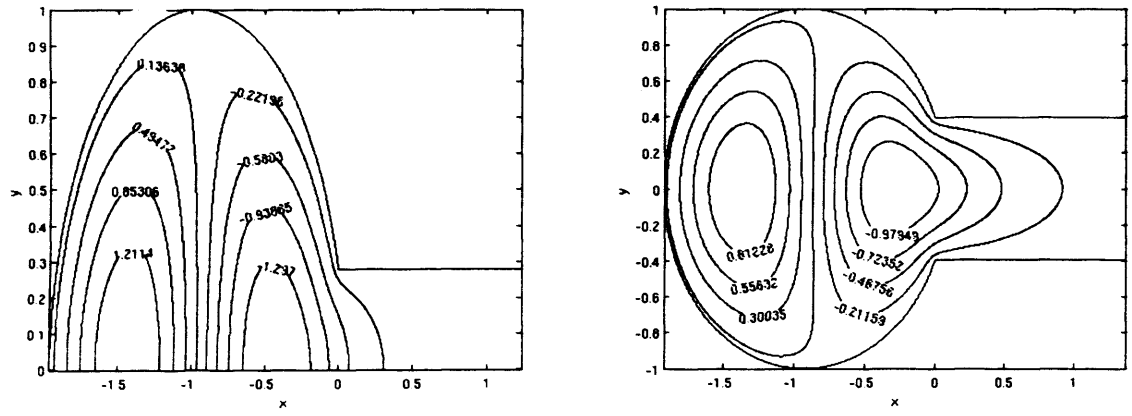

Figure 5.19: Contour plot of λ_2 for $\theta = 0.09\pi$ and $\theta = 0.13\pi$

θ	$\dot{\lambda}_1$	$\dot{\lambda}_2$	$\dot{\lambda}_3$	$\dot{\lambda}_4$	$\dot{\lambda}_5$	$\dot{\lambda}_8$	$\dot{\lambda}_{10}$	$\dot{\lambda}_{12}$
0.09π	-0.603	-4.41	-0.0614	-17.1	-0.462	-1.70	-0.297	-4.60
0.1π	-0.723	-5.50	-0.0890	-31.9	-0.679	-2.55	-0.477	-7.10
0.11π	-0.838	-6.97	-0.122	-	-0.950	-3.67	-0.755	-10.96
0.12π	-0.980	-9.04	-0.166	-	-1.31	-5.29	-1.20	-17.75
0.13π	-1.12	-11.80	-0.216	-	-1.76	-7.55	-2.17	-32.67
0.14π	-1.30	-15.9	-0.285	-	-2.39	-11.2	-4.75	-

Table 5.7: Theoretical values for the derivative of λ with respect to δ for various δ

5.10 A parabolic potential

We now consider the full domain and modify the potential to

$$V = \begin{cases} Ax^2 & \mathrm{x} < 0 \\ By^2 \sin^2(x) & \mathrm{x} \geq 0 \end{cases} \tag{5.40}$$

where A and B are some positive constants. The aim of using this potential is to force the solution to the right of the domain into the waveguide. Taking $B = 1$ with $\theta = 0.08\pi$, $\theta = 0.09\pi$ and $\theta = 0.1\pi$ gives us spectral gaps at $\lambda \in (-\infty, 39.895)$, $\lambda \in (-\infty, 31.700)$ and $\lambda \in (-\infty, 25.839) \cup (26.088, 26.090)$ respectively. As A increases the solution moves into the waveguide and it's total density is reduced thus increasing the eigenvalue. We shall let $A = 21$.

θ	0.095π	0.105π	0.115π	0.125π	0.135π
λ_1	-0.67	-0.78	-0.91	-1.1	-1.2
$P_1'(\theta)$	-0.82	-0.94	-1.1	-1.2	-1.4
λ_2	-4.9	-6.2	-7.9	-10.3	-13.6
$P_2'(\theta)$	-5.8	-7.2	-8.9	-11.3	-14.5
λ_3	-0.076	-0.10	-0.14	-0.19	-0.25
$P_3'(\theta)$	-0.092	-0.13	-0.17	-0.22	-0.29
λ_4	-24.5	-	-	-	-
$P_4'(\theta)$	-25.6	-	-	-	-
λ_5	-0.57	-0.80	-1.1	-1.5	-2.0
$P_5'(\theta)$	-0.69	-0.96	-1.3	-1.8	-2.3
λ_8	-2.3	-3.1	-4.4	-6.3	-9.1
$P_8'(\theta)$	-2.5	-3.6	-5.0	-7.0	-9.9
λ_{10}	-0.38	-0.60	-0.95	-1.6	-3.2
$P_{10}'(\theta)$	-0.43	-0.68	-1.1	-1.8	-3.3
λ_{12}	-6.7	-8.9	-13.7	-23.7	-
$P_{12}'(\theta)$	-6.7	-9.9	-15.0	-24.3	-

Table 5.8: Comparison of the theoretical and actual derivatives obtained for λ with respect to δ continued.

In this case the Hamiltonian as in (3.7) becomes

$$A_{pq} = \begin{cases} 1 & \text{if } q = p+n \\ \frac{k^2\pi^2}{\delta^2} + \frac{\delta^3}{4}\left(\frac{1}{6} - \frac{1}{m^2\pi^2}\right)\sin(x) - \lambda & \text{if } p = q+n \\ \frac{2\delta^3 kl(\cos(l\pi)\cos(k\pi)-1)}{\pi^2(k-l)^2(k+l)^2}\sin(x) & \text{if } p > n \;\; q < n \;\; p \neq q+n; \end{cases} \tag{5.41}$$

Table 5.9 contains eigenvalues as a function of θ for $A = 21$.

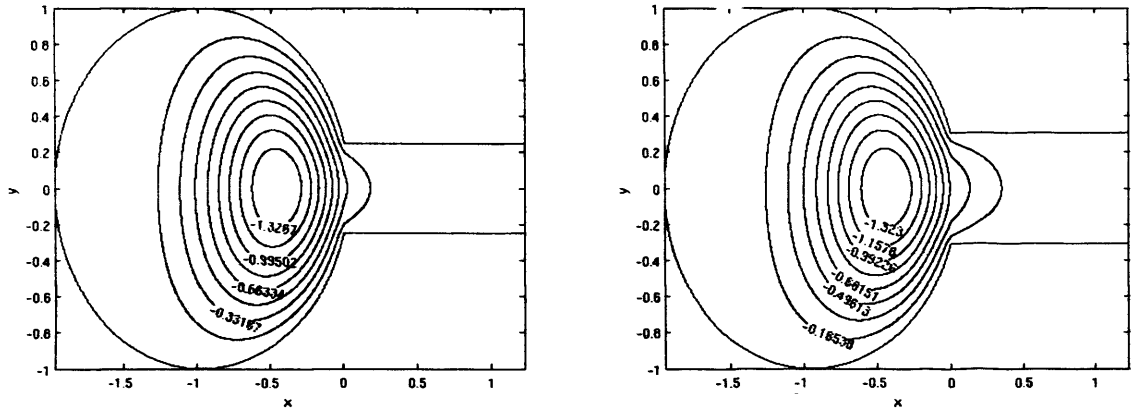

Figure 5.20: Contour plot of λ_1 for $\theta = 0.8\pi$ and $\theta = 0.1\pi$

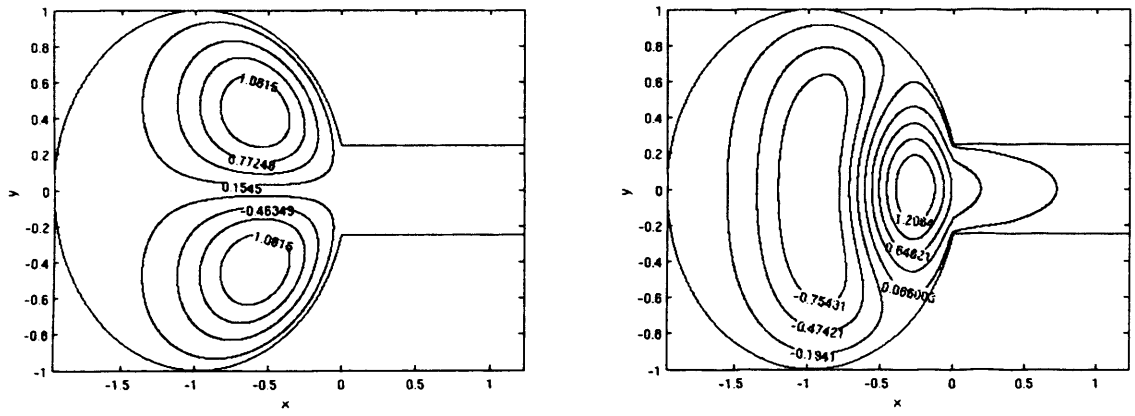

Figure 5.21: Contour plot of λ_1 and λ_3 for $\theta = 0.8\pi$

(m,n,p)	θ	λ_1	λ_2	λ_3
(53,15,3)	0.08π	16.8676	28.6950	32.3882
(53,15,4)	0.08π	16.8674	28.6948	32.3873
(53,15,3)	0.09π	16.3970	28.4500	-
(53,15,4)	0.09π	16.3967	28.4502	-
(51,17,3)	0.1π	15.8547	-	-
(51,17,4)	0.1π	15.8541	-	-

Table 5.9: Eigenvalues of the periodic potential for various tube widths

5.11 The error in $\frac{\partial\lambda}{\partial\delta}$

Let us consider a small section of the domain near the corners of Fig 5.1 with radius ϵ

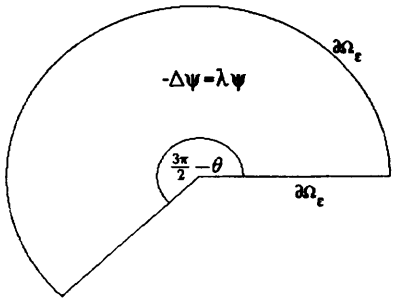

Assuming that $\psi|_{\partial\Omega_\epsilon} = 0$ then the solutions are $\psi_n(r,\theta) = J_{\frac{n\pi}{\Theta}}(\sqrt{\lambda}r)\sin(\frac{n\pi}{\Theta}\theta)$ for $n \in \{1,...,\infty\}$ and in terms of θ in Fig 5.1 $\Theta = \frac{3\pi}{2} - \theta$. We will now find to which Sobolev space these solutions belong.

Given that the n^{th} order Bessel function is given by

$$J_n(r) = \left(\frac{r}{2}\right)^n \sum_{k=0}^{\infty} \frac{(-1)^k}{2^{2p}p!(n+1)!} r^{2p}$$

then near the corner

$$J_{\frac{n\pi}{\Theta}}(r) \approx cr^{\frac{n\pi}{\Theta}}.$$

Differentiating this function ν times and integrating over r in polar coordinates we obtain

$$c\int_0^{\epsilon} |r^{\frac{n\pi}{\Theta}-\nu}|^2 r dr = cr^{\frac{2n\pi}{\Theta}+2-2\nu}|_0^{\epsilon}$$

and we require $\frac{2n\pi}{\Theta} - 2\nu + 2 > 0$ to guarantee convergence or

$$\nu < 1 + \frac{n\pi}{\Theta}.$$

In the case where $\theta = \frac{\pi}{10}$ we have $\Theta = \frac{7\pi}{5}$ and so $\nu < \frac{12}{7}$. As $r \to 0$ then $\nu < \frac{5}{3}$.

The following theorem is taken from [4, Theorem 3.1.5].

Theorem: For a given triangle K in the mesh there exists a constant c_K such that

$$||\psi - \Pi_K \psi||_{H^m(K)} < c_K |\psi|_{H^{k+1}(K)}$$

for $0 \leq m \leq k+1$ where k is the order of the interpolating polynomial which in our case is 1 and $\Pi_K \psi$ is the interpolated solution. From this we see that our solutions will converge in H^k for $k \leq 2$. In deriving $\dot{\lambda}$ we required the first order derivative on the boundary $\partial\Omega$ as in (5.36) and we see that the solution near the corner is in $H^{\frac{12}{7}}$. We can thus expect convergence but not a very good rate of convergence as is evidenced by the poor agreement between theoretical and experimental values for $\frac{\partial\psi}{\partial\delta}$.

5.12 Conclusion

Looking at the derivative of the eigenfunction with respect to tube width and the plots, we see that eigenfunctions which penetrate strongly into the tube are more susceptible to changes in δ. As the tube is widened the eigenvalues become more sensitive to the tube width since more of the eigenfunction is able to get into the tube. In comparing the theoretical and experimental values for the derivative of the eigenvalue with respect to tube width it can be seen that for eigenvalues which are not strongly sensitive to tube width that the theoretical estimate is an underestimate by approximately 15%. For eigenvalues more sensitive to the tube width δ, we see that the theoretical estimate starts as an underestimate but eventually becomes an overestimate as δ increases.

In the following chapter we will use the finite element method to find the eigenvalues of Fig 5.1 by deriving an analogous expression to (5.24) for the finite element method. Given these two sets of eigenvalues calculated using the finte element and finte differences methods, we shall imake a comparison between them in the last chapter.

Chapter 6

Calculation of the eigenvalues using the finite element method

6.1 Introduction

In this last chapter we shall use the method of finite elements instead of the method of finite differences as we did in the previous chapter to solve $-\Delta\psi + \lambda\psi = 0$ subject to $\psi|_{\partial\Omega\setminus\Gamma} = 0$ and $\frac{\partial\psi}{\partial x}|_\Gamma = \Lambda(\lambda)\psi|_\Gamma$ in the modified part of the circular domain.

As a consequence of the work to be undertaken in this chapter, we will conclude with a comparison of the eigenvalues obtained from the method of finite differences and that of finite elements.

6.2 The Method of Finite Elements

We begin with an integral expression for the weak formulation which we shall show that when minimised we obtain the original problem namely that shown in Fig 5.1. Let $I[\psi]$ be

$$I[\psi] = \frac{1}{2}\int_\Omega (|\nabla\psi|^2 - \lambda\psi^2)d\mathbf{x} - \frac{1}{2}\int_\Gamma \langle\psi, \Lambda(\lambda)\psi\rangle \mathbf{n}.d\mathbf{l}, \tag{6.1}$$

where $\Lambda(\lambda)$ is a pseudo differential operator. $I[\psi]$ can be minimised by setting $I[\psi + \delta\psi] - I[\psi]$ to zero and solving (where $\delta\psi$ is a small increment in ψ or more precisely $\delta\psi(x, y) = \psi(x + \delta x, y + \delta y) - \psi(x, y)$) thus

$$I[\psi+\delta\psi]-I[\psi] = \frac{1}{2}\int_\Omega (|\nabla(\psi+\delta\psi)|^2-\lambda(\psi+\delta\psi)^2)d\mathbf{x}-\frac{1}{2}\int_\Gamma \langle\psi+\delta\psi, \Lambda(\lambda)(\psi+\delta\psi)\rangle\mathbf{n}.d\mathbf{l}$$

$$-\frac{1}{2}\int_{\Omega}(|\nabla\psi|^2-\lambda\psi^2)d\mathbf{x}+\frac{1}{2}\int_{\Gamma}\langle\psi,\Lambda(\lambda)\psi\rangle\mathbf{n}.d\mathbf{l}$$

which reduces to

$$\int_{\Omega}(\nabla\psi.\nabla\delta\psi-\lambda\psi\delta\psi)d\mathbf{x}-\frac{1}{2}\int_{\Gamma}(\langle\psi,\Lambda(\lambda)\delta\psi\rangle+\langle\delta\psi,\Lambda(\lambda)\psi\rangle)\mathbf{n}.d\mathbf{l}$$

$$-\frac{1}{2}\int_{\Gamma}\langle\delta\psi,\Lambda(\lambda)\delta\psi\rangle\mathbf{n}.d\mathbf{l}+\frac{1}{2}\int_{\Omega}(\nabla\delta\psi.\nabla\delta\psi-\lambda(\delta\psi)^2)d\mathbf{x}=0.$$

The second line of the above is negligible compared to those on the first line provided that $\delta\psi << \psi$ and so neglecting it we obtain

$$\int_{\Omega}(\nabla\psi.\nabla\delta\psi-\lambda\psi\delta\psi)d\mathbf{x}-\frac{1}{2}\int_{\Gamma}(\langle\psi,\Lambda(\lambda)\delta\psi\rangle+\langle\delta\psi,\Lambda(\lambda)\psi\rangle)\mathbf{n}.d\mathbf{l}=0. \quad (6.2)$$

We now apply the divergence theorem giving from (6.2)

$$\int_{\Omega}\nabla\psi.\nabla\delta\psi d\mathbf{x}=\frac{1}{2}\int_{\Omega}\nabla.(\delta\psi\nabla\psi)d\mathbf{x}+\frac{1}{2}\int_{\Omega}\nabla.(\psi\nabla\delta\psi)d\mathbf{x}-\frac{1}{2}\int_{\Omega}\psi\Delta\delta\psi d\mathbf{x}-\frac{1}{2}\int_{\Omega}\delta\psi\Delta\psi d\mathbf{x}.$$

We thus obtain

$$\int_{\Omega}(\frac{1}{2}\delta\psi\Delta\psi+\frac{1}{2}\psi\Delta\delta\psi+\lambda\psi\delta\psi)d\mathbf{x}=\frac{1}{2}\int_{\Gamma}\langle\delta\psi,\nabla\psi\rangle.d\mathbf{l}+\frac{1}{2}\int_{\Gamma}\langle\psi,\nabla\delta\psi\rangle.d\mathbf{l}$$

$$-\frac{1}{2}\int_{\Gamma}(\langle\delta\psi,\Lambda(\lambda)\psi\rangle+\langle\psi,\Lambda(\lambda)\delta\psi\rangle)\mathbf{n}.d\mathbf{l}.$$

Making use of the fact that $\psi|_{\partial\Omega\setminus\Gamma} = 0$ and rearranging we may rewrite the above expression as

$$\frac{1}{2}\int_{\Omega}(\Delta\psi + \lambda\psi)\delta\psi d\mathbf{x} + \frac{1}{2}\int_{\Omega}(\Delta\delta\psi + \lambda\delta\psi)\psi d\mathbf{x} = \frac{1}{2}\int_{\Gamma}\langle\delta\psi, \nabla\psi - \mathbf{n}\Lambda(\lambda)\psi\rangle.d\mathbf{l}$$

$$+\frac{1}{2}\int_{\Gamma}\langle\psi, \nabla\delta\psi - \mathbf{n}\Lambda(\lambda)\delta\psi\rangle.d\mathbf{l}.$$

This yields $\Delta\psi + \lambda\psi = 0$ and $n \cdot \nabla\psi = \Lambda(\lambda)\psi$ where $n = \begin{pmatrix} 1 \\ 0 \end{pmatrix}$ on the interface Γ. We see that in minimising this integral we obtain the equations for ψ which when solved yield solutions to our problem.

Thus the minimum of (6.1) over a finite element mesh gives a solution of the problem. Now consider a finite element mesh in Ω consisting of N_t triangles and N_p nodes, then we can minimise (6.1) on this mesh using a particular linear combination of functions $\phi_k(x, y)$ for $k = 1, 2, ..., N_p$. Consider the following:

$$\psi(x, y) = \sum_{k=1}^{N_p} \gamma_k \phi_k(x, y) \tag{6.3}$$

where γ_k is the value of ψ at the point (x_k, y_k) for $k = 1, 2, ..., N_p$ and $\phi_k(x, y)$ is a piecewise linear function whose properties will now be explained.

Given a node (x_l, y_l) then the function $\phi_l(x_1, y_1) = 1$ and zero on the other nodes of the triangles of the domain, or $\phi_k(x_l, y_l) = \delta_{kl}$ for $\{k, l\} \in \{1, ..., N_p\}$. Consider a section of mesh for a particular triangle, such as triangle number n which we shall denote by T_n as illustrated below:

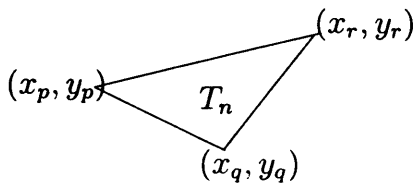

Figure 6.1: Example of a triangle amongst the finite element mesh

Then we may define a function f as follows. Let $f(n,1) = p$, $f(n,2) = q$ and $f(n,3) = r$. Then $\phi_{f(n,s)}(x,y) := a_n^{(s)} + b_n^{(s)}x + c_n^{(s)}y$ for $s = \{1,2,3\}$ and according to the desired properties of the hat function on letting $t = \{1,2,3\}$ we may impose the following condition:

$$\phi_{f(n,s)}(x_{f(n,t)}, y_{f(n,t)}) = \delta_{s,t}$$

which produces the following equation

$$\begin{pmatrix} 1 \\ 0 \\ 0 \end{pmatrix} = \begin{pmatrix} 1 & x_p & y_p \\ 1 & x_q & y_q \\ 1 & x_r & y_r \end{pmatrix} \begin{pmatrix} a_n^{(1)} \\ b_n^{(1)} \\ c_n^{(1)} \end{pmatrix}.$$

For the node (x_p, y_p) and for the nodes (x_q, y_q) and (x_r, y_r) we have

$$\begin{pmatrix} 0 \\ 1 \\ 0 \end{pmatrix} = \begin{pmatrix} 1 & x_p & y_p \\ 1 & x_q & y_q \\ 1 & x_r & y_r \end{pmatrix} \begin{pmatrix} a_n^{(2)} \\ b_n^{(2)} \\ c_n^{(2)} \end{pmatrix} \text{ and } \begin{pmatrix} 0 \\ 0 \\ 1 \end{pmatrix} = \begin{pmatrix} 1 & x_p & y_p \\ 1 & x_q & y_q \\ 1 & x_r & y_r \end{pmatrix} \begin{pmatrix} a_n^{(3)} \\ b_n^{(3)} \\ c_n^{(3)} \end{pmatrix}$$

respectively. We thus see that $\phi_k(x,y)$ is a piecewise linear function since its coefficients a, b and c depend on which triangle the function is defined over. Note that the hat function is continuous but not differentiable across the edges of the triangles.

This leads to the following approximation for $\psi(x,y)$ over the triangle T_n:

$$\psi(x,y) \approx \gamma_{f(n,1)}\phi_{f(n,1)}(x,y) + \gamma_{f(n,2)}\phi_{f(n,2)}(x,y) + \gamma_{f(n,3)}\phi_{f(n,3)}(x,y)$$

or

$$\psi(x,y) \approx \gamma_p\phi_p(x,y) + \gamma_q\phi_q(x,y) + \gamma_r\phi_r(x,y)$$

for $(x,y) \in \Omega_{T_n}$ where $\bigcup_{k=1}^{N_T} \Omega_{T_k} = \Omega$ and

$$\phi_{f(n,k)}(x,y) = \begin{pmatrix} 1 & x & y \end{pmatrix} \begin{pmatrix} 1 & x_p & y_p \\ 1 & x_q & y_q \\ 1 & x_r & y_r \end{pmatrix}^{-1} e_k$$

for $k = \{1,2,3\}$ and e_k is the unit normal vector with the k^{th} component equal to 1 and the rest zero.

We now proceed to minimise (6.1) by choosing appropriate values of γ_k in (6.3). Substituting (6.3) into (6.1) we have

$$I[\psi] = \frac{1}{2}\int_\Omega \left[\left(\sum_{k=1}^{N_p} \gamma_k \frac{\partial \phi_k}{\partial x} \right)^2 + \left(\sum_{k=1}^{N_p} \gamma_k \frac{\partial \phi_k}{\partial y} \right)^2 - \lambda \left(\sum_{k=1}^{N_p} \gamma_k \phi_k \right)^2 \right] d\mathbf{x}$$

$$-\int_{-\frac{\delta}{2}}^{\frac{\delta}{2}} \frac{1}{2} \sum_{k=1}^{N_p} \sum_{l=1}^{N_p} \gamma_k \gamma_l \langle \phi_k, \Lambda(\lambda) \phi_l \rangle dy$$

The above expression can be minimised by differentiating with respect to γ_j and equating to zero as follows:

$$0 = \int_\Omega \left(\sum_{k=1}^{N_p} \gamma_k \frac{\partial \phi_k}{\partial x} \frac{\partial \phi_j}{\partial x} + \sum_{k=1}^{N_p} \gamma_k \frac{\partial \phi_k}{\partial y} \frac{\partial \phi_j}{\partial y} - \lambda \sum_{k=1}^{N_p} \gamma_k \phi_k \phi_j \right) d\mathbf{x}$$

$$+ \int_{-\frac{\delta}{2}}^{\frac{\delta}{2}} \sum_{k=1}^{N_p} \frac{1}{2} \gamma_k \langle \phi_j, \Lambda(\lambda) \phi_k \rangle dy + \int_{-\frac{\delta}{2}}^{\frac{\delta}{2}} \sum_{k=1}^{N_p} \frac{1}{2} \gamma_k \langle \phi_k, \Lambda(\lambda) \phi_j \rangle dy. \tag{6.4}$$

Here we write $\psi(0, y) = \psi(y)$ and likewise $\phi_k(0, y) = \phi_k(y)$ and denote the interface by Γ. We therefore make the following linear approximation to the derivative on Γ

$$\frac{\partial \psi}{\partial x}(y) = \sum_{k=1}^{N_\Gamma} \tau_k \phi_k(y)$$

where N_Γ is the number of nodes on the boundary Γ and τ_k is the derivative of the ψ at node $(0, y_k)$ ie $\frac{\partial \psi}{\partial x}(y_k)|_\Gamma = \tau_k$. This together with the fact that $\psi(y) = \sum_{k=1}^{N_\Gamma} \gamma_k \phi_k(y)$ then

$$\sum_{k=1}^{N_\Gamma} \gamma_k \langle \phi_j(y), \Lambda(\lambda) \phi_k(y) \rangle = \sum_{k=1}^{N_\Gamma} \langle \phi_j(y), \phi_k(y) \rangle \tau_k$$

and for the second term

$$\sum_{k=1}^{N_\Gamma} \gamma_k \langle \Lambda^*(\lambda) \phi_k(y), \phi_j(y) \rangle = \sum_{k=1}^{N_\Gamma} \langle \phi_k(y), \phi_j(y) \rangle \tau_k.$$

From (5.21) and (5.22) we have

$$\tau_k = \sum_{l=1}^{N_\Gamma} \Lambda_{kl}(\lambda)\gamma_l \quad \text{and thus} \quad \frac{\partial \psi}{\partial x}(y) = \sum_{k=1}^{N_\Gamma}\sum_{l=1}^{N_\Gamma} \Lambda_{kl}(\lambda)\gamma_l \phi_k(y).$$

The integrals in (6.4) thus become

$$\int_{-\frac{\delta}{2}}^{\frac{\delta}{2}} \sum_{k=1}^{N_\Gamma}\sum_{l=1}^{N_\Gamma} \phi_j(y)\Lambda_{kl}(\lambda)\gamma_l\phi_k(y)dy = \sum_{k=1}^{N_\Gamma}\sum_{l=1}^{N_\Gamma} \Lambda_{kl}(\lambda)\gamma_l \int_{-\frac{\delta}{2}}^{\frac{\delta}{2}} \phi_j(y)\phi_k(y)dy.$$

Since ϕ_k is a hat function there are three values of k namely $k = j-1$, $k = j$ and $k = j+1$ for which the integral is non zero. We have

$$\phi_k(y) = \frac{y - y_{k-1}}{y_k - y_{k-1}} \text{ for } y \in [y_{k-1}, y_k) \text{ and } \phi_k(y) = \frac{y_{k+1} - y}{y_{k+1} - y_k} \text{ for } y \in [y_k, y_{k+1})$$

and thus if $k = j-1$ we have

$$\int_{-\frac{\delta}{2}}^{\frac{\delta}{2}} \phi_{j-1}(y)\phi_j(y)dy = \int_{y_{j-1}}^{y_j} \frac{(y_j - y)(y - y_{j-1})}{(y_j - y_{j-1})^2}dy = \frac{1}{6}(y_j - y_{j-1})$$

likewise

$$\int_{-\frac{\delta}{2}}^{\frac{\delta}{2}} \phi_j(y)\phi_{j+1}(y)dy = \frac{1}{6}(y_{j+1} - y_j).$$

The diagonal elements of (6.4) are

$$\int_{-\frac{\delta}{2}}^{\frac{\delta}{2}} \phi_k^2(y)dy = \int_{y_{k-1}}^{y_k} \frac{(y - y_{k-1})^2}{(y_k - y_{k-1})^2}dy + \int_{y_k}^{y_{k+1}} \frac{(y_{k+1} - y)^2}{(y_{k+1} - y_k)^2}dy = \frac{1}{3}(y_{k+1} - y_{k-1}).$$

This leads to the following expression for a given value of j in the second line

of (6.4)

$$\sum_{l=1}^{N_\Gamma}\left(\frac{1}{6}\Lambda_{(j-1)l}(\lambda)(y_j-y_{j-1})+\frac{1}{3}\Lambda_{jl}(\lambda)(y_{j+1}-y_{j-1})+\frac{1}{6}\Lambda_{(j+1)l}(\lambda)(y_{j+1}-y_j)\right)\gamma_l$$

which when we interpret (6.4) as the quadratic form of a matrix we obtain the expression

$$C_{jk}=\int_\Omega\left(\frac{\partial\phi_k(x,y)}{\partial x}\frac{\partial\phi_j(x,y)}{\partial x}+\frac{\partial\phi_k(x,y)}{\partial y}\frac{\partial\phi_j(x,y)}{\partial y}\right)d\mathbf{x} \qquad (6.5)$$

$$+\sum_{l=1}^{N_\Gamma}\left(\frac{1}{6}\Lambda_{(j-1)l}(\lambda)(y_j-y_{j-1})+\frac{1}{3}\Lambda_{jl}(\lambda)(y_{j+1}-y_{j-1})+\frac{1}{6}\Lambda_{(j+1)l}(\lambda)(y_{j+1}-y_j)\right)$$

iff $y_j\in\Gamma$ and

$$C_{jk}=\int_\Omega\left(\frac{\partial\phi_k(x,y)}{\partial x}\frac{\partial\phi_j(x,y)}{\partial x}+\frac{\partial\phi_k(x,y)}{\partial y}\frac{\partial\phi_j(x,y)}{\partial y}\right)d\mathbf{x}$$

iff $y_j\notin\Gamma$ with $\{l,k\}\in\{1,2,...,N_p\}$ and

$$B_{jk}=\int_\Omega\phi_k(x,y)\phi_j(x,y)d\mathbf{x}$$

where we define the matrices $B=(B_{ij})_{i,j=1}^{N_p}$ and $C=(C_{ij})_{i,j=1}^{N_p}$ for $\{l,k\}\in\{1,2,...,N_p\}$. Letting $\mathbf{d}=[\gamma_1,...,\gamma_p]^T$ we obtain

$$C\mathbf{d}=\lambda B\mathbf{d}.$$

The integrals involved in obtaining B are calculated by evaluating $\phi_k(x,y)$

at the centroid and multiplying by the area of the triangle. The coordinates of the centroid (x_c, y_c) are given by

$$x_c = \frac{x_p + x_q + x_r}{3} \quad \text{and} \quad y_c = \frac{y_p + y_q + y_r}{3}$$

and thus we have

$$\int_{T_n} \phi_k(x,y)\phi_l(x,y)d\mathbf{x} = \phi_k(x_c,y_c)\phi_l(x_c,y_c)A_{T_n} = \frac{A_{T_n}}{9} \tag{6.6}$$

where A_{T_n} is the area of triangle T_n. The table below gives the eigenvalues calculated using this method of approximating the mass matrix B.

(N_T, N_p, N_Γ)	θ	λ_1	λ_2	λ_3
$(4336, 2239, 11, 9)$	0.09π	5.69415	14.1518	14.7183
$(17344, 8813, 23, 21)$	0.09π	5.67782	14.1136	14.6873
$(4416, 2281, 15, 13)$	0.1π	5.66846	13.9707	14.7153
$(17664, 8977, 31, 23)$	0.1π	5.66273	13.9369	14.6846
$(4608, 2377, 15, 13)$	0.11π	5.64069	13.7589	14.7111
$(18432, 9361, 31, 23)$	0.11π	5.63483	13.7246	14.6806
$(4480, 2313, 15, 13)$	0.12π	5.60943	13.4972	14.7067
$(17920, 9105, 31, 23)$	0.12π	5.60339	13.4627	14.6759
$(4432, 2291, 19, 17)$	0.13π	5.57332	13.1622	14.7009
$(17728, 9013, 39, 27)$	0.13π	5.56764	13.1322	14.6696
$(4400, 2275, 19, 17)$	0.14π	5.53390	12.7405	–
$(17600, 8949, 39, 27)$	0.14π	5.52822	12.7135	–

Table 6.1: Eigenvalues for several widths and mesh densities where the mass matrix is evaluated using quadrature

We remind the reader that the above calculations have been performed using approximation (6.6) to the mass matrix.

We can perform the integrals of the mass matrix exactly. If one does this then one obtains the following results

$$\int_{T_n} \phi_k(x,y)\phi_l(x,y)d\mathrm{x} = \begin{cases} \frac{A_n}{6} & \text{iff } k = l \\ \frac{A_n}{12} & \text{iff } k \neq l. \end{cases} \tag{6.7}$$

In Table 6.2, we have the eigenvalues obtained from using this more accurate calculation of the mass matrix. We note that the exact calculations of the mass matrix results in an improvement of order 10^{-3} in the eigenvalues calculated.

$(N_T, N_p, N_\Gamma, N_b)$	θ	λ_1	λ_2	λ_3	λ_4	λ_5	λ_6
(4336,2239,11,9)	0.09π	5.69179	14.1373	14.7024	24.9752	26.4203	29.7855
(17344,8813,23,21)	0.09π	5.68724	14.1100	14.6833	24.8975	26.3586	29.7056
(69376,34969,47,21)	0.09π	5.68582	14.1016	14.6785	24.8741	26.3424	29.6833
(69376,34969,47,31)	0.09π	5.68585	14.1017	14.6785	24.8744	26.3425	29.6834
(4416,2281,15,13)	0.1π	5.66621	13.9572	14.6989	24.1808	26.4058	-
(17664,8977,31,23)	0.1π	5.66220	13.9337	14.6804	24.1198	26.3372	-
(70656,35617,63,23)	0.1π	5.66098	13.9265	14.6757	24.1013	26.3217	-
(70656,35617,63,31)	0.1π	5.66102	13.9268	14.6757	24.1017	26.3218	-
(4608,2377,15,13)	0.11π	5.63847	13.7461	14.6952	-	-	-
(18432,9361,31,23)	0.11π	5.63431	13.7216	14.6767	-	-	-
(73728,37153,63,23)	0.11π	5.63300	13.7139	14.6720	-	-	-
(73728,37153,63,31)	0.11π	5.63305	13.7142	14.6720	-	-	-
(4480,2313,15,13)	0.12π	5.60724	13.4852	14.6906	-	-	-
(17920,9105,31,23)	0.12π	5.60288	13.4599	14.6719	-	-	-
(71680,36219,63,23)	0.12π	5.60147	13.4518	14.6671	-	-	-
(71680,36219,63,31)	0.12π	5.60153	13.4521	14.6671	-	-	-
(4432,2291,19,17)	0.13π	5.57114	13.1518	14.6848	-	-	-
(17728,9013,39,27)	0.13π	5.56720	13.1301	14.6656	-	-	-
(70912,35753,79,23)	0.13π	5.56591	13.1233	14.6607	-	-	-
(70912,35753,79,31)	0.13π	5.56600	13.1235	14.6607	-	-	-
(4400,2275,19,17)	0.14π	5.53175	12.7317	-	-	-	-
(17600,8949,39,27)	0.14π	5.52780	12.7118	-	-	-	-
(70400,35497,79,23)	0.14π	5.52655	12.7053	-	-	-	-
(70400,35497,79,31)	0.14π	5.52659	12.7057	-	-	-	-

Table 6.2: Eigenvalues for different tube widths and mesh densities for the exact calculation of the mass matrix

6.3 The parabolic potential again

Here we have the same potential as in section (5.10). The differences arising from using the potential (5.40) to (6.5) are to U and V in the calculation of $\Lambda(\lambda)$ in (5.22) which we call $\tilde{\Lambda}(\lambda)$ and thus (6.5) becomes

$$C_{jk} = \int_{\Omega} \left(\frac{\partial \phi_k(x,y)}{\partial x} \frac{\partial \phi_j(x,y)}{\partial x} + \frac{\partial \phi_k(x,y)}{\partial y} \frac{\partial \phi_j(x,y)}{\partial y} + 21x^2 \phi_k(x,y)\phi_j(x,y) \right) d\mathbf{x}$$

$$+ \sum_{l=1}^{N_\Gamma} \left(\frac{1}{6} \tilde{\Lambda}_{(j-1)l}(\lambda)(y_j - y_{j-1}) + \frac{1}{3} \tilde{\Lambda}_{jl}(\lambda)(y_{j+1} - y_{j-1}) + \frac{1}{6} \tilde{\Lambda}_{(j+1)l}(\lambda)(y_{j+1} - y_j) \right)$$

iff $y_j \in \Gamma$ and

$$C_{jk} = \int_{\Omega} \left(\frac{\partial \phi_k(x,y)}{\partial x} \frac{\partial \phi_j(x,y)}{\partial x} + \frac{\partial \phi_k(x,y)}{\partial y} \frac{\partial \phi_j(x,y)}{\partial y} + 21x^2 \phi_k(x,y)\phi_j(x,y) \right) d\mathbf{x}$$

iff $y_j \notin \Gamma$.

Table 7.3 contains the eigenvalues as a function of tube width and mesh density.

$(N_\Gamma, N_p, N_\Gamma, N_b)$	θ	λ_1	λ_2	λ_3
$(4304, 2223, 11, 9)$	0.08π	16.9134	28.7466	32.5274
$(17216, 8749, 23, 21)$	0.08π	16.8835	28.7083	32.4319
$(68864, 34713, 47, 21)$	0.08π	16.8732	28.6983	32.4038
$(68864, 34713, 47, 31)$	0.08π	16.8734	28.6983	32.4044
$(4336, 2239, 11, 9)$	0.09π	16.4466	28.5051	–
$(17344, 8813, 23, 21)$	0.09π	16.4144	28.4648	–
$(69376, 34969, 47, 21)$	0.09π	16.4031	28.4542	–
$(69376, 34969, 47, 31)$	0.09π	16.4034	28.4543	–
$(4416, 2281, 15, 9)$	0.1π	15.8925	–	–
$(17662, 8977, 31, 23)$	0.1π	15.8643	–	–
$(70656, 35617, 63, 23)$	0.1π	15.8585	–	–
$(70656, 35617, 63, 31)$	0.1π	15.8592	–	–

Table 6.3: Eigenvalues of the parabolic potential for several tube widths and mesh densities

Chapter 7

Comparison of the finite differences and finite element methods

7.1 Comparison of the eigenvalues

In this chapter we shall make a comparison of the eigenvalues obtained from the method of finite differences with those obtained from the method of finite elements. Table 7.1 gives eigenvalues obtained by both methods where for each λ the left column below λ contains the eigenvalues obtained by finite differences and the right column contains the eigenvalues obtained by the method of finite elements for different values of θ on the full domain.

θ	λ_1		λ_2	
0.09π	5.68508	5.68585	14.0972	14.1017
0.1π	5.66038	5.66102	13.9231	13.9268
0.11π	5.63235	5.63305	13.7101	13.7142
0.12π	5.60074	5.60153	13.4476	13.4521
0.13π	5.56535	5.56600	13.1199	13.1235
0.14π	5.52591	5.52659	12.7023	12.7057
θ	λ_3		λ_4	
0.09π	14.6769	14.6785	24.8622	24.8744
0.1π	14.6741	14.6757	24.0924	24.1017
0.11π	14.6703	14.6720	-	-
0.12π	14.6653	14.6671	-	-
0.13π	14.6588	14.6607	-	-
θ	λ_5		λ_6	
0.09π	26.3368	26.3425	29.6731	29.6834
0.1π	26.3166	26.3218	-	-

Table 7.1: Comparison of eigenvalues obtained by finite differences on the left and the method of finite elements on the right

Table 7.2 compares the eigenvalues obtained for the half domain and has the same layout as Table 7.1. The eigenvalues in Table 7.2 calculated via the method of finite elements for the half domain have not previously appeared

in this thesis. These eigenvalues have only being calculated for the densest possible mesh as are the last values appearing in Table 6.2 for each value of θ and λ.

θ	λ_1		λ_2		λ_3	
0.09π	5.68466	5.68570	14.0947	14.1009	14.6768	14.6786
0.1π	5.66010	5.66105	13.9215	13.9270	14.6741	14.6759
0.11π	5.63202	5.63304	13.7082	13.7142	14.6702	14.6721
0.12π	5.60041	5.60149	13.4456	13.4519	14.6652	14.6672
0.13π	5.56496	5.56613	13.1177	13.1243	14.6587	14.6608
0.14π	5.52560	5.52668	12.7007	12.7062	14.6504	14.6526
θ	λ_4		λ_5		λ_6	
0.09π	24.8622	24.8722	26.3360	26.3426	29.6711	29.6831
0.1π	24.0924	24.1022	26.3152	26.3223	-	-
0.11π	-	-	26.2866	26.2941	-	-
0.12π	-	-	26.2481	26.2562	-	-
0.13π	-	-	26.1970	26.2058	-	-
0.14π	-	-	26.1303	26.1395	-	-
θ	λ_8		λ_{10}		λ_{12}	
0.09π	40.5678	40.5864	49.1905	49.2163	57.2269	57.2666
0.1π	40.4924	40.5124	49.1772	49.2037	57.0255	57.0670
0.11π	40.3862	40.4072	49.1570	49.1821	56.7283	56.7617
0.12π	40.2384	40.2613	49.1252	49.1501	56.2819	56.3291
0.13π	40.0335	40.0576	49.0729	49.0979	55.5677	56.6182
0.14π	39.7476	39.7735	48.6754	49.0010	-	-

Table 7.2: Comparison of eigenvalues obtained by finite differences on the left and the method of finite elements on the right for the half domain

Notice that λ_3 in Table 7.1 and Table 7.2 are virtually the same. This is the first antisymmetric eigenvalue about the x axis. This is not the case for the other eigenvalues since they are calculated by imposing Neumann boundary conditions at $y = 0$ on the half domain. This means that we use

5.39 instead of 5.38 which itself is symmetric to 5.19. The same comparison is done in Table 7.3 containing the eigenvalues for the parabolic potential.

θ	λ_1		λ_2		λ_3	
0.08π	16.8674	16.8734	28.6948	28.6983	32.3873	32.4044
0.09π	16.3967	16.4034	28.4502	28.4543	-	-
0.1π	15.8541	15.8592	-	-	-	-

Table 7.3: Comparison of eigenvalues obtained from the method of finite differences on the left and the method of finite elements on the right

7.2 The eigenvalues in relation to theory

These results for the eigenvalues calculated by the methods of finite differences and finite elements agree with the theory that the finite differences method is an approximation from below and the finite elements method gives an approximation from above. This is the case for the comparison Table 7.1, Table 7.2 and Table 7.3.

7.3 Conclusion

In this thesis we have examined a spectral problem for a semi infinite waveguide with a perturbed periodic potential. We have shown numerically that the perturbation induces eigenvalues into the spectral gaps of the unperturbed problem as well as inducing eigenvalues into the spectral bands. These

results have been obtained using both the methods of finite difference and finite elements and a comparison between the quality of them has been made. As waveguides are often used for models of quantum switches (and triadic logic) it would be interesting to repeat this investigation, but now assuming the underlying problem is governed by the Maxwell system.

Bibliography

[1] L. Aceto, P. Ghelardoni, and M. Marletta. Numerical computation of eigenvalues in spectral gaps of Sturm-Liouville operators. *J. Comput. Appl. Math.*, 189(1-2):453–470, 2006.

[2] A. Aslanyan, L. Parnovski, and D. Vassiliev. Complex resonances in acoustic waveguides. *Quart. J. Mech. Appl. Math.*, 53(3):429–447, 2000.

[3] M. Callan, C. M. Linton, and D. V. Evans. Trapped modes in two-dimensional waveguides. *J. Fluid Mech.*, 229:51–64, 1991.

[4] P G. Ciarlet. *The finite element method for elliptic problems*, volume 40 of *Classics in Applied Mathematics.* Society for Industrial and Applied Mathematics (SIAM), Philadelphia, PA, 2002. Reprint of the 1978 original [North-Holland, Amsterdam; MR0520174 (58 #25001)].

[5] S. Clark, F. Gesztesy, H. Holden, and B. Levitan. Borg-type theorems for matrix-valued Schrödinger operators. *J. Differential Equations*, 167(1):181–210, 2000.

[6] E. A. Coddington and N. Levinson. *Theory of ordinary differential equations.* McGraw-Hill Book Company, Inc., New York-Toronto-London, 1955.

[7] M. S. P. Eastham. *The asymptotic solution of linear differential systems*, volume 4 of *London Mathematical Society Monographs. New Series.* The Clarendon Press Oxford University Press, New York, 1989. Applications of the Levinson theorem, Oxford Science Publications.

[8] M.S.P Eastham. *The spectral theory of periodic differential equations.* Scottish Academic Press London, Edinburgh, 1973.

[9] D.E. Edmunds and W. D. Evans. *Spectral theory and differential operators.* Oxford Mathematical Monographs. The Clarendon Press Oxford University Press, New York, 1987. Oxford Science Publications.

[10] D.V. Evans, M. Levitin, and D. Vassiliev. Existence theorems for trapped modes. *J. Fluid Mech.*, 261:21–31, 1994.

[11] D.V. Evans and C.M. Linton. Trapped modes in open channels. *J. Fluid Mech.*, 225:153–175, 1991.

[12] D.R. Gardner, S.A Trogdon, and R.W. Doughlas. A modified tau spectral method that eliminates spurious eigenvalues. *Journal of Computational Physics*, 80(1):137–167, 1989.

[13] J. R. Gilbert, G L. Miller, and S-H Teng. Geometric mesh partitioning: Implementation and experiments. *SIAM Journal on Scientific Computing*, 19(6):2091–2110, 1998.

[14] V. Hutson, J.S. Pym, and J.C Michael. *Applications of functional analysis and operator theory*, volume 200 of *Mathematics in Science and Engineering*. Elsevier B. V., Amsterdam, second edition, 2005.

[15] M K. Kadalbajoo and D Kumar. Geometric mesh FDM for self-adjoint singular perturbation boundary value problems. *Appl. Math. Comput.*, 190(2):1646–1656, 2007.

[16] Y. Kuznetsov, K. Lipnikov, and M. Shashkov. The mimetic finite difference method on polygonal meshes for diffusion-type problems. *Comput. Geosci.*, 8(4):301–324 (2005), 2004.

[17] M. Levitin and E. Shargorodsky. Spectral pollution and second-order relative spectra for self-adjoint operators. *IMA J. Numer. Anal.*, 24(3):393–416, 2004.

[18] C.M. Linton and D.V. Evans. Integral equations for a class of problems concerning obstacles in waveguides. *J. Fluid Mech.*, 245:349–365, 1992.

[19] M. Marletta. Automatic solution of regular and singular vector sturm-liouville problems. *Numerical Algorithms*, 4(1):66–99, 1993.

[20] M. Marletta. Numerical solution of eigenvalue problems for hamiltonian systems. *Advances in Computational Mathematics*, 2(2):155–184, 1994.

[21] M. Marletta. Numerical solution of eigenvalue problems for Hamiltonian systems. *Adv. Comput. Math.*, 2(2):155–184, 1994.

[22] M. McIver. An example of non-uniqueness in the two-dimensional linear water wave problem. *J. Fluid Mech.*, 315:257–266, 1996.

[23] M. McIver, C. M. Linton, and J. Zhang. The branch structure of embedded trapped modes in two-dimensional waveguides. *Quart. J. Mech. Appl. Math.*, 55(2):313–326, 2002.

[24] M. McIver, C.M. Linton, P. McIver, J. Zhang, and R. Porter. Embedded trapped modes for obstacles in two-dimensional waveguides. *Quart. J. Mech. Appl. Math.*, 54(2):273–293, 2001.

[25] P. McIver, C.M. Linton, and M. McIver. Construction of trapped modes for wave guides and diffraction gratings. *R. Soc. Lond. Proc. Ser. A Math. Phys. Eng. Sci.*, 454(1978):2593–2616, 1998.

[26] M. A. Naĭmark. *Linear differential operators. Part II: Linear differential operators in Hilbert space.* With additional material by the author, and a supplement by V. È. Ljance. Translated from the Russian by E. R. Dawson. English translation edited by W. N. Everitt. Frederick Ungar Publishing Co., New York, 1968.

[27] W. N. Everitt P. B. Bailey and A. Zettl. Algorithm 810: The sleign2 sturm-liouville code. *ACM Trans. Math. Softw.*, 27(2):143–192, 2001.

[28] B Pavlov and K Robert. Resonance optical switch: calculation of resonance eigenvalues. In *Waves in periodic and random media (South Hadley, MA, 2002)*, volume 339 of *Contemp. Math.*, pages 141–169. Amer. Math. Soc., Providence, RI, 2003.

[29] K. M. Schmidt. Critical coupling constants and eigenvalue asymptotics of perturbed periodic Sturm-Liouville operators. *Comm. Math. Phys.*, 211(2):465–485, 2000.

[30] B. Straughan and D.W. Walker. Two very accurate and efficient methods for computing eigenvalues and eigenfunctions in porous convection problems. *J. Comput. Phys.*, 127(1):128–141, 1996.

[31] K. Wright. Continuous orthonormalization algorithms for boundary value problems. *Department of Computer Science, Newcastle Univeristy*, http://www.cs.ncl.ac.uk/publications/trs/papers/257.pdf, 1988.